The Role of the Meniscus in Knee Joint Load Transmission: A Three-Dimensional Finite Element Study

by

Catherine Mary Ford

B.S.E., University of Pennsylvania (1990)

Submitted to the Department of Mechanical Engineering
in partial fulfillment of the requirements for the degree of

Master of Science in Mechanical Engineering

at the

MASSACHUSETTS INSTITUTE OF TECHNOLOGY

May 1992

Author .....
Department of Mechanical Engineering
May 8, 1992

Certified by .....
Derek R. Rowell
Professor
Thesis Supervisor

Accepted by .....
Ain A. Sonin
Departmental Committee on Graduate Students

The Role of the Meniscus in Knee Joint Load Transmission: A Three-Dimensional Finite Element Study

by

Catherine Mary Ford

Submitted to the Department of Mechanical Engineering
on May 8, 1992, in partial fulfillment of the
requirements for the degree of
Master of Science in Mechanical Engineering

Abstract

Treatment of meniscal pathology through removal of the meniscus (meniscectomy) is one of the most common intra-articular procedures. Clinical studies have demonstrated a link between meniscectomy and degenerative joint disease. Quantitative knowledge of meniscal mechanics is crucial to understanding the mechanisms of meniscal lesions, the effects of meniscectomy, and the pathogenesis of osteoarthritis in the knee. Modeling of the meniscus is needed to estimate variables which cannot be measured experimentally, such as subchondral bone stresses.

A two-dimensional axisymmetric model of the meniscus has been developed by Brown [12]. The goal of this project was to develop a three-dimensional, non-axisymmetric finite element model of the meniscus to further investigate the role of the meniscus in load bearing. A three-dimensional model allows the use of more realistic meniscal geometry, and significantly expands the meniscal functions which can be examined. The results of the two- and three-dimensional models were compared in order to evaluate the efficacy of modeling the meniscus as an axisymmetric structure. The parameters used for the comparison were contact pressure in the tibial articular cartilage, overall joint stiffness, meniscal displacement, meniscal circumferential strain, and subchondral bone stress.

The three-dimensional meniscus model was verified by comparing the model predictions for peak articular cartilage contact pressures, meniscal circumferential strains and meniscal radial displacements to experimental values from the literature. The three-dimensional meniscus model predicitons demonstrated better agreement with experiment than the axisymmetric meniscus model. Although axisymmetric modeling is effective in providing a qualitative description of meniscal mechanics, non-axisymmetric modeling is necessary for quantitative description of the role of the meniscus in knee joint load transmission.

Thesis Supervisor: Derek R. Rowell
Title: Professor

Acknowledgements

I would like first of all to acknowledge and thank my faculty advisor, Professor Derek Rowell, for his support and wisdom throughout this project. Your ability to see "the big picture", your willingness to provide support, and your assistance in overcoming obstacles were invaluable.

I would also like to thank my "other" advisor, Greg Brown. This project would not have been possible without both the scientific groundwork that you laid and your significant efforts in formulating the project and seeing it through to completion. Your willingness to spend time helping me even when you were in the thick of medical school adds to the respect that I hold for you. Your mentorship and caring attitude have been invaluable to me not just as a Master's student, but as a student in the MEMP program and as a future PhD (I hope!!).

I wish as well to express my gratitude to Professor Robert Mann for providing an environment for research in biomechanics like the Newman Laboratory. Thanks to all the students in the lab, particularly Keita (for sharing your ADINA wisdom), Pat (for all the advice on computer hardware and letting me use your "Personal" Iris), Sylvain, Denis, Naomi, Tony and all the other students who made the lab a great place in which to work.

Thanks are also due to all of the people in the MEMP program for their constant support and friendship. Special thanks to Brian and Naomi for getting me through the qualifying exams. Thank you Edwin for all the fun we had throwing softballs around in Killian Court (when we should have been working!).

No list of people to thank could be complete without acknowledging the love and support of my family. Thanks Mom, Dad, and Beverly for everything. Words can't even begin to express what I owe you all. And special thanks to my surrogate "family" here in Cambridge, my roomates Tobi and Sue. I didn't even know you when we moved in, but after two years I can't believe how lucky I was to find you! And how could I forget the best across-the-street neighbor, fellow student, friend and travel companion anyone could have, Marie-José.

Student support for this project was provided by the National Science Foundation and the Harvard-MIT Division of Health Sciences and Technology. Portions of this work were performed on a CRAY X-MP at the MIT Supercomputing Facility and on a CRAY Y-MP at the San Diego Supercomputing Center.

Contents

List of Figures

Chapter 1

Introduction

The knee is a six degree-of-freedom synovial joint whose complex design fulfills the competing requirements of stability, range of motion, and load transmission. The articular surfaces of the femur and tibia are highly incongruous and therefore require several passive and active elements to maintain joint stability. In addition to maintaining a high degree of mobility, the knee is capable of transmitting large dynamic loads. The relatively simple act of walking requires the knee to transmit loads of 3-5 times body weight (Harrington,1976[27]). Impact loads sustained by the knee during more strenuous and sudden movements can be significantly higher. Thus it is evident that the knee joint has a tremendous capacity for transmitting loads as well as maintaining mobility and stability. The meniscus is an extremely important structure which contributes to the knee's ability to perform these competing functions. The menisci are highly mobile, crescent-shaped wedges of fibrocartilage located between the femur and tibia. Geometrically, the menisci serve to increase the congruence between the femoral and tibial articular surfaces (MacConaill,1932[41]).

1.1 Meniscal Pathology and Treatment

The delicate biomechanical balance within the knee joint makes the meniscus a common site for difficulties. Meniscal pathology can take several forms, and can be brought on by acute injury or can develop over time due to degeneration. Appel re-

ported that meniscal lesions were the most common intra-articular injuries, and that meniscectomy was therefore the most common intra-articular procedure (1970[4]). This report reflected the trend in the past of complete removal of damaged menisci. A common belief was that the damaged meniscus caused erosion of the articular cartilage, which could be halted or even reversed by meniscectomy (1959[29]). Since no weight-bearing role had ever been ascribed to the meniscus, total meniscectomy appeared to be a relatively benign procedure. The lack of belief in any load bearing meniscal function lead to the belief that "a normally functioning knee usually results when one or both menisci are removed at operation (1941[11])." The belief of the time is also described in a 1932 paper by MacConaill [41]:

> ... it is a well-known fact the the removal of the internal meniscus of the knee is an operation not necessarily followed by discomfort of the patient in the use of the limb. There exists, then, the paradox that structures clearly of great importance for the normal working of a part can be removed (at least to the extent of one-half) without the production of ill effects.

1.2 Clinical Effects of Meniscectomy

The first investigator to lend support to the idea of a load-bearing role for the meniscus was Fairbank in 1948. Fairbank's radiological study of knees following meniscectomy led him to conclude that meniscectomy was not a benign procedure, and that the menisci play an integral part in weight-bearing in the knee joint. He also suggested that meniscectomy could predispose the knee to degenerative changes [21].

Since the time of Fairbank, several investigators have examined the possible link between meniscectomy, joint degeneration, and osteoarthritis. There have been a number of clinical, long-term follow-ups of meniscectomized knees which have shown a correlation between meniscectomy and degenerative joint disease [30, 63, 4, 32, 2, 34]. Although there is still debate concerning the precise mechanisms of joint degeneration following meniscectomy, it is now well-established that meniscectomy is not a benign procedure as was once thought. Clinically, there is a fair amount of agreement that

meniscectomy should be approached conservatively, and that the meniscus should be spared or repaired whenever possible [2, 17, 30, 32].

1.3 The Meniscus as a Load-Bearing Structure

Clinical studies showing the correlation between meniscectomy and degeneration in the knee joint have been accompanied by several investigations attempting to quantify the biomechanical effects of meniscal removal. A large proportion of these studies focused on quantifying the role of the meniscus as a weight bearing and load transmitting structure. Techniques used to evaluate the load transmission characteristics of the meniscus include contact stress and area studies of cadaver knees and load-deflection tests during joint compression. For example, a study performed by Seedhom *et al.* (1979[56, 58]) examined the amount of load carried by the menisci in cadaver knees at different degrees of flexion, and used a staining technique to estimate contact areas. The authors concluded that knees with no meniscus have significantly reduced contact areas and increased stress, and calculated that the menisci support 70% to 99% of the total joint load.

Numerous other in vitro studies have been performed in an attempt to further understand and quantify the effects of meniscectomy. Although studies such as these provide valuable information, they are limited. There are few relevant parameters which can be directly measured without interfering with the normal function of the joint. The stress values that can be calculated based on contact area estimates are only average stresses; they give little information regarding the distribution of stress. Such studies can give estimates of the percentage of load carried by the meniscus; however, they do not further our understanding of the *mechanisms* by which the meniscus transmits loads.

The essential first step in truly understanding the effects of meniscectomy is a better understanding of how the meniscus transmits loads. Modeling of the meniscus under normal conditions is needed in order to evaluate important quantities which cannot be directly measured, such as subchondral bone stresses and internal meniscal

stresses. An effective model is also extremely helpful in understanding the mechanisms of meniscal tearing and joint degeneration. Once established, a model which uses fundamental engineering and physiological principles to understand meniscal behavior can be verified by experiments. This approach is significantly more effective than performing invasive experiments first and then working backwards to describe general behavior. In addition, once an effective model has been developed, parameters such as geometry, material properties, and loading conditions can be varied with relative ease.

1.4 Previous Modeling of the Meniscus

Brown (1990[12]) has developed a two-dimensional, axisymmetric finite element model of the meniscus using the approach described above. The model includes articular cartilage layers on the femoral and tibial surfaces, as well as anisotropic meniscal material properties. The philosophy behind the work was to derive as much meaningful information as possible from a relatively simple model. The model succeeds in providing significant insight into the mechanisms of meniscal load-bearing while maintaining relatively simple axisymmetric geometry and loading.

The next logical step in the modeling process is to expand the meniscus model into three dimensions. A three-dimensional model with non-axisymmetric meniscal geometry can be used to evaluate the two-dimensional model, and to determine if the two-dimensional model is sufficient to describe the general behavior of the system under simple loading conditions. This is an extremely important issue, given that the cost of three-dimensional analysis is significantly higher than two-dimensional analysis. In addition to allowing for more realistic geometry, a three-dimensional model can be used to study a much greater range of proposed meniscal functions. While an axisymmetric model can be used primarily for the study of meniscal weight bearing under axial loading, a three-dimensional model can provide insight into many areas including the meniscus's role in joint stability, the mechanisms of meniscal tearing, as well as normal load bearing under both axial and non-axial loading conditions.

1.5 Research Objectives

The meniscus is clearly an important functional structure within the human knee joint. Its proposed functions are numerous, as are the types of meniscal pathologies. The role of the meniscus in prevention of joint degeneration has been well established clinically; however, the precise mechanisms by which the meniscus transmits loads and "protects" underlying bone are not sufficiently quantified. Modeling of knee joint contact with the meniscus is needed in order to elucidate quantitatively the mechanisms of meniscal load-bearing. Knowledge of these mechanisms will provide insight into normal meniscal function, the causes and effects of meniscal pathology, and biomechanical changes that occur as a result of meniscal surgery.

Based on these observations, the goal of this project is to develop a three dimensional finite element model of the human knee meniscus, including non-axisymmetric meniscal geometry. Development of such a model will serve a dual purpose. First, the model will provide an accessible environment for the quantitative study of meniscal mechanics. A realistic, working model can calculate subchondral bone stresses and internal meniscal stresses, which are extremely difficult to measure experimentally. Secondly, the model will be used to evaluate the efficacy of two-dimensional axisymmetric modeling in describing general meniscal behavior. This will be accomplished by comparing results from Brown's axisymmetric model to results of the three-dimensional model and using the same material properties, geometry, and loading conditions. Going from two to three dimensions, then, will provide both a means of verification of two-dimensional modeling and a significant expansion of the type of meniscal functions that can be examined.

Chapter 2

Review of Meniscal Functions

2.1 Meniscectomy and Joint Degeneration

Since the first suggestion of the possible link between meniscectomy and degenerative change by Fairbank (1948[21]), there have been several clinical studies of meniscectomized knees performed in an attempt to quantify such a connection. Several of these studies are long-term follow-ups of meniscectomy patients. Jackson (1968[30]) performed a radiological review of 577 meniscectomized knees at a minimum of five years post-operatively, and concluded that a significantly higher proportion of meniscectomized knees underwent degenerative changes than did normal knees. The qualitative nature of the study made it difficult to establish the causes of degeneration, but the author suggests that the degenerative changes were a direct result of loss of the meniscus.

Some investigators have attempted to evaluate the effect of numerous factors on joint degeneration following meniscectomy (Tapper & Hoover, 1969[63]; Appel, 1970[4]; Johnson *et al.*, 1974[32]; Allen *et al.*, 1984[2]). These factors include age at operation, sex, varus or valgus deformity, and type of lesion, just to name a few. These studies were retrospective in nature, making it difficult to account for how symptoms change over time. Jorgensen (1987[34]) attempted to relate clinical findings to time elapsed since operation in athletes. He found that degenerative changes increased in amount and severity with time since operation. The differences in ex-

perimental methods and the subjectiveness of symptoms and clinical findings makes it very difficult to draw many consistent conclusions from these studies. All of these studies, however, came to the same general conclusion that degeneration is more likely to occur in a meniscectomized knee than in a normal knee. The difficulty in interpreting these observational studies is that they only establish a correlation between meniscectomy and knee degeneration. Modeling of the meniscus is needed to clarify a pathophysiologic etiology of knee degeneration following meniscectomy.

2.2 The Meniscus as a Load-Bearing Structure

Investigators have used several experimental methods in an attempt to quantify the load-bearing role of the meniscus. One of these techniques is measurement of contact areas. Contact area measurements provide an indirect measure of average stress within the joint. The techniques for measuring contact area include the use of polymethylmethacrylate castings (Walker & Hajek, 1972[68]), radiographic contrast techniques (Kettelkamp & Jacobs, 1972[35]; Maquet, 1976[42]), articular cartilage staining techniques (Krause *et al.*, 1976[36]; Seedhom and Hargreaves, 1979[58]), silicone rubber castings (Fukubayashi *et al.*, 1980[24]; Kurosawa *et al.*, 1980[38]), and pressure sensitive films (Baratz *et al.*, 1986[9]; Riegger *et al.*, 1987[52]). It is very difficult to compare the quantitative results of these experiments because of differences in experimental procedures, in particular the loading conditions and specimen preparation. It is also difficult to extrapolate the results to what occurs *in vivo* because of the non-physiologic nature of the loading constraints. The only consistent qualitative conclusion that can be drawn from these studies is that the contact area of the knee joint decreases following meniscectomy.

Several investigators have also attempted to measure the contact pressure within the joint directly. Walker and Erkman (1975[69]) used a miniaturized pressure transducer to measure contact pressure. Ahmed and Burke (1983[1]) used a micro indentation transducer to determine the pressure distribution and calculate the percentage of joint load transmitted by the meniscus. Pressure sensitive films have been used

by Fukubayashi and Kurosawa (1980[24]), Baratz *et al.* (1986[9]), and Riegger *et al.* (1987[52]). Brown and Shaw (1984[13]) used miniature piezoresistive pressure transducers set in the femoral articular cartilage to measure contact pressure. Due to the nature of the piezoresistive transducers used by Brown and Shaw, low frequency dynamic measurements were possible. This significantly reduced the error due to poroelastic effects of articular cartilage. Brown and Shaw's technique is an improvement over pressure-sensitive films due to the ability to measure pressure instantaneously; however, the method provides very low spatial resolution. As with the contact area studies described above, the invasiveness of the experiments casts doubt on the applicability of the results to *in vivo* load bearing.

Another experimental technique used to evaluate the load-bearing role of the meniscus is the use of load deflection measurements with and without the meniscus (Seedhom *et al.*, 1974[57], 1979[56, 58]; Shrive, 1974[60]; Walker & Erkman, 1975[69]; Krause *et al.*, 1976[36]; Kurosawa *et al.*, 1980[38]; Newman *et al*, 1989[46]). These studies provide estimates of the percentage of joint load carried by the meniscus. The values reported range from 40% to 100%. The experiments are difficult to compare quantitatively because of the high variability of the loading rates and kinematic constraints imposed during loading. There is general agreement, however, that the menisci play an important load-bearing role in the knee joint.

Other investigators have used meniscal load-deflection and strain measurements to characterize meniscal behavior. Krause *et al.* (1976[36]) used a hump-backed displacement transducer to measure the circumferential displacement of the meniscus, and calculated circumferential strain. Bylski *et al.* (1986[16]) measured the motion and deformation of intact menisci using lead markers cemented to the superior surface of the menisci. These investigators found that meniscal deformation is highly dependent on the integrity of the peripheral attachments. Thompson (1990[64]) used magnetic resonance imaging to determine meniscal kinematics. Brown (1990[12]) used x-ray stereophotogrammetry to measure circumferential strains and displacements of the meniscus under axial joint loading.

Several investigators have performed photoelastic studies of planar knee models

to study stress patterns (Chand *et al.*, 1976[18]; Maquet, 1976[42]; Nishizaki *et al.*, 1981[47];Radin *et al.*, 1984[49]). These models give qualitative assessments of stress patterns but are limited by their two-dimensional nature.

As can be seen from the investigations described above, accurate quantification of the load-bearing role of the meniscus is extremely difficult to achieve experimentally. All of the experiments described above were highly invasive, and the preparations often did not undergo physiological loading and constraints. In many of the experiments, the joints were disarticulated during preparation. This interferes with soft tissue and ligamentous constraints. In addition, the use of cadaverous tissue loses the effect of muscular co-contraction, which can have a significant effect on the magnitude and direction of joint loads. The placement of transducers and pressure-sensitive films within the joint space interferes significantly with the natural lubrication and functioning of the joint. Another factor which can cause problem is the loading rate used. The time-dependent behavior of articular cartilage makes the loading rate and time between loading and taking of measurements extremely important issues. The issue of cartilage time-dependency was often omitted from these studies. All of these experimental difficulties emphasize the need to model the meniscus in order to learn more about meniscal mechanics without disrupting the joint integrity experimentally.

2.3 The Role of the Meniscus in Joint Stability

Besides helping to quantify the role of the meniscus in knee joint load transmission, a three-dimensional model of the meniscus can aid in understanding the role of the meniscus in joint stability. This is a subject of significant debate, which several investigators have examined experimentally. Several different techniques have been used to assess joint stability. Investigators have used force versus displacement responses for anterior/posterior motion of the tibia (Markolf *et al.*, 1981[43]; Levy *et al.*, 1982[40], 1989[39]; Shoemaker & Markolf, 1986[59], Askew *et al.*, 1987[6]), force versus displacement responses for medial/lateral motion of the tibia (Markolf *et al.*, 1981[43]), rotatory laxity tests (Markolf *et al.*, 1981[43]; Wang & Walker, 1974[70];

Seale *et al.*, 1981[54]; Askew *et al.*, 1987[6]), and varus/valgus laxity tests (Seale *et al.*, 1981[54]; Askew *et al.*, 1987[6]). Several of these studies focused on the role of the meniscus in stabilization of knees from which the anterior cruciate ligament has been removed (Levy *et al.*, 1982[40, 39]; Askew *et al.*, 1987[6]; Seale *et al.*, 1981[54]; Shoemaker and Markolf, 1986[59]). All of the experiments used different constraints and loading techniques, and significantly different applied joint loads. This makes direct comparison of results extremely difficult. The widely varying results of these studies emphasize the need for a model in which parameters can be easily adjusted to a particular physiological situation (for example, a meniscal lesion or meniscectomy). This would allow for consistent, direct comparison of stability measurements from different physiological situations. The use of a model is also helpful in that it avoids the invasiveness of experiments, and also the inconsistencies associated with cadaver knee geometry.

Chapter 3

Finite Element Modeling of the Meniscus

3.1 The Finite Element Method

Given that the objective of this research is to develop a model of knee joint contact that will elucidate the load-bearing role of the meniscus, it is clear that the major emphasis of the model should be to predict pressures, stresses, and strains within the joint. It is useful, therefore, to approach the questions involved in modeling as questions in solid mechanics. The finite element method is extremely useful in examining systems from a solid mechanical point of view and is thus the method of choice for the model developed here. A general definition of the finite element method is as follows:

> The FEM (finite element method) is a computer-aided mathematical technique for obtaining approximate numerical solutions to the abstract equations of calculus that predict the response of physical systems subjected to external influences (Burnett, 1987[15]).

The method is thus directly applicable to the problem of developing a model to predict stresses and strains within the knee joint.

The analysis of a system using the finite element technique begins with division of the continuous system into subdivisions called elements. The geometry of each element is defined by a set of nodal points. The finite element discretization reduces the set of differential equations which describe the continuous physical system into a set of algebraic equations of the form

$$\mathbf{KU} = \mathbf{R}$$

where **K** is the structural stiffness matrix, **U** is the vector of nodal point displacements, and **R** is the vector of applied loads. The stiffness matrix is formed by lumping the material properties of each element at the nodal points. The boundary conditions on the system take the form of prescribed displacements.

The solution to the finite element system of equations is the vector **U** of nodal point displacements. The strains within elements are calculated directly from the displacements, and the stresses are calculated from the strains based on the appropriate constitutive relations. This is a highly simplified explanation of the solution of the finite element equations, particularly given the fact that the contact surfaces in the meniscus model render the model non-linear. For a thorough treatment of the non-linear solution scheme, the reader is referred to Bathe (1982[10]).

3.2 Practical Modeling Considerations

A useful and practical approach to finite element modeling is to begin with the simplest model that can provide meaningful information. To that end, Brown (1990[12]) has developed a two-dimensional axisymmetric finite element model of the meniscus. The axisymmetric model showed that the meniscus transmits a significant portion of the joint load when loaded axially. The next logical step in the modeling process, then, is to create a model which facilitates the study of meniscal mechanics under non-axisymmetric loading conditions and with more realistic geometry. Since this situation cannot be idealized in two dimensions, it is necessary to model the joint

contact problem in three dimensions.

The expansion from a two-dimensional to a three-dimensional finite element model involves a tremendous increase in the number of nodes and elements needed to adequately represent both the geometry and the state of stress within the system. A standard procedure is to begin with a relatively coarse mesh to qualitatively assess the state of stress within the system, and then to refine the mesh by shrinking the element size where necessary, thus increasing the number of nodes. In general three-dimensional analysis, a standard node contains three translational degrees of freedom. A mesh refinement which merely doubles the number of nodes in the model results in an eightfold increase in the number of degrees of freedom and thus the size of the stiffness matrix. Assuming the size of the stiffness matrix is roughly proportional to the computing time and temporary storage required to solve the equations of the model, it is not difficult to imagine the solution of a three-dimensional model becoming infeasible without tremendous amounts of expensive supercomputing time. The expansion to a three-dimensional model brings with it the competing requirements of computing cost and adequate mesh refinement which are significantly less important issues in two-dimensional analysis. Given these practical constraints, great care was taken in the discretization stage to provide sufficient mesh refinement in high-stress areas, and less refinement in low stress areas.

The fact that the problem to be examined is by nature a contact problem also significantly contributes to the cost of solution. One reason is that the contact regions require a relatively high degree of mesh refinement in order to adequately represent the state of stress. Secondly, the presence of contact surfaces renders the model non-linear, since the boundary conditions change as higher loads are applied and the contact areas change. Solution of the non-linear contact problem therefore requires a step-by-step, iterative scheme which is considerably more costly than the solution of a linear model.

3.3 Model Accuracy and Verification

The term 'adequate mesh refinement' has been used above to describe an important requirement of the finite element model to be developed. What exactly is meant by 'adequate mesh refinement', and how does one know when it has been achieved? Even more importantly, how does one verify that the finite element results obtained are meaningful to the problem being studied? It is not sufficient to merely accept numerical results without some form of verification and recognition of potential sources of error.

From a theoretical standpoint, finite element modeling involves the mechanical idealization of an actual physical problem (represented by the differential equations describing the system), followed by the finite element solution of the equations (Bathe, 1982[10]). An in-depth discussion of convergence of finite element results is not appropriate here; it suffices to state that the finite element solution will converge to the exact solution of the mechanical idealization as the mesh is refined provided the requirements of completeness and compatibility are met. Completeness of a finite element is the ability of the element to represent rigid body displacements and constant strain states. This requirement is inherently satisfied by the element formulation implemented within the finite element software used. Compatibility requires that displacements across element boundaries are continuous, and is achieved by using adjacent elements which employ the same displacement interpolation functions (Bathe, 1982[10]).

Given that the model meets the completeness and compatibility requirements, it remains to determine how much mesh refinement is sufficient to obtain meaningful information from the model. Compatibility requires that displacements across element boundaries are continuous. This requirement, however, does not guarantee that stresses will be continuous between elements since stresses are calculated from the derivatives of displacement (Sussman & Bathe, 1986[62]). Therefore, the continuity of stresses across element boundaries is a useful indicator of mesh refinement sufficiency and will be helpful in determining optimal mesh characteristics for the finite

element model.

Analytical solutions can be an extremely useful tool in the verification of finite element results. Of course, most problems cannot be solved using purely analytical methods (otherwise the FEM solution would not be necessary); their solutions must be approximated numerically. It is at times possible, however, to simplifiy the problem at hand in such a way that an analytical solution can be used as a basis for comparison to finite element results. Convergence of finite element results of the simplified system to the analytical solution can then be used as a basis for extrapolating the convergence of a more complicated system which cannot be solved analytically.

3.4 Hertz Theory of Elastic Contact

The system that will be used for verification of mesh characteristics consists of an elastic sphere in contact with a planar surface. This general class of problems is known as Hertzian contact. Although highly simplified, the Hertzian contact problem can provide significant insight into how much mesh refinement is needed to model knee joint contact. The problem of a sphere in contact with a flat surface is a reasonable simplification of unicondylar contact without the meniscus under axial loading. The analytical solution for Hertzian contact problems is based on the following assumptions:

1. The bodies in contact are infinite elastic half-spaces.
2. The surfaces are frictionless, continuous, and non-conforming.
3. The strains are small.
4. The radius of the contact area is much smaller than the radius of curvature of the sphere ($a << R$).

It is important to bear these assumptions in mind when comparing the analytical solution to the finite element results.

The analytical solution for stresses at the contact of two elastic bodies was first presented by Hertz in 1881. The following are the results for the case of an elastic

sphere in contact with an elastic semi-infinite half-plane. The equations presented here were taken from Johnson (1985[31]) and Timoshenko and Goodier (1970[65]), to which the reader is referred for a more complete derivation.

A downward compressive load P is applied to the sphere, and a hemispherical pressure distribution is created in both bodies near the area of contact:

$$\left(\frac{p_0}{a}\right)\left(\frac{2}{3}\pi a^3\right) = P \tag{3.1}$$

where p_0 is the peak pressure and a is the radius of the contact area. Solving for the peak pressure, we find that it is equal to 1.5 times the uniform pressure:

$$p_0 = \frac{3}{2}\frac{P}{\pi a^2} = \frac{3}{2}p_{uniform} \tag{3.2}$$

In the case where one of the bodies is planar and the material constants are identical, the contact pressure distribution is

$$p(r) = p_0\sqrt{1-\left(\frac{r}{a}\right)^2} = \frac{3P}{2\pi a^2}\sqrt{1-\left(\frac{r}{a}\right)^2} \tag{3.3}$$

The contact radius is given by

$$a = \sqrt[3]{\frac{3\left(1-\nu^2\right)}{2E}PR_1} \tag{3.4}$$

where E is Young's modulus, ν is Poisson's ratio, and R_1 is the radius of the spherical surface. The contact pressure distribution from the finite element solution will be compared to the analytical expression for contact pressure.

The stiffness of the system can be determined by considering the mutual approach of two points far from the contact region as a function of applied load. This distance is given by

$$\alpha = \sqrt[3]{\frac{9(1-\nu^2)^2}{4E^2}\frac{P^2}{R_1}} \tag{3.5}$$

The load-displacement curve of the finite element model will be compared to this expression.

The vertical displacement of the planar surface as a function of radial distance r from the original contact point is given by

$$u_z = \begin{cases} \left(\frac{1-\nu^2}{E}\right)\left(\frac{\pi p_0}{4a}\right)(2a^2 - r^2) & r \leq a \\ \left(\frac{1-\nu^2}{E}\right)\left(\frac{p_0}{2a}\right)\left[(2a^2 - r^2)\,sin^{-1}\left(\frac{a}{r}\right) + a\sqrt{r^2 - a^2}\right] & r > a \end{cases} \tag{3.6}$$

The stresses along the axis of symmetry in the planar solid through the original contact point will also be compared to the finite element results. The analytical expressions are

$$\sigma_{rr} = \sigma_{\theta\theta} = -p_0(1+\nu)\left[1 - \left(\frac{z}{a}\right)tan^{-1}\left(\frac{a}{z}\right)\right] + \frac{p_0}{2}\left(1 + \frac{z^2}{a^2}\right)^{-1} \tag{3.7}$$

$$\sigma_{zz} = -p_0\left(1 + \frac{z^2}{a^2}\right)^{-1} \tag{3.8}$$

Since these are principal stresses, the maximum shear stress is given by

$$\tau_{max} = \frac{1}{2}\left|\sigma_{zz} - \sigma_{rr}\right| \tag{3.9}$$

These analytical expressions, along with interelement pressure band continuity, will serve as criteria for finite element mesh optimization and verification of results.

3.5 Previous Finite Element Models

Sauren *et al.* (1984[53]) were the first investigators to use the finite element method to study meniscal mechanics. The axisymmetric model employed isotropic meniscal material properties, and no articular cartilage. The authors used the model to perform a parametric analysis of bone and meniscal material properties. Sauren's mesh is shown in Figure 3-1. The mesh is composed of triangular elements, and the meniscus and femur are fully conforming. Brown (1990[12]) developed a model using Sauren's geometry for comparison purposes and found that the sharp corner at the inner edge of the meniscus caused stress concentrations which are non-physiological, since the normal meniscus has a tapered inner edge.

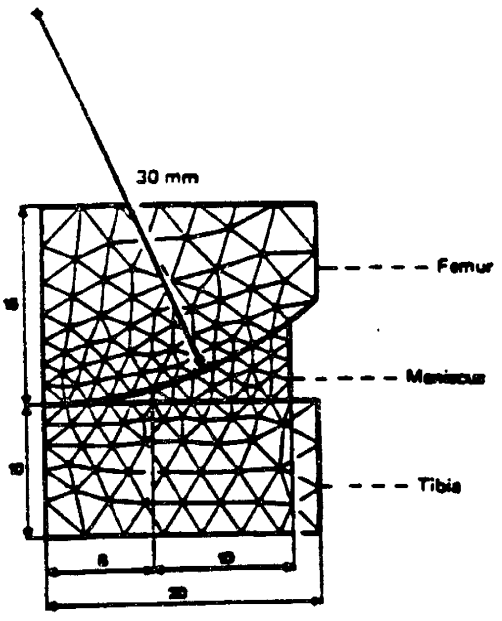

Figure 3-1: Finite element mesh used by Sauren *et al.* [53]

Sauren *et al.* concluded that the meniscus transmits a significant portion of the total joint load, with the inner half of the meniscus accounting for most of the meniscal load transmission; the meniscus serves to considerably reduce tibiofemoral contact stresses; and the axial joint stiffness and radial meniscal displacement are non-linear functions of applied axial load. The conclusion of the parametric study was that the combination of meniscal and bone material properties are more of a factor in meniscal load bearing than the meniscal dimensions. The authors caution against the extrapolation of numerical results to reality due to the highly simplified geometry and material properties used. This warning is reasonable since the model contained no articular cartilage, producing unrealistic bone on bone contact.

Hefzy *et al.* (1987[28]) developed an axisymmetric model of the meniscus using the same geometry as Sauren. The model included direct bone-on-bone contact, as well as isotropic meniscal material properties. The mesh was generated using triangular elements which were highly distorted near the contact surface, which is clearly an area of high stress. Figure 3-2 shows the finite element mesh used by Hefzy *et al.* In addition, the point load applied to the top of the femoral section does not accurately

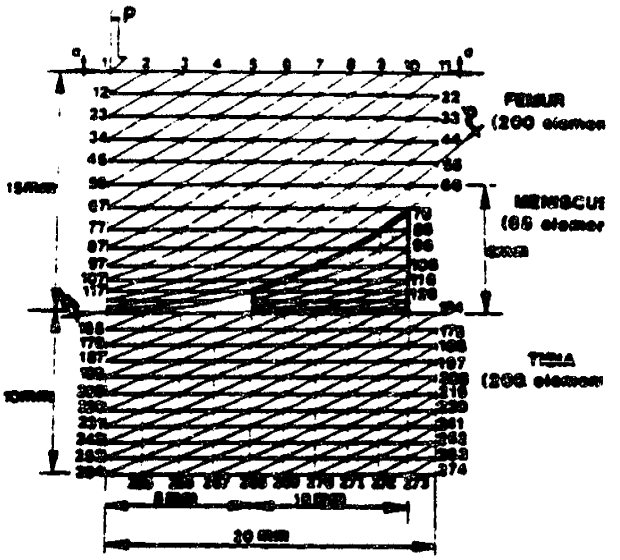

Figure 3-2: Finite element mesh used by Hefzy *et al.* The mesh contains highly distorted elements in the tibiofemoral and meniscotibial contact regions [28].

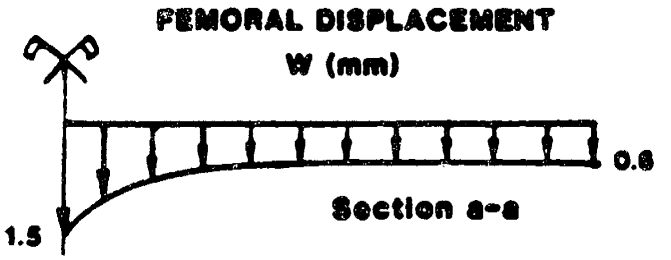

Figure 3-3: Results of Hefzy's finite element model for displacement of the top femoral surface [28].

represent physiological loading conditions. (The results for the displacement of the top femoral surface are precisely what one would expect from the application of a point load along the axis of symmetry, see Figure 3-3). It is doubtful that the application of the load in this manner caused contact conditions that are physiologically meaningful, casting doubt on the reported results.

Aspden (1985[8]) developed an axisymmetric finite element model of the meniscus to investigate the response of the meniscus to a compressive load. The meniscus is modeled as a wedge-shaped toroid resting on a compliant base, which represents

the articular cartilage of the tibial plateau (see Figure 3-4). Aspden presents only qualitative results due to the absence of experimental values for meniscal material properties. The meniscus was modeled as anisotropic, so the three elastic parameters (Young's modulus, shear modulus, and Poisson's ratio) were varied independently. The results predict development of positive circumferential strain throughout the entire meniscal cross-section. In addition, the author qualitatively correlates regions of radial and shear strain with common types of meniscal tears.

Spilker *et al.* (1990[61]) developed an axisymmetric finite element model of the meniscus using a biphasic model for soft hydrated tissue. The authors compared results from biphasic and isotropic material models. The meniscal geometry is triangular in cross section, and the proximal surface of the meniscus is subjected to a time-dependent parabolic displacement (See Figure 3-5) No physiological basis is given for the particular prescribed displacement that was used. The isotropic model predicts positive circumferential stresses at the peripheral edge, which become negative as the radius decreases. This result casts doubt on the prescribed displacements and geometry used since it conflicts with all current experimental and modeling results. Spilker's anisotropic model predicts positive hoop stresses throughout the meniscus, but these results remain suspect as well due to the unrealistic displacement conditions and geometry.

Tissakht *et al.* (1989[67], 1990[66]) performed a three-dimensional finite element study of the meniscus in order to examine the effect of the transverse and medial collateral ligaments on meniscal response, as well as the effect of axial rotation combined with compressive load. The meniscus is modeled as a linear transversely isotropic material covered by an isotropic membrane (see Figure 3-6). A compressive load was distributed over the menisci and tibial plateau based on experimental measurements from Ahmed and Burke (1983[1]). These pressure results were obtained with a .285 mm thick micro-indentation transducer placed within the knee joint space. Given the invasiveness of the technique used to obtain the pressure results, the loading conditions used for the finite element model are somewhat suspect. In addition to the compressive load, the tibia was subject to 20 degrees of external axial rotation. The

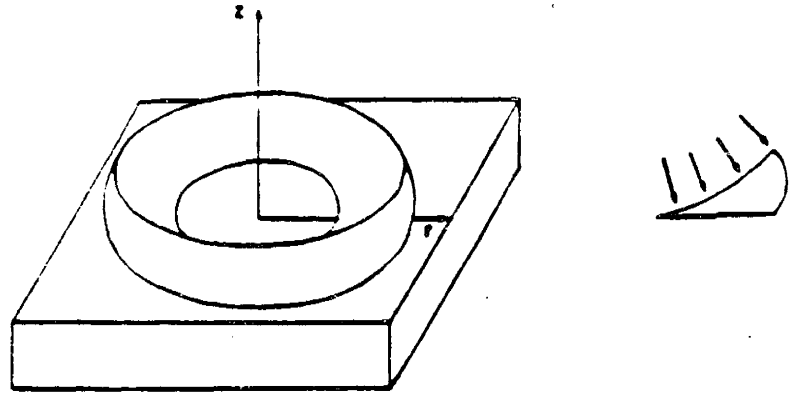

(a)

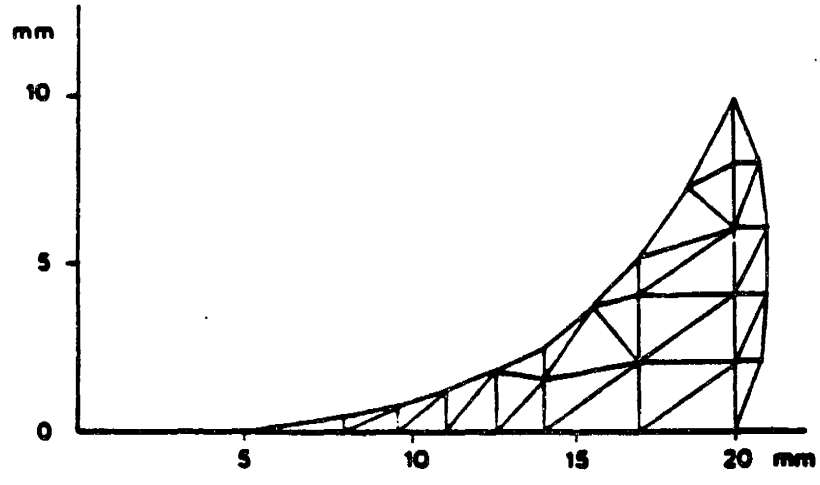

(b)

Figure 3-4: Aspden's finite element model. (a) The axisymmetric meniscus resting on a compliant base. (b) Cross-section of the meniscus showing the finite element mesh [8].

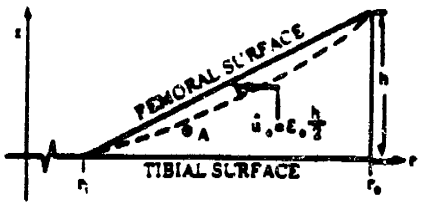

Figure 3-5: Cross-section of Spilker's axisymmetric meniscus model showing prescribed parabolic displacement [61].

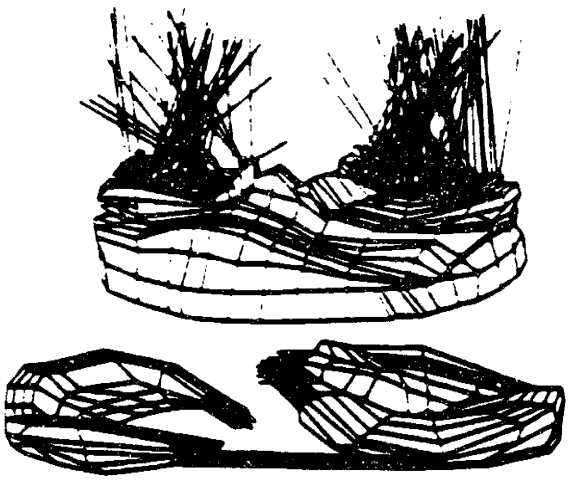

(a)

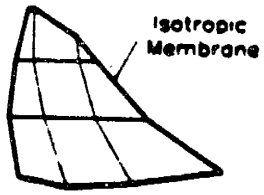

(b)

Figure 3-6: Three-dimensional knee model developed by Tissakht *et al.* [67, 66] (a) Finite element mesh. (b) Cross-section of meniscal mesh showing isotropic membrane.

model predicts a significant increase in tensile meniscal stresses when axial rotation is applied with compressive load. The study also predicts that the medial collateral ligament has a considerable effect on motion of the medial meniscus.

A striking similarity among all of the finite element studies described above is the lack of any discussion of error analysis. Most of the meshes seem quite coarse, and no mention is made of efforts to establish mesh refinement criteria. Errors can be estimated in several ways, for example using convergence analysis or interelement stress continuity. It is not clear from the reported results of these studies that either of these methods would reveal that a sufficiently refined mesh was used. The finite element method will always yield a solution, given that the model converges numerically. This solution, however, is only as valid as the assumptions that went into the mesh development. There is always some amount of error in a finite element solution; without some estimate of this error, the results are uninterpretable. Confidence in the mesh characteristics must be established in order to have confidence in the results.

3.6 Anisotropic Axisymmetric Meniscus Model

Brown (1990[12]) has developed a two-dimensional axisymmetric finite element model of the meniscus which uses anisotropic material properties. The meniscus was modeled as a wedge-shaped toroid, confroming with the femur along the outer circumference and tapering to a thin inner edge. The model included articular cartilage on the femoral and tibial surfaces, which produced an order of magnitude reduction in peak contact stresses when compared to the model without articular cartilage. The model also predicted that radial meniscal displacement is an order of magnitude lower when anisotropic meniscal material properties are employed. Brown used x-ray stereophotogrammetry to measure meniscal circumferential strains and found some correlation between the experimental results and model predictions. Brown also used analytical solutions and interelement stress continuity to establish sufficient mesh refinement. Brown's model predicted that the intact meniscus transmits from 70% to 100% of the total joint load. Brown's axisymmetric mesh is shown in Figure 3-7.

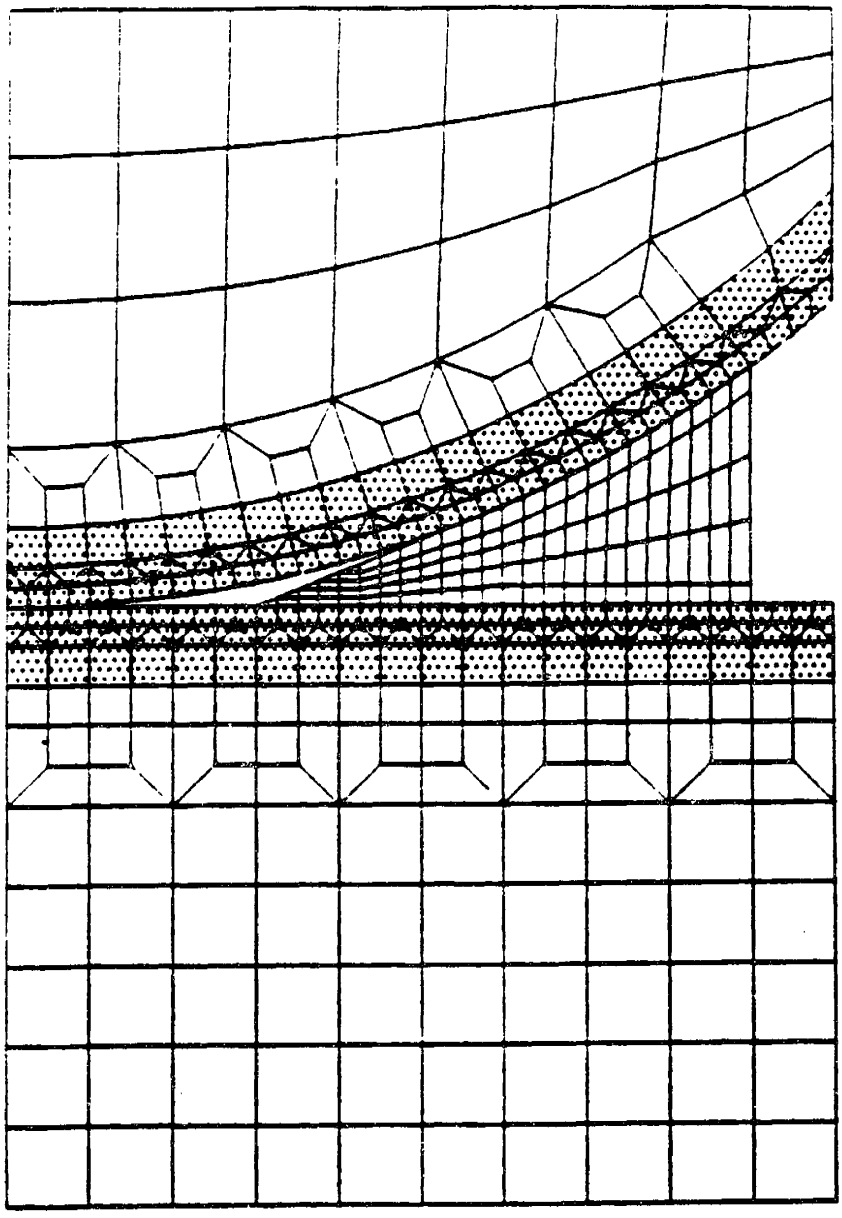

Figure 3-7: Brown's axisymmetric finite element model of the meniscus, including articular cartilage and anisotropic meniscal material properties [12].

The three-dimensional model developed in this project uses the same geometry, material properties and loading conditions as Brown's model. This will allow quantitative comparison between axisymmetric and non-axisymmetric model predictions. The numerical results from the three-dimensional model will be compared to Brown's results to determine if the two-dimensional axisymmetric model is sufficient for describing meniscal behavior under simple loading conditions.

Chapter 4

Preliminary Model Development

4.1 Overview of Model Development

Research objectives and constraints surrounding the model have been established, and a method of verifying finite element results has been identified. The next step in the process, then, is the actual finite element model development. This development will occur in step-by-step fashion, beginning with simple meshes and culminating in a three-dimensional model of knee joint contact with non-axisymmetric meniscal geometry. The specific steps to be taken are as follows:

1. Develop a simple, two-dimensional model of Hertzian contact which adequately reproduces the analytical contact pressure distribution with a minimum number of elements.

2. Use the results of the two-dimensional models to establish criteria for the development of a three-dimensional model of Hertzian contact.

3. Use these criteria to develop a manageable three-dimensional model of Hertzian contact which will later be appropriate for modeling the knee joint contact problem including the meniscus.

4. Perform an in-depth comparison of Hertzian contact analytical expressions to finite element results of the initial three-dimensional mesh; refine the mesh until

satisfactory results are obtained.

5. Add axisymmetric meniscal geometry and articular cartilage to the model.

6. Proceed with the addition of non-axisymmetric meniscal geometry to the model.

4.2 Computational Environment

All analyses in this project were performed using the ADINA (Automatic Dynamic Incremental Nonlinear Analysis) finite element program, version 6.0, ADINA R & D, Inc., Watertown, MA. ADINA-IN and ADINA-PLOT were used for pre- and post-processing, respectively. All two-dimensional modeling and preliminary three-dimensional modeling was performed using a Silicon Graphics Personal Iris 4D20 workstation with 32 Megabytes of RAM and approximately 1 Gigabyte of storage. The final three-dimensional modeling was performed on a CRAY Y-MP at the MIT Supercomputing Facility.

4.3 Two-Dimensional Modeling

Several two-dimensional axisymmetric meshes of the Hertzian contact problem were developed in order to gain quick insight into how much mesh refinement will be necessary in three dimensions. Once a satisfactory axisymmetric mesh is obtained, the result can be expanded into three dimensions.

The radius of curvature of the elastic sphere was chosen to be 30 *mm*, and contact was considered frictionless. Each body had a modulus of elasticity of 1000 *MPa*, and Poisson's ratio of 0.3. The geometry and material properties were chosen to be consistent with previous finite element models for comparison purposes [12]. A concentrated downward load was applied to the top node along the axis of symmetry, and all nodes along the top surface were constrained to undergo the same vertical displacement as the loaded node. This constraint is in keeping with the fact that the analytical solution for Hertzian contact assumes the bodies are semi-infinite; therefore

points far from the contact region should have the same vertical displacements. The models were loaded to levels of 50, 100, 200, and 1000 N, and each load step was divided by 2π to account for modeling only a one radian wedge of the structure. The bottom node along the axis of symmetry was fixed in space, and the remainder of the bottom row of nodes had only the y (horizontal) degree of freedom free to allow radial expansion. A highly compliant truss connected the sphere to ground in order to prevent rigid body motion in the unloaded configuration.

4.3.1 Two-Dimensional Meshes

Several two-dimensional meshes were analyzed. The first was a simple, relatively coarse mesh of 4-node linear elements shown in Figure 4-1. The second mesh contained the same number of elements as the first, but utilized 9-node parabolic elements; see Figure 4-2. Model 3 contained the same number of 9-node elements as model two, but with a finer mesh near the contact area and a coarser mesh in low stress areas. This mesh is shown in Figure 4-3.

As modeling progressed and meshes became finer, it became more efficient to model only the region immediately around the contact area. Based on analytical predictions of contact radius, all subsequent meshes modeled only 4 millimeters out from the axis of symmetry, as compared to 15 millimeters modeled in the first three meshes. This scaling down of the modelled region will become particularly important when the model is expanded into three dimensions. Model 4, shown in Figure 4-4 used a fine mesh of 9-node elements with 8 elements along the 4 millimeter radius. Since each element face contains three nodes, each element along the line of contact represents two contact segments (two-dimensional contact segments are defined by only two nodes). Therefore, model 4 contains four contact segments per millimeter of contact radius. Model 5 (Figure 4-5) was half as fine as model four, employing two contact segments per millimeter of contact radius.

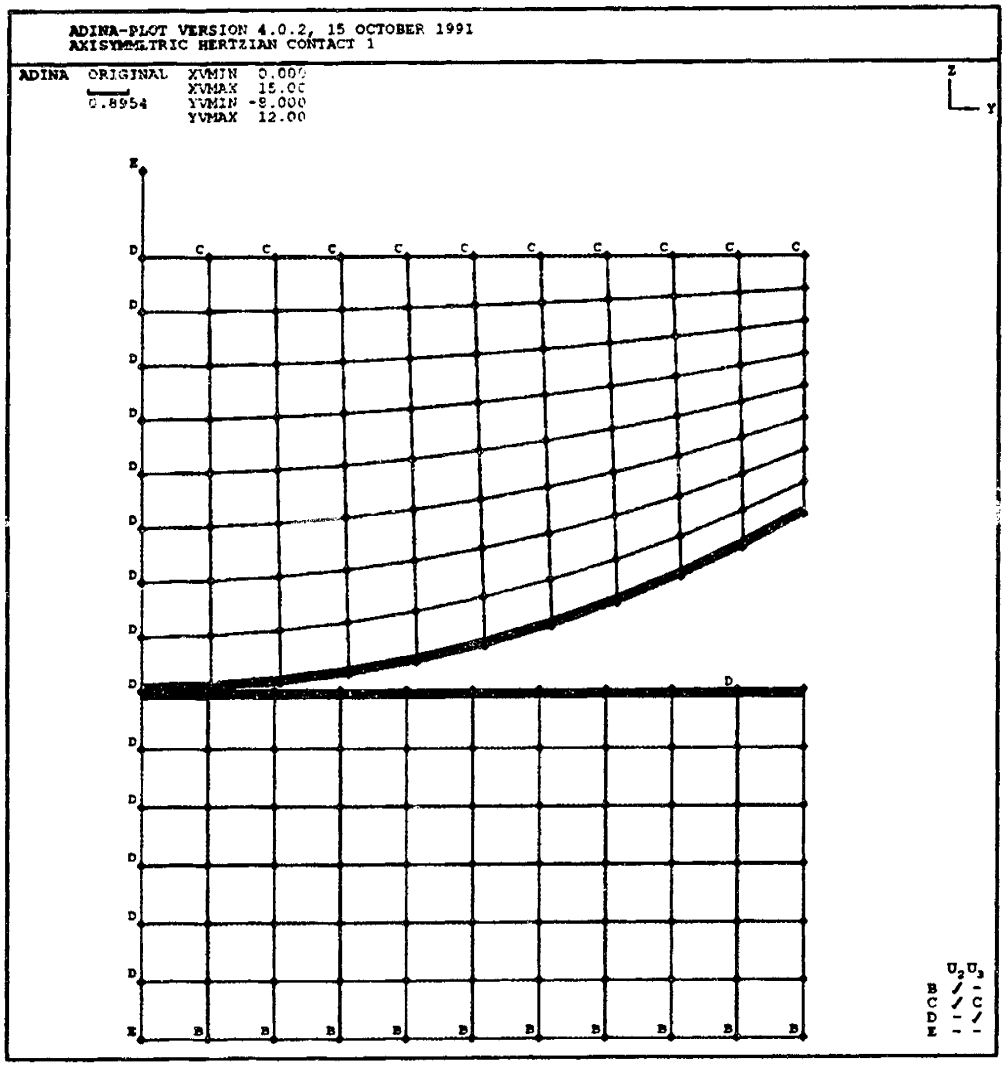

Figure 4-1: Original mesh for axisymmetric model 1, using four-node linear elements.

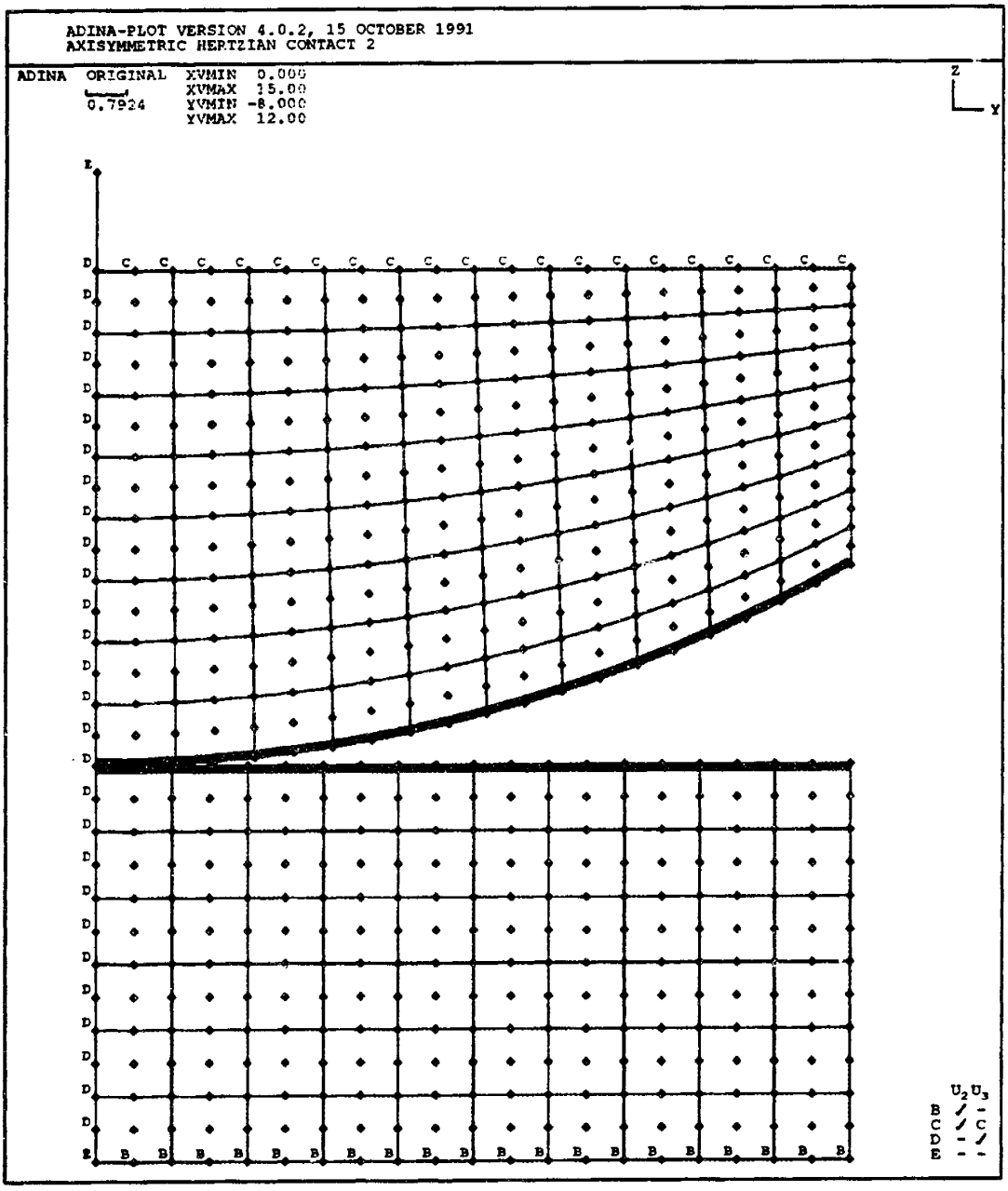

Figure 4-2: Original mesh for axisymmetric model 2, using nine-node parabolic elements.

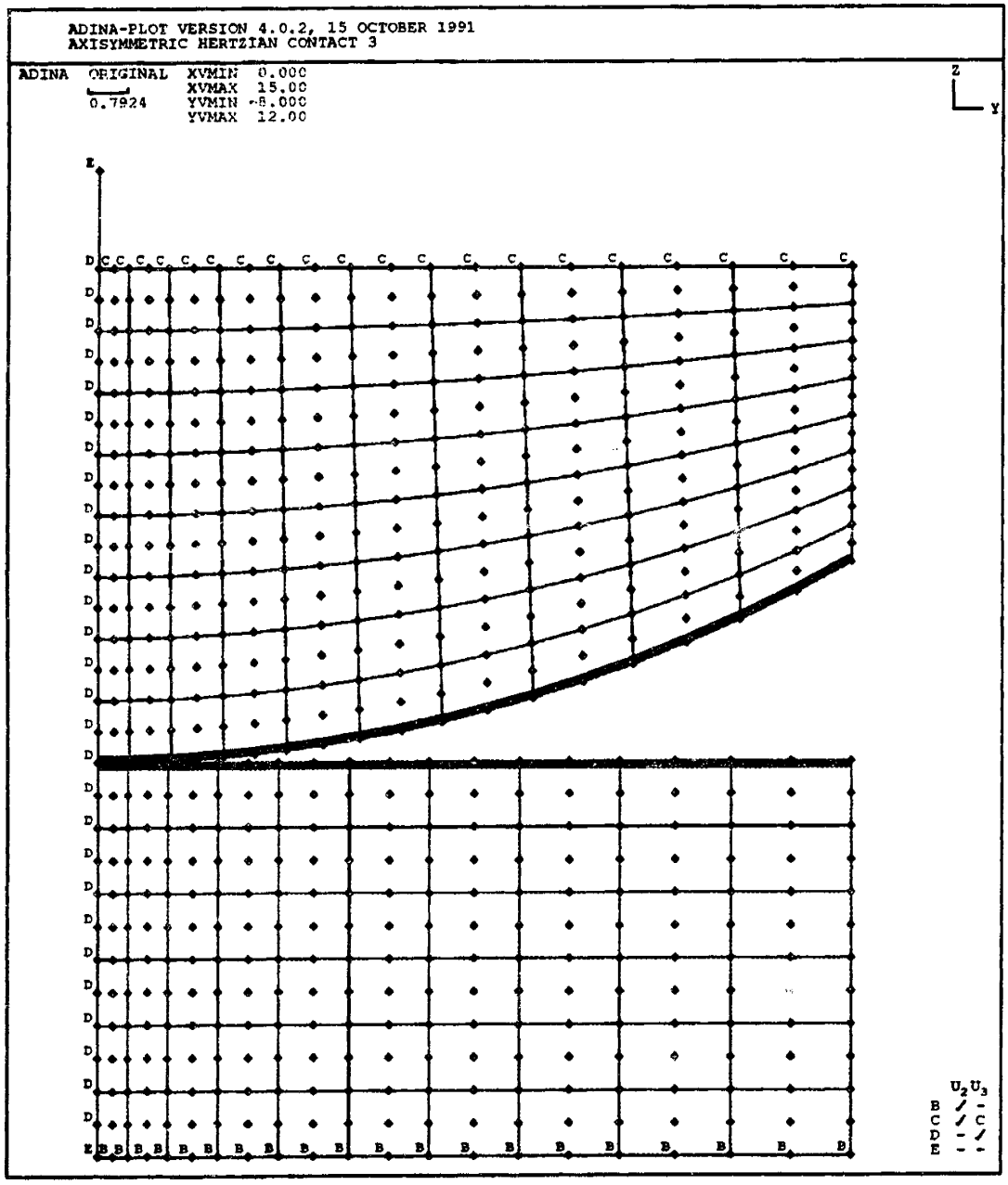

Figure 4-3: Original mesh for axisymmetric model 3; uses nine-node elements with more refined mesh near the contact region.

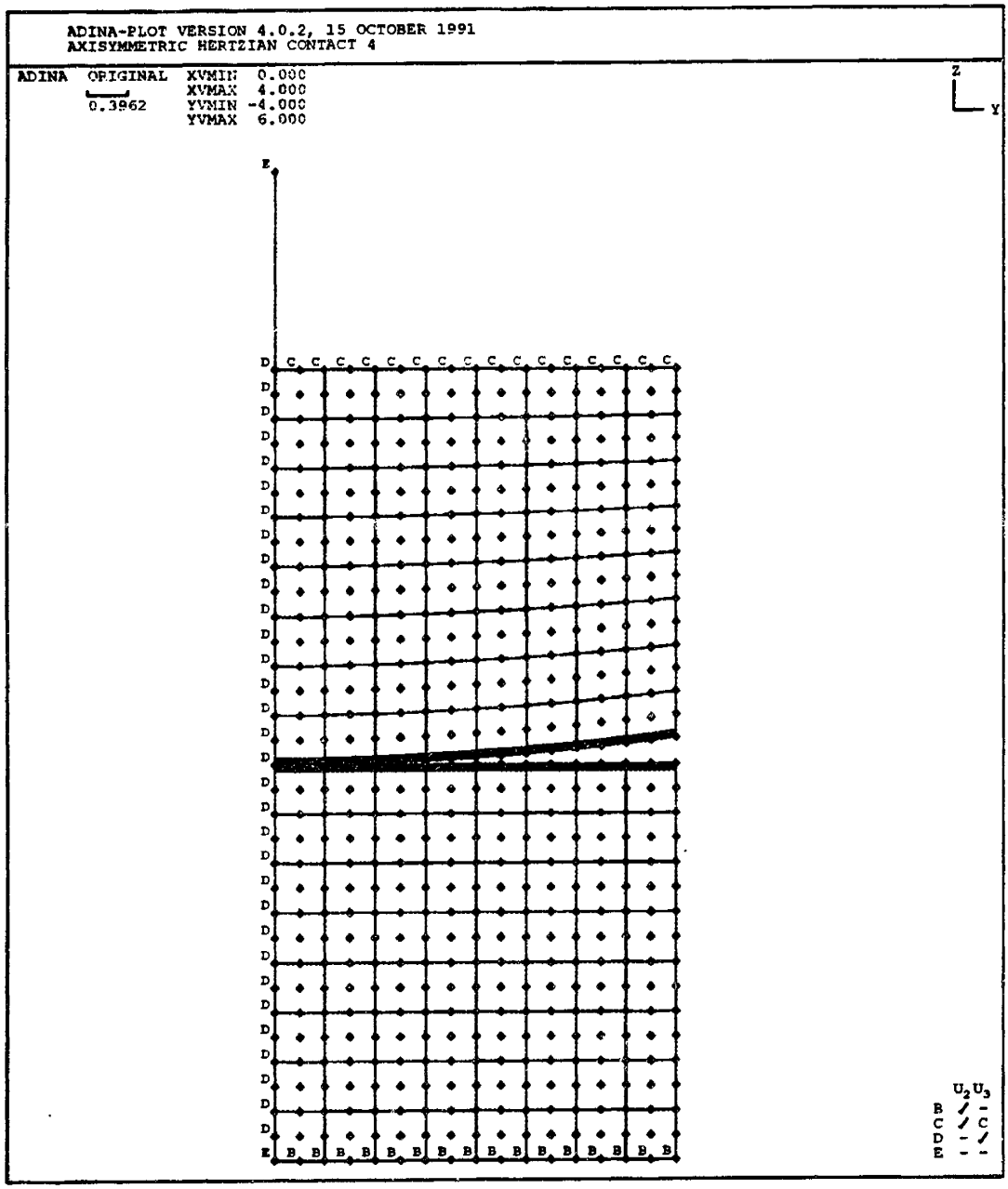

Figure 4-4: Original mesh for axisymmetric model 4; includes four contact segments per millimeter measured radially outward from the contact point.

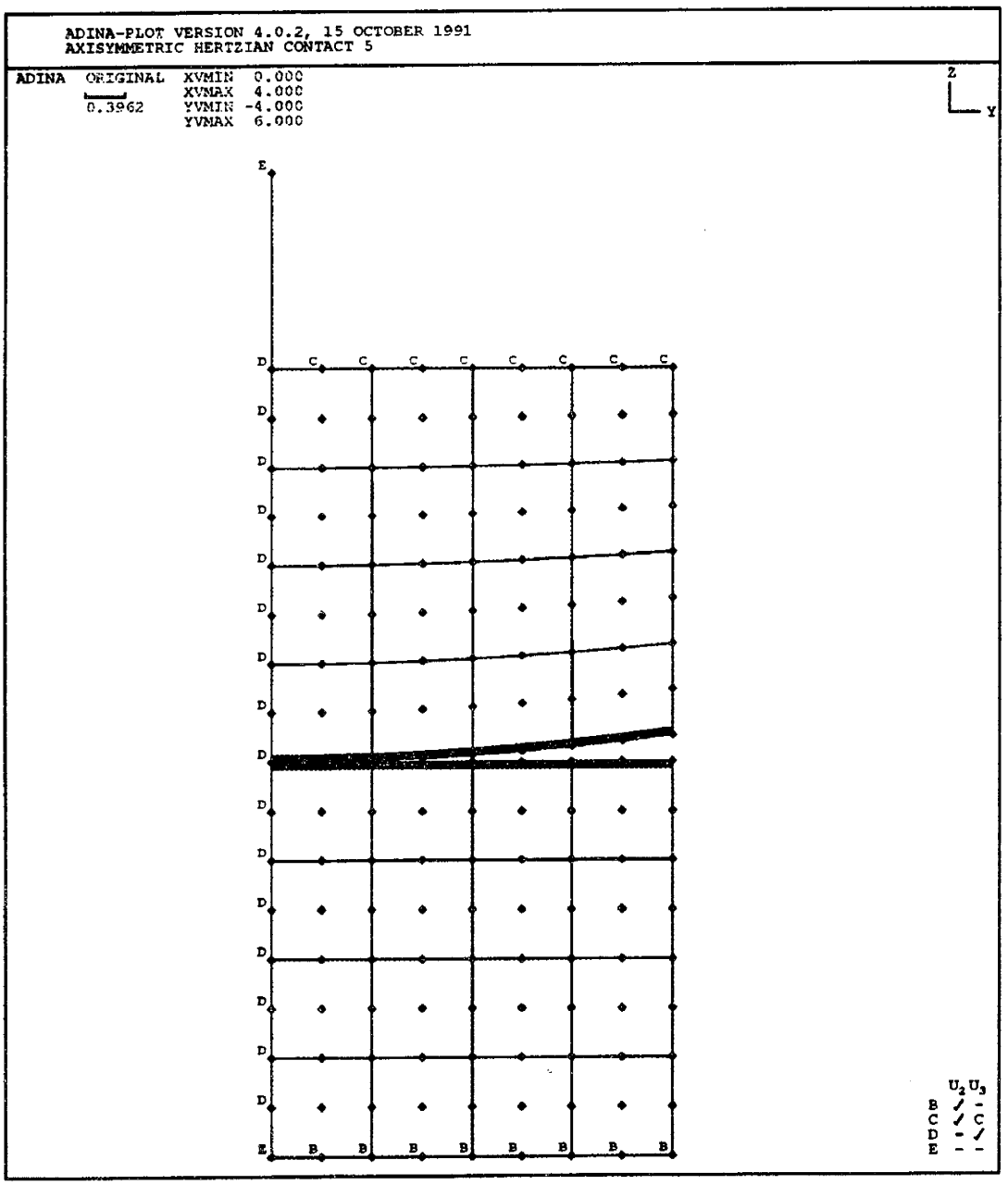

Figure 4-5: Original mesh for axisymmetric model 5; includes two contact segments per millimeter measured radially outward from the contact point.

4.3.2 Discussion of Two-Dimensional Results

Both pressure band plots and contact pressure distributions were used to evaluate the two-dimensional models. In order to evaluate stress continuity between elements, the hydrostatic pressure is used:

$$p = \frac{-(\sigma_{xx} + \sigma_{yy} + \sigma_{zz})}{3} \tag{4.1}$$

This is a scalar quantity and thus does not vary with coordinate transformations (Sussman & Bathe, 1986[62]).

The pressure band plot for Model 1 in Figure 4-6 shows significant interelement pressure discontinuities, indicating that the mesh does not contain sufficient degrees of freedom near the contact area to accurately represent the state of stress. It is also clear from the graph of contact pressure that the contact surface did not contain enough result points to reproduce the correct contact pressure distribution.

The pressure band plot for Model 2 shows considerable improvement over Model 1. The stress bands near the contact region are smooth and distinguishable. The contact pressure distribution, however, is not reproduced very accurately (see Figure 4-7).

Model 3 shows a very similar pressure band pattern to Model 2; see Figure 4-8. In addition, Model 3 shows a significant improvement over all previous meshes in representing the expected contact pressure distribution, particularly at the highest loading level.

Mesh 4 shows the best interelement pressure continuity of all of the two dimensional models (Figure 4-9). It also can best represent the analytical contact pressure distribution at all loading levels.

The pressure band plot for Model 5 lacks some of the smoothness of Model 4, but the bands are nevertheless distinguishable (Figure 4-10). Model 5 does an adequate job of reproducing the proper contact stress distribution.

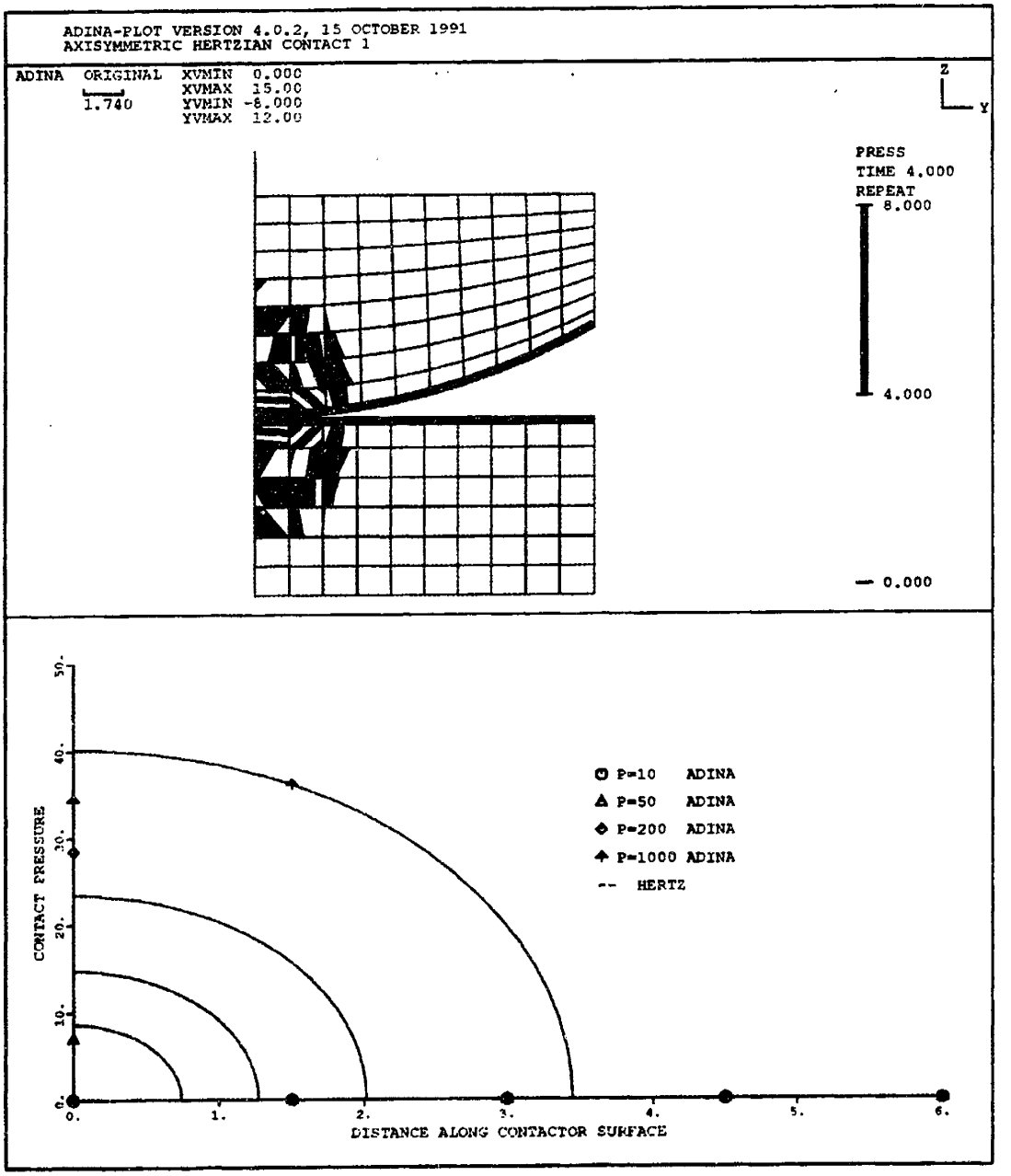

Figure 4-6: Pressure band plot and contact pressure distribution, axisymmetric model 1. The pressure bands are indistinguishable and the contact pressure distribution is not well-reproduced.

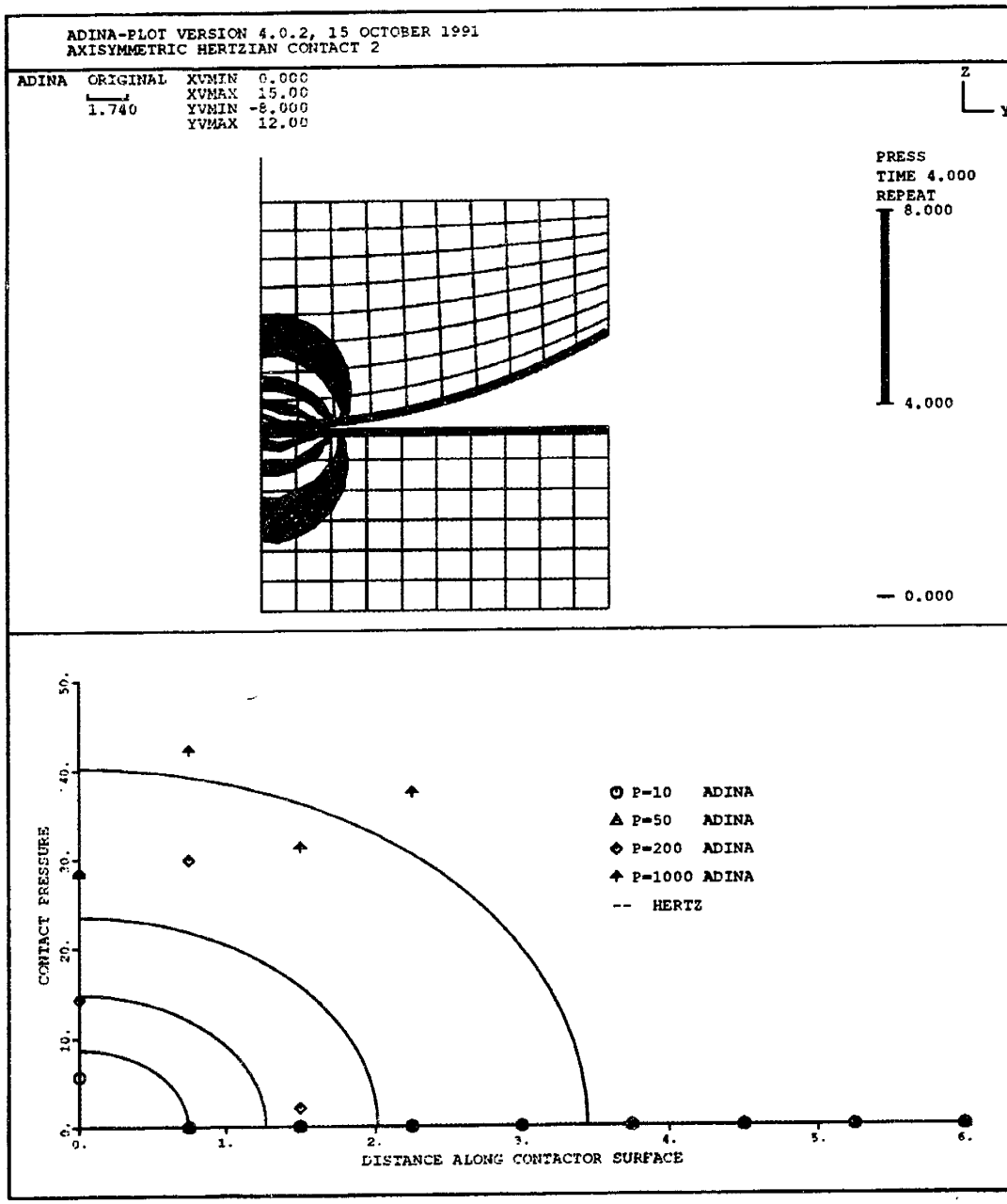

Figure 4-7: Pressure band plot and contact pressure distribution for axisymmetric model 2. The pressure bands are smooth and distinguishable, but the contact pressure distribution is not represented properly.

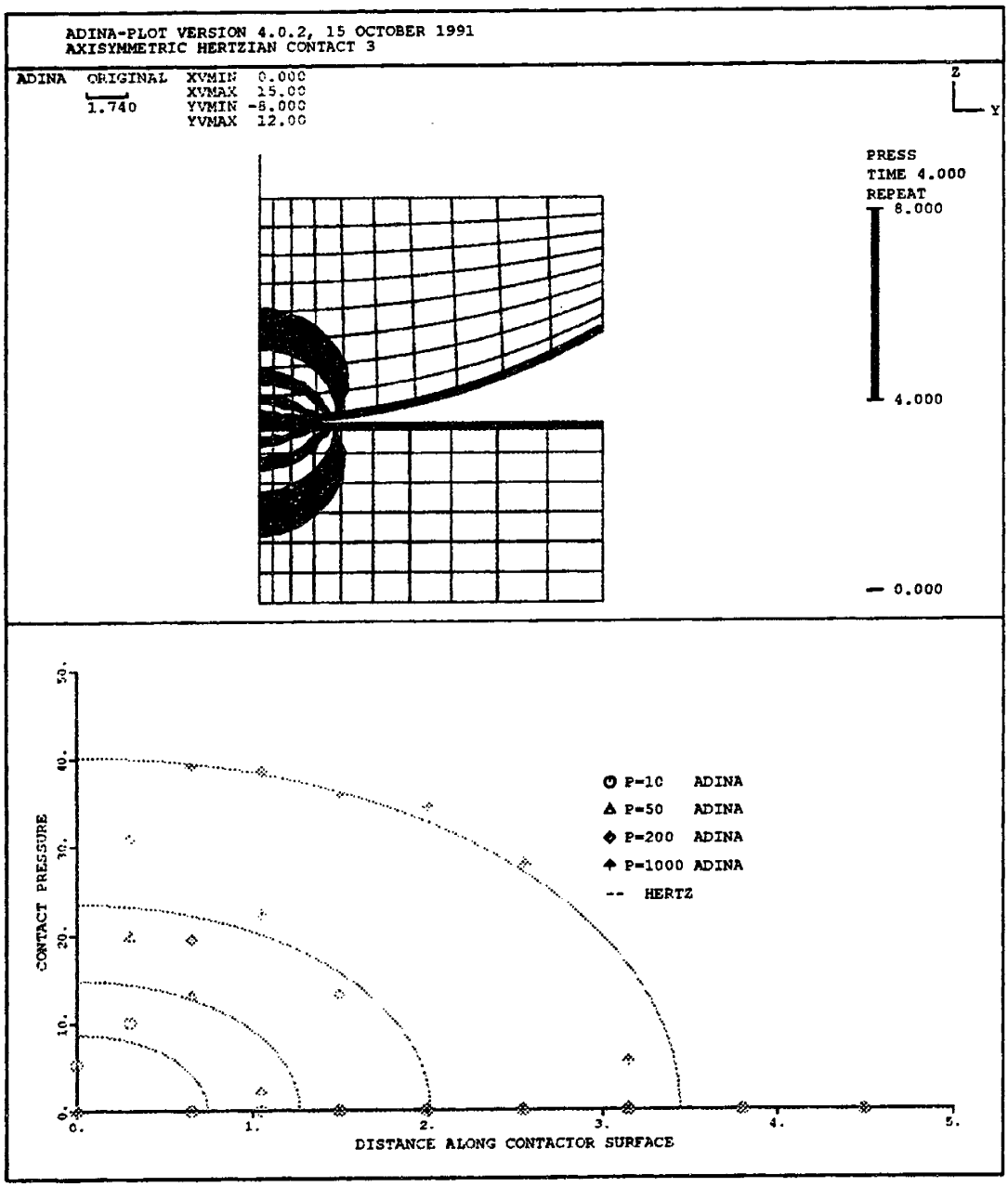

Figure 4-8: Pressure band plot and contact pressure distribution for axisymmetric model 3. Smooth pressure bands, improved contact pressure distribution.

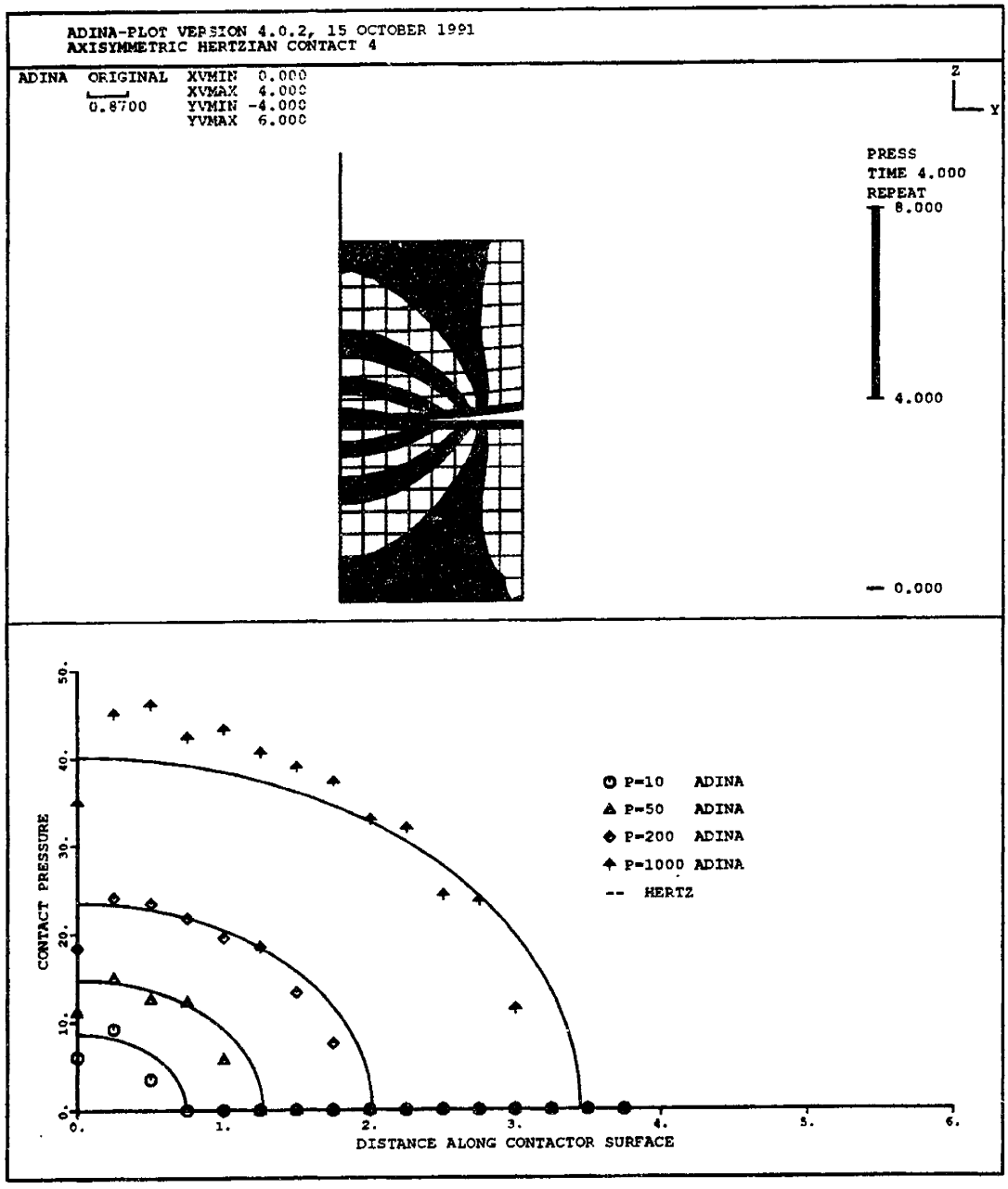

Figure 4-9: Pressure band plot and contact pressure distribution for axisymmetric model 4. High interelement pressure band continuity, good contact pressure distribution.

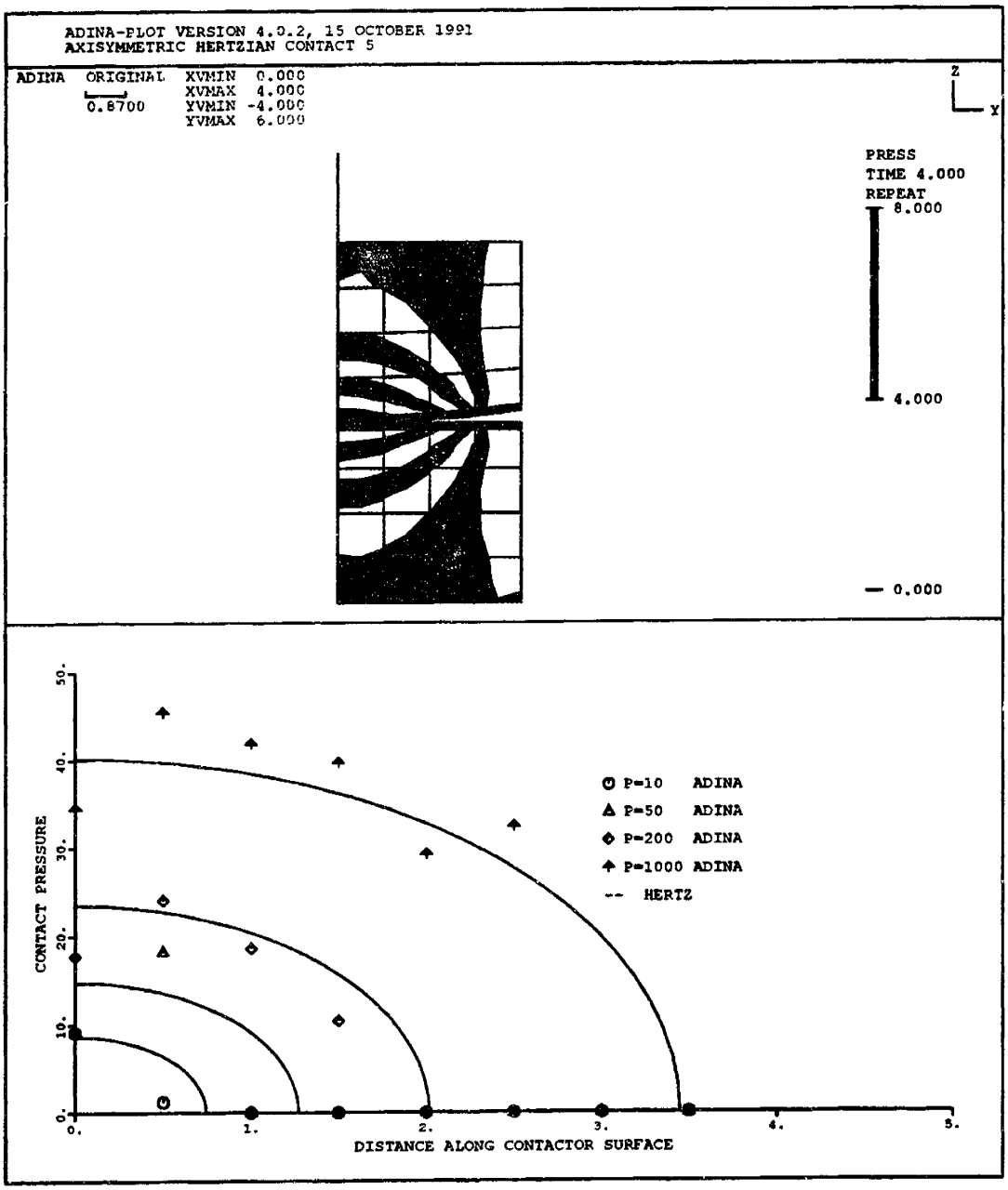

Figure 4-10: Pressure band plot and contact pressure distribution for axisymmetric model 5. Pressure bands are distinguishable and contact pressure distribution is reproduced adequately.

4.3.3 Conclusions of Two-Dimensional Analysis

The purpose of the two-dimensional analysis was to establish roughly the requirements for a three-dimensional model of Hertzian contact, given the constraints discussed earlier. The following conclusions were drawn based on the two-dimensional analysis:

1. Elements which employ parabolic displacement interpolation functions are more effective than linear elements in producing continuous pressure bands.

2. The contact area should contain a minimum of approximately 2 contact segments per millimeter of contact area radius in order to adequately reproduce the proper contact stress distribution.

3. The contact pressure distribution is the more stringent of the two requirements.

4.3.4 Expansion into Three Dimensions

The most obvious way of expanding the Hertzian contact model into three dimensions is to simply rotate the planar geometry about the axis of symmetry through 360 degrees. This approach, however, was not taken for several reasons. First, this method would have resulted in degenerate elements at the point of contact, which is undesirable since this is the area of highest stress. Also, the element faces which comprise the contact surfaces must employ linear interpolation functions, since higher order contact segments are not permitted by the software used. Due to these constraints, the contact region of the sphere was modelled as a block with a spherical bottom surface. In order to achieve the refinement necessary for adequate contact pressure results while retaining a manageable number of nodes, the elements were designed to be significantly longer than they are wide. This seemingly disproportionate scaling, however, is mitigated by using midnodes (i.e. parabolic interpolation functions) on the vertical element faces.

4.4 3-D Hertzian Contact Model

4.4.1 Mesh Design

The criteria for development of a three-dimensional Hertzian contact model have now been established based on the axisymmetric analysis, model size requirements, the assumptions of Hertzian contact, and acceptable finite element practices. They are:

1. Near the contact region, use tall, thin elements which are linear along horizontal faces and parabolic along vertical faces, in order to accurately reproduce the contact pressure distribution with a minimum number of degrees of freedom.

2. Use a minimum of two contact segments per millimeter of contact radius to produce an accurate contact pressure distribution.

3. Model 15 millimeters of material vertically from the original contact point so that edge effects do not interfere with stresses near the contact region (Brown, 1990[12]).

4. Design the portion of the mesh which will eventually come in contact with the meniscus to minimize overlap of nodes between the bone and meniscal surfaces.

Based on these criteria, several three-dimensional meshes were developed and analyzed. The meshes were refined and adjusted until the goal of adequate mesh refinement with minimum computational cost was achieved. Views of the final, undeformed mesh are shown in Figures 4-11 and 4-12. The area of the mesh near the contact region contains tall, thin elements with midnodes on the vertical edges. Just outside this area is a region of transitional elements. The outer portion of the mesh was generated in a cylindrical coordinate system, to conform with the meniscal mesh to be added later. Stabilizing trusses are present to prevent rigid body motions; the trusses are highly compliant and therefore carry a negligible amount of load.

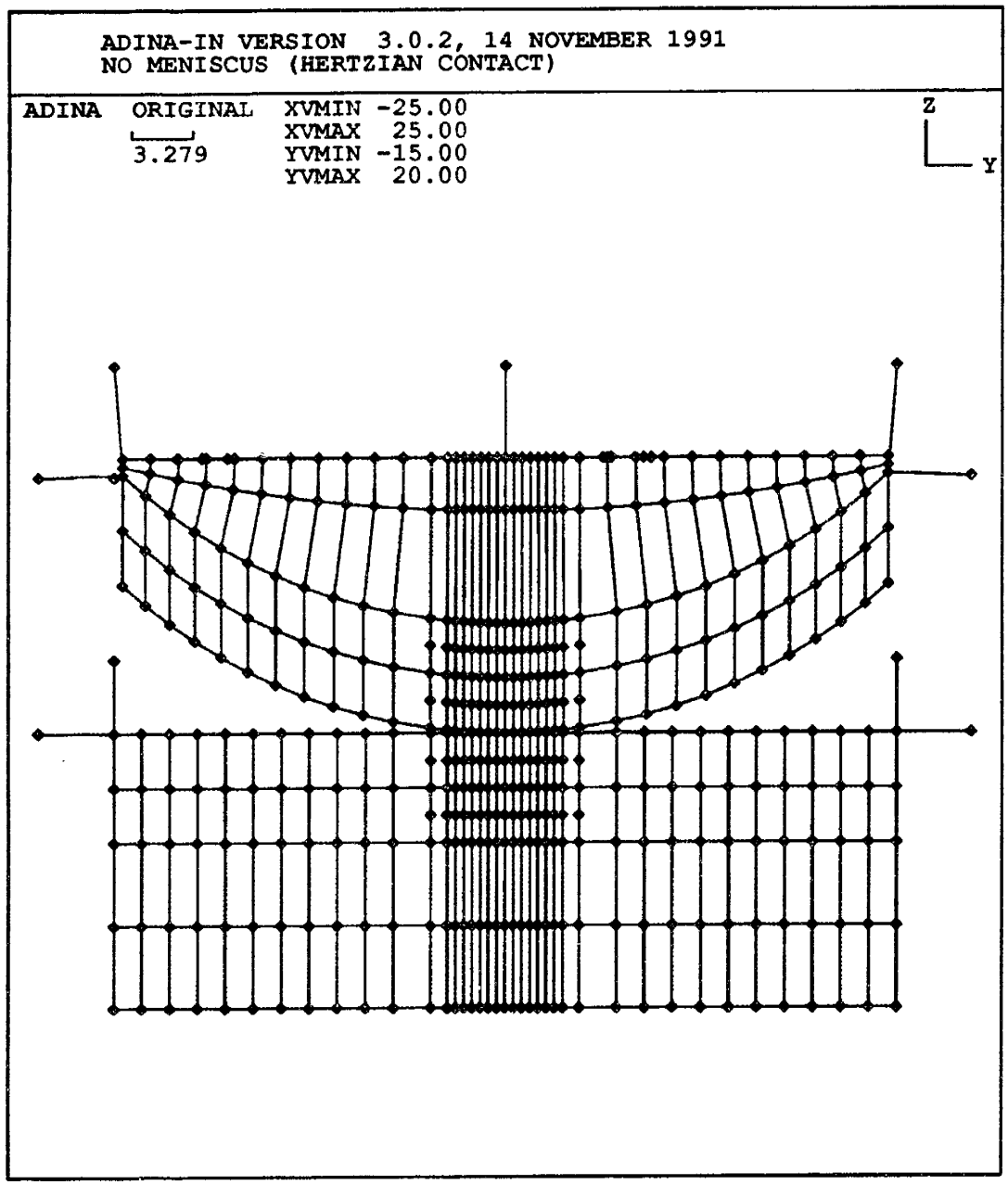

Figure 4-11: Undeformed 3D Hertzian contact model, cut view. Note the stabilizing trusses used to prevent rigid body motion.

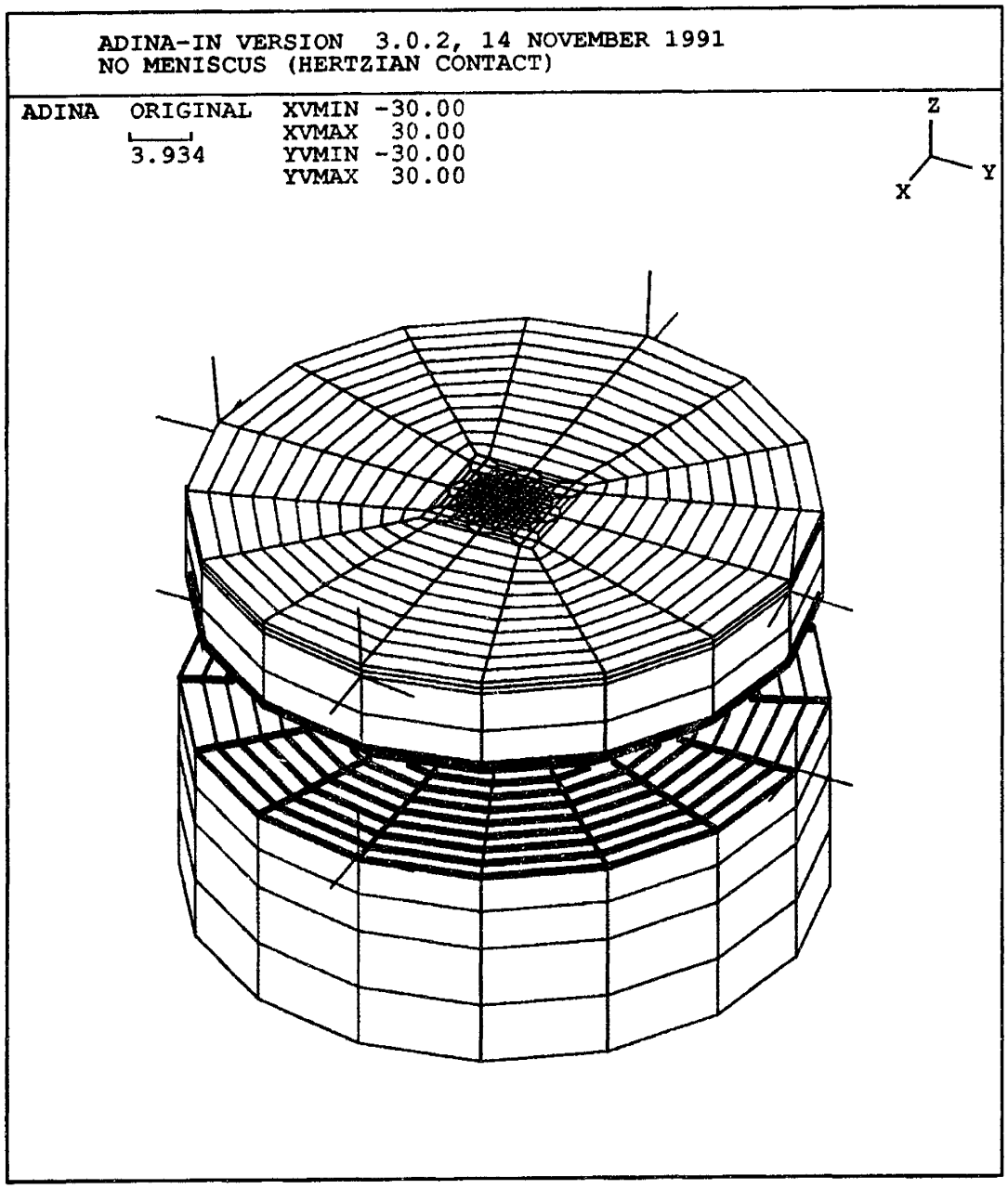

Figure 4-12: Undeformed 3D Hertzian contact model. Note the region of transitional elements.

4.4.2 Results of 3D Hertzian Contact Model

The final 3D Hertzian contact model was verified in depth using the analytical expressions for Hertzian contact discussed in Section 3.4. The quantities used for evaluation are radial and circumferential compressive stress, maximum shear stress, contact pressure, axial compressive stress, overall stiffness, and vertical displacement of the planar surface. Results of the finite element and analytical solutions for these quantities are shown in Figures 4-13–4-15.

All of these quantities show good agreement with analytical results. Small offsets that occur between the finite element and analytical solutions are due inpart to the fact that the analytical solution assumes the contacting bodies are semi-infinite. This is particularly evident near the rigid boundary conditions in the finite element model. The finite element contact pressure distribution agrees well with analytical solution except for a pressure spike in the transition region. This is probably due to the fact that the transition elements are not as uniform as the central contact elements. The distortion of the elements results in an artifact in the FEM contact solution algorithm. When the meniscus is added to the mesh, however, the central contact region will become smaller, and the contact stresses in the transitional zone will become much less important than the contact stresses in the central and meniscal contact regions.

The use of pressure bands to evaluate the mesh is an intuitive process. The first step is to define a fraction of the maximum stress which represents the highest tolerable stress discontinuity. Pressure band plots are then produced using a bandwidth equal to this fraction. If the pressure bands are distinguishable (i.e. can be followed from one element to another), then the mesh is sufficiently refined. It is not necessary that the pressure bands be totally smooth; in that case the mesh is probably overrefined (Sussman & Bathe, 1986[62]). This idea is particularly important in three-dimensional analysis where the number of degrees of freedom is extremely large. Figures 4-16 and 4-17 are pressure band plots of the contact region, showing sufficiently distinguishable pressure bands. The bandwidth chosen is approximately 6% of the maximum stress. Given all of the modeling assumptions made regarding geometry, material properties, and loading conditions, this is clearly a sufficient crite-

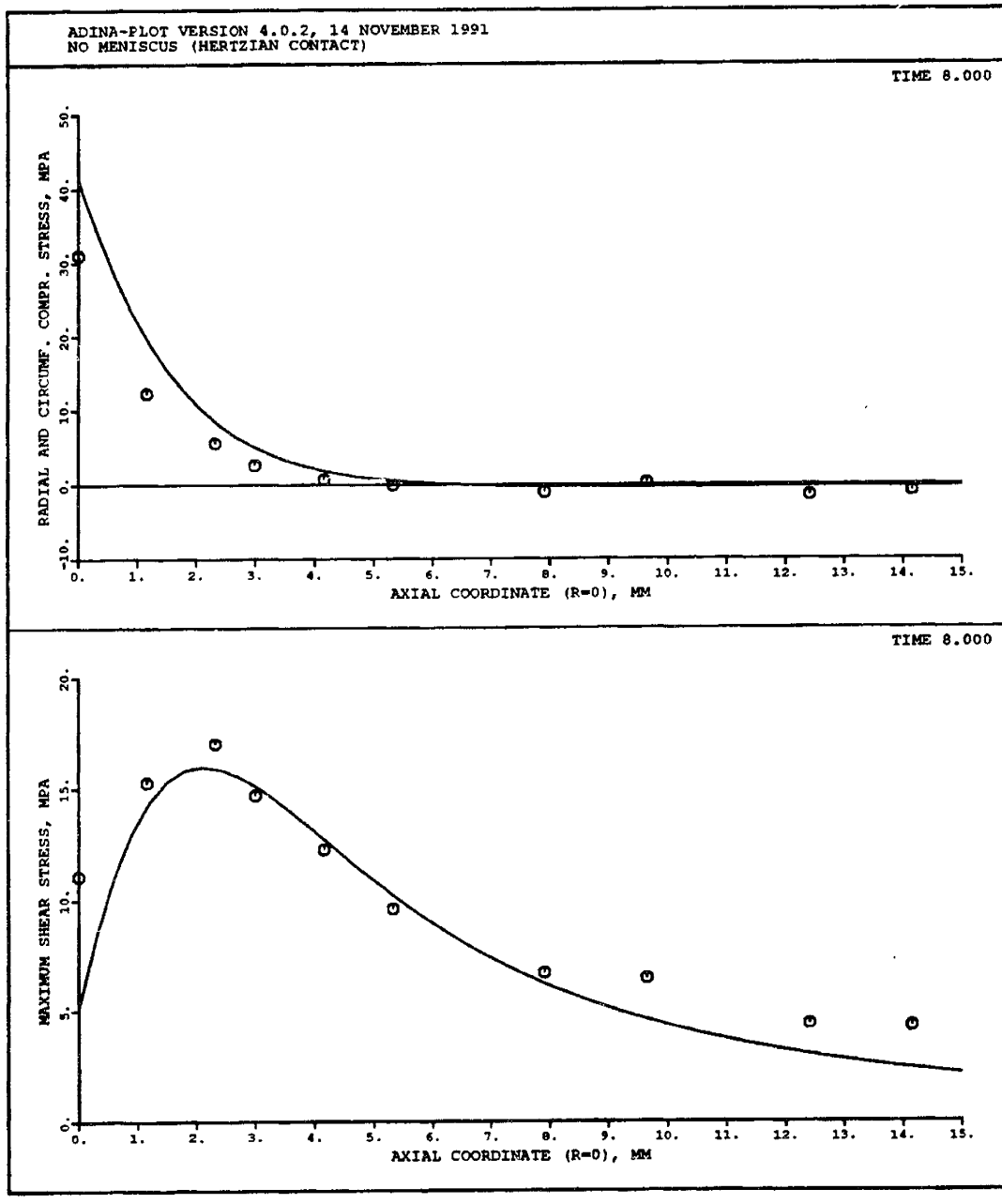

Figure 4-13: Radial and circumferential compressive stress, maximum shear stress vs. axial coordinate

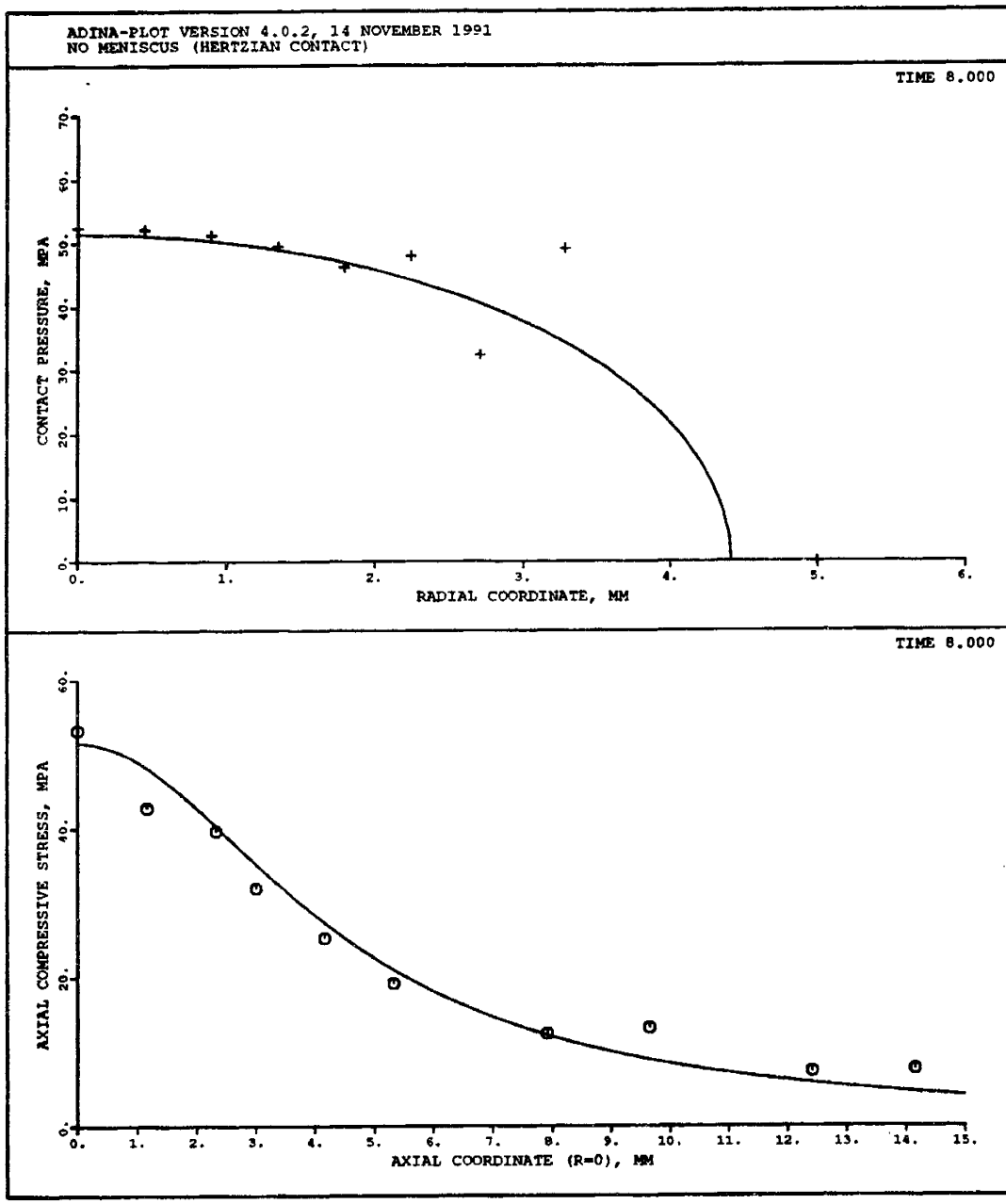

Figure 4-14: Contact pressure distribution vs. radial coordinate, axial compressive stress vs. axial coordinate

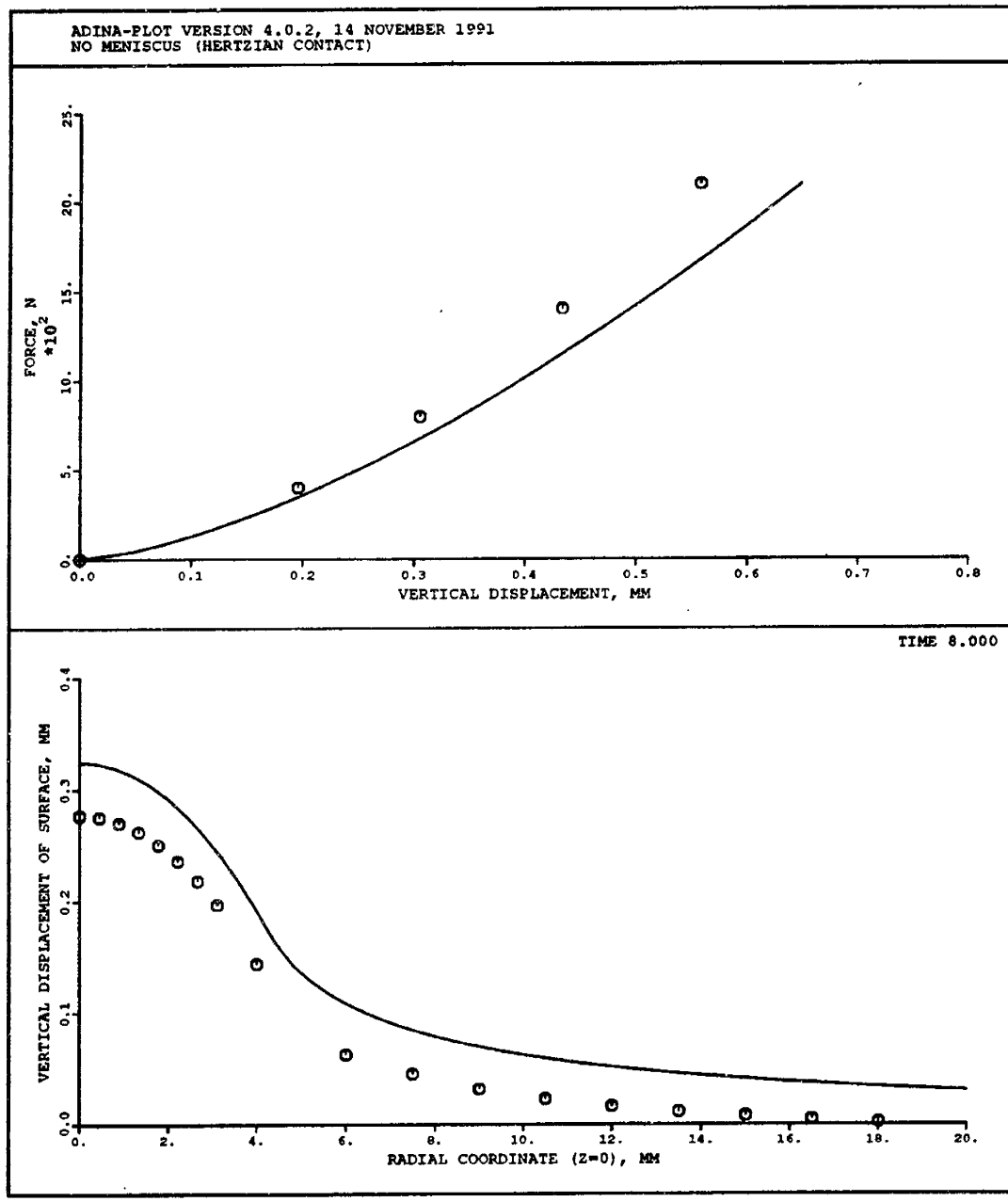

Figure 4-15: Overall model stiffness, vertical displacement of planar surface vs. radial coordinate

rion for examining interelement stress continuity. In addition, the small improvement that could be obtained does not justify the large cost that would be involved in further refining the mesh.

A three-dimensional mesh appropriate for modeling the meniscus has now been established. The next step is to add the meniscus and articular cartilage to the model, which is the subject of the next chapter.

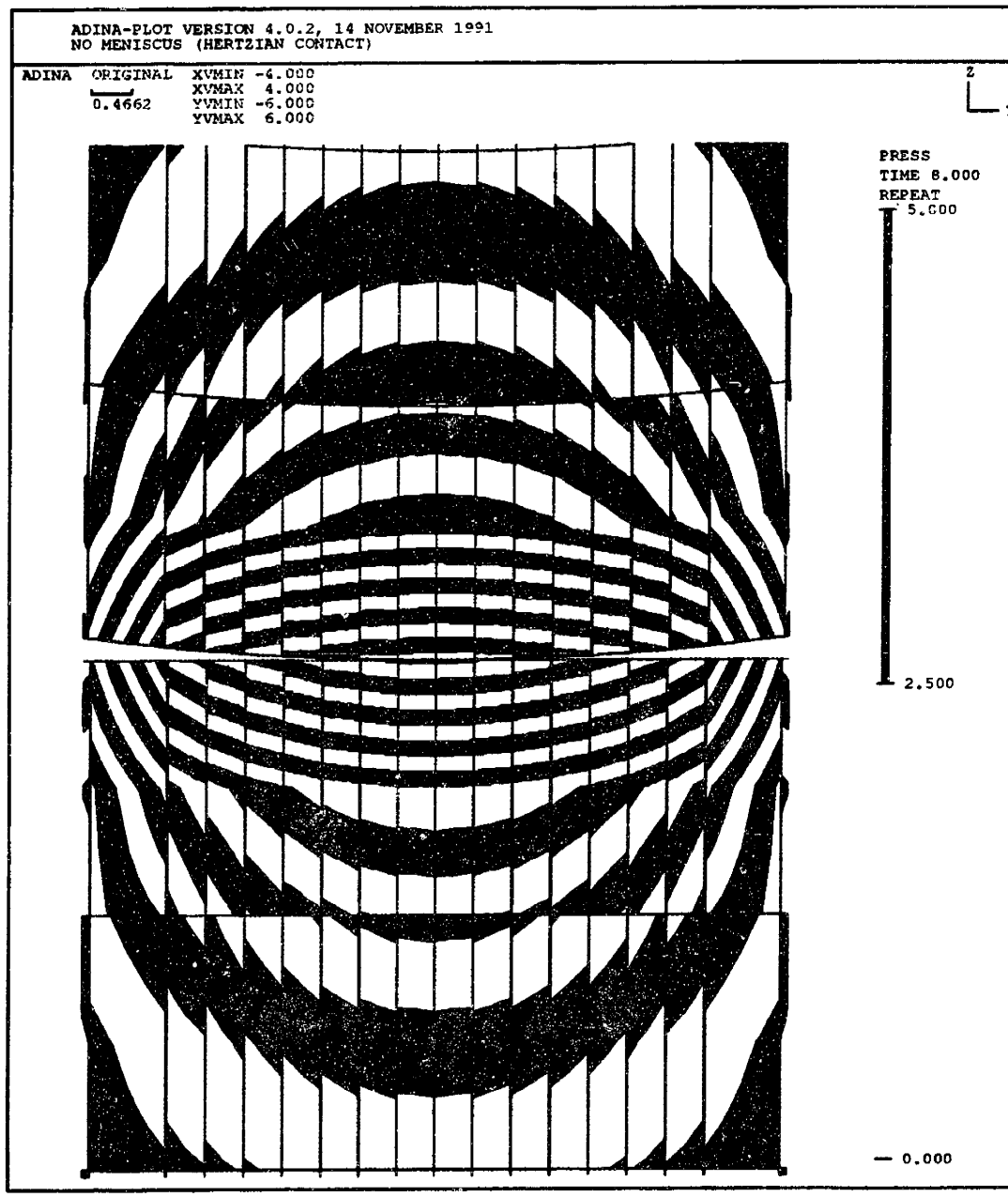

Figure 4-16: Pressure band plot of contact region for 3D Hertzian contact model, side view. The bands are sufficiently distinguishable.

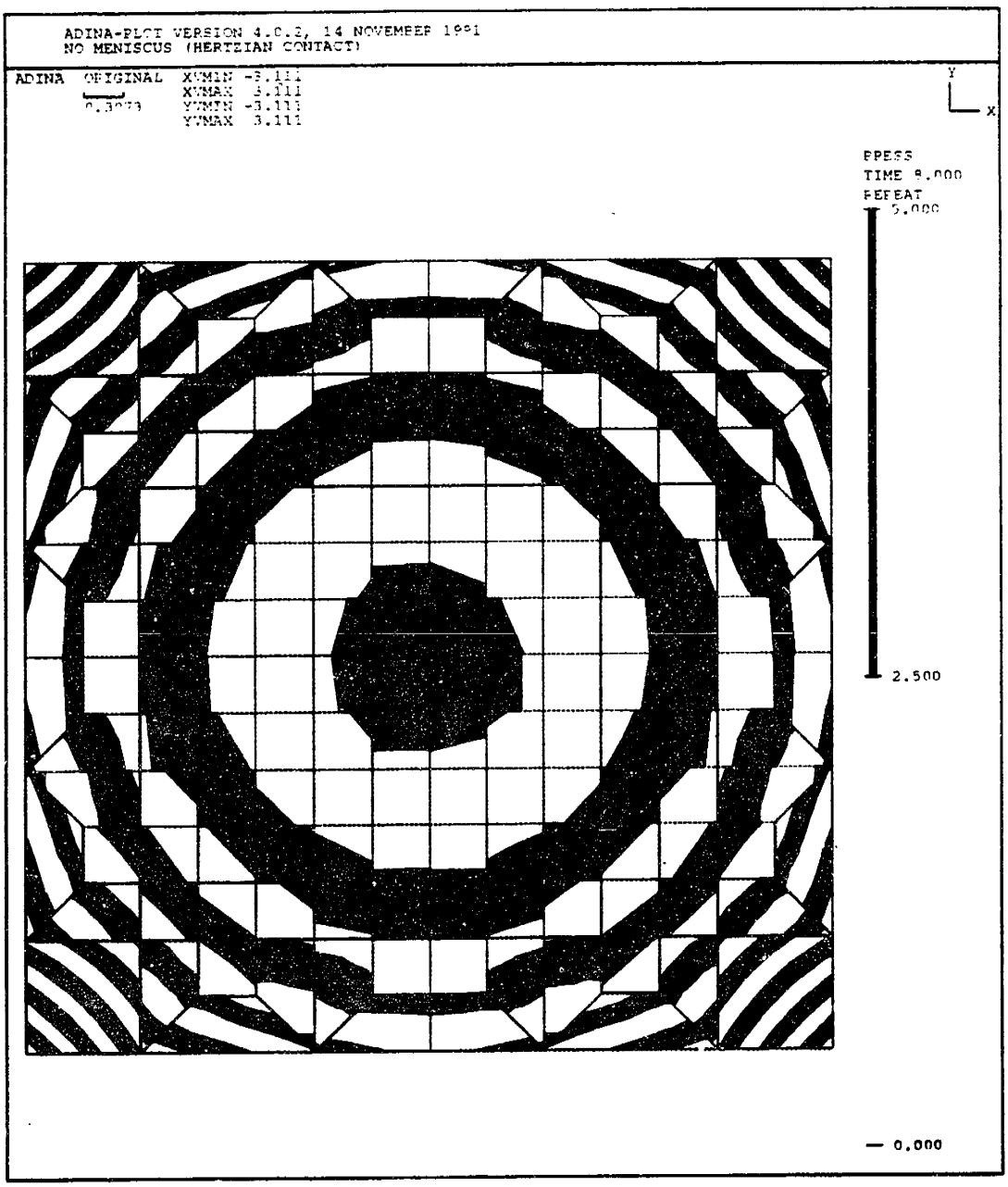

Figure 4-17: Pressure band plot of contact region for 3D Hertzian contact model, top view. Pressure bands are distinguishable.

Chapter 5

3D Meniscus Model Development

5.1 Overview

The previous chapter described the finite element mesh development for the femoral and tibial sections of the model. The subject of this chapter is the addition of both the meniscus and articular cartilage layers to complete the model. It is appropriate here to include discussions of meniscal anatomy, as well as material properties of the meniscus and articular cartilage. These discussions are not exhaustive; they are intended only to provide sufficient information for understanding the modeling assumptions.

5.2 Meniscal Anatomy

The menisci are essentially two semilunar fibrocartilages which are interposed between the distal femur and proximal tibia. The thick, convex peripheral edges of the medial and lateral menisci are attached to the joint capsule. The inside border of each meniscus tapers out to a thin, free edge. The proximal surfaces of the menisci are concave, thus improving joint congruence, and the distal surfaces are relatively flat (Gray, 1973[26]).

The medial meniscus is semicircular in shape, is wide posteriorly and narrower anteriorly (Gray,1973[26];Johnson, 1978[33]). The posterior horn of the medial menis-

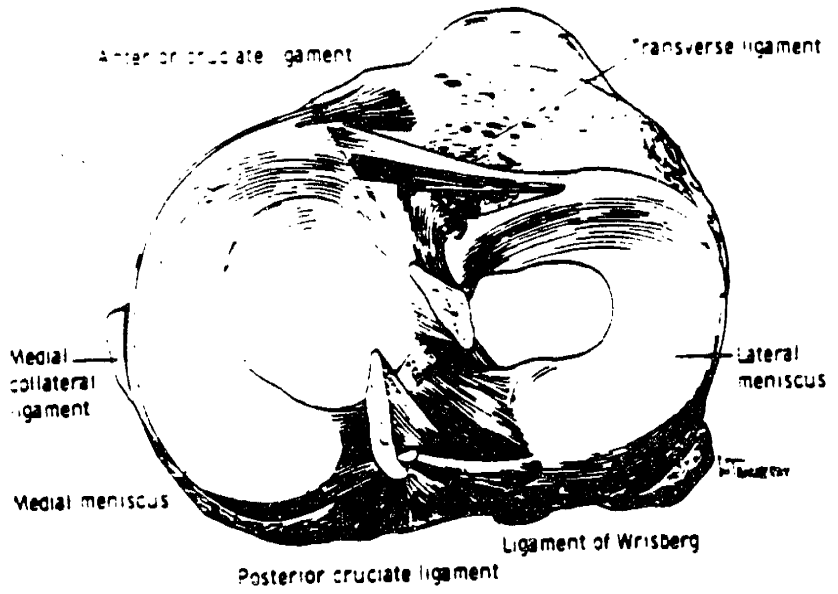

Figure 5-1: Superior view of the proximal tibia, showing medial and lateral menisci.

cus attaches to the intercondylar eminence of the tibia, between the attachment of the lateral meniscus and the posterior cruciate ligament (Gray, 1973[26]). Anteriorly, the medial meniscus attaches to the front edge of the tibial articular surface (Johnson,1978[33]). The semimembranosus muscle inserts into the posterior portion, and the deep medial collateral ligament, or medial capsular ligament, is also attached to the medial meniscus (Johnson, 1978[33] (see Figure 5-1).

In general, the lateral meniscus has a more circular shape than the medial, and has a more constant width when viewed from above. In addition, the lateral menicus covers a significantly larger portion of the tibial articular surface than does the medial meniscus (Gray, 1973[26]). The anterior horn of the lateral meniscus is attached anterior to the intercondylar eminence of the tibia and blends with the anterior cruciate ligament (Gray, 1973[26]). The posterior horn inserts into the posterior part of the intercondylar eminence, anterior to the medial meniscal attachment (Gray, 1973[26]; Johnson, 1978[33]). The ligament of Wrisberg, or posterior meniscofemoral ligament, originates near the posterior attachment and inserts into the medial femoral condyle (Gray, 1973[26]). In some specimens, the ligament of Humphrey, or anterior meniscofemoral ligament, arises from the posterior horn and attaches into the medial femoral condyle as well (Gray, 1973[26]; Johnson, 1978[33]). The posterior part

of the lateral meniscus contains a groove for the popliteus tendon (Gray, 1973[26]; Johnson, 1978[33]), and the popliteus muscle inserts into the posterior horn (Johnson, 1978[33]).

5.3 Material Modeling

5.3.1 Meniscus

The meniscus is basically a composite material, reinforced by collagen fibers. The orientation of collagen fibers in the core of the meniscus is primarily circumferential, as shown by Bullough *et al* (1970[14]). The circumferentially oriented fibers allow the meniscus to develop significant hoop stresses when the knee is axially loaded. In addition to the circumferential fibers, there are a small number of radially oriented collagen fibers which tend to resist splitting of the tissue longitudinally. The central region of the meniscus is surrounded by a surface layer containing randomly oriented collagen fibers, which lie parallel to the adjacent articular surfaces. This layer is approximately 100 μm thick (Arnoczky, 1987[5]). The collagen fiber orientations in different planes of the meniscus are shown in Figure 5-2.

Given the distribution of collagen fibers, the meniscus is clearly an anisotropic material. There is a wide range of experimentally obtained values for the tensile, compressive, and shear moduli of the meniscus. This wide range is due to both differences in specimen orientation and the region from which specimens were obtained. In addition, meniscal material properties are frequency-dependent due to the poroelastic nature of the meniscus. For a complete review of the relevant experimental work, the reader is referred to Brown (1990[12]).

In his axisymmetric finite element model of the meniscus, Brown (1990[12]) modeled the meniscus as a transversely isotropic material, with a higher modulus in the circumferential direction than in the plane orthogonal to the circumferential direction. In addition to being anisotropic, the meniscus is a bimodular material, having different elastic moduli in tension and compression. Therefore, the material properties

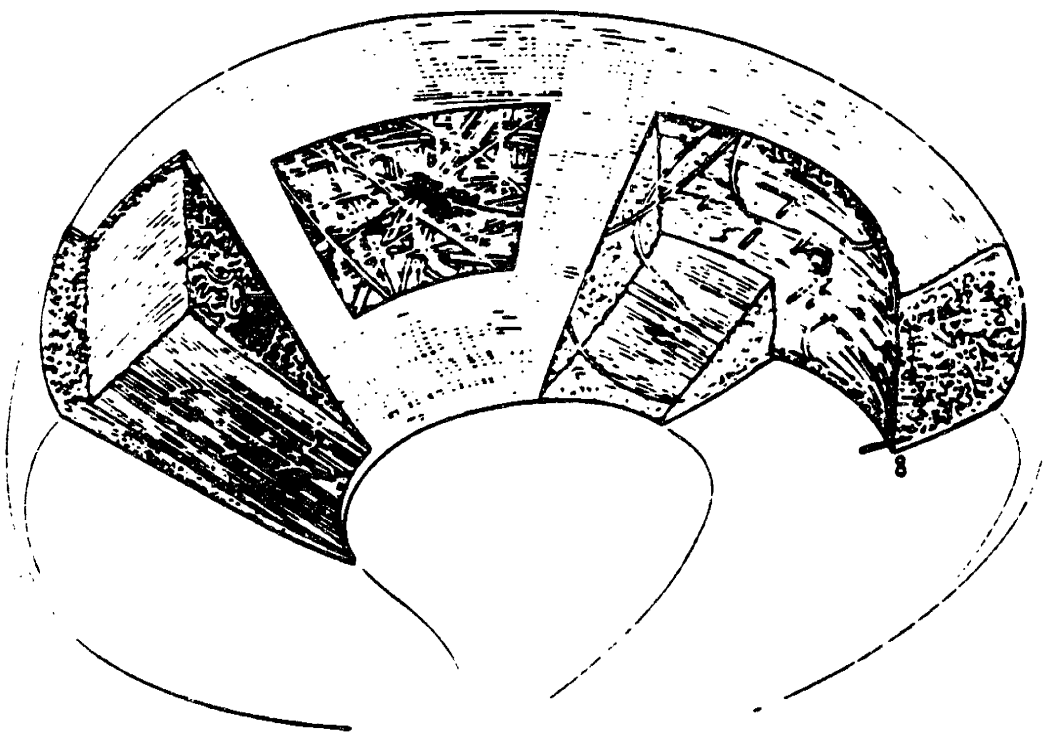

Figure 5-2: Cut view of the meniscus showing different collagen fiber orientations.

chosen for the model must be based on the assumed state of stress in the meniscus. The assumed stress state under axial loading is compressive in the radial and axial directions, and tensile in the circumferential direction. All of the assumptions regarding material properties are consistent with Brown's, to allow for direct comparison between the axisymmetric and non-axisymmetric meniscus models.

5.3.2 Articular Cartilage

Articular cartilage is a poroelastic material which exhibits complex behavior and is thus a subject of significant controversy in the literature. At high loading rates, such as those which occur during walking and running, however, it is reasonable to model the articular cartilage as an isotropic, elastic solid. The results for biphasic and elastic models of cartilage differ by negligible amounts at high loading rates, as demonstrated by Eberhardt *et al* (1990[20]). For the purposes of this model, articular cartilage is modeled as a linear elastic solid.

5.4 Summary of Modeling Assumptions

5.4.1 Femoral and Tibial Geometry

The articular surface of the femoral condyle is modeled as a sphere with a radius of curvature of 30 *mm*. This is a reasonable radius of curvature given the value reported by Kurosawa *et al.* (1985[37]) for the average frontal plane radius of the medial condyle at full extension (21.4 *mm*), and the value reported by Mensch *et al.* (1975[44]) for the average anterior medial condylar radius in the saggital plane (37.5 *mm*). The tibial plateau is modeled as a planar surface. Both the femur and tibia are axisymmetric, with radial widths of 20 *mm*. The proximal femoral surface and the distal tibial surfaces are 15 *mm* from the point of initial contact. This distance is sufficient to prevent the surface boundary conditions from affecting the state of stress near the contact region. Both the femoral and tibial surfaces are covered with layers of articular cartilage 2 *mm* thick. This value for articular cartilage thickness is

consistent with that used by other investigators (Askew, 1978[7]; Galbraith, 1989[25]).

5.4.2 Meniscal Geometry

The first three-dimensional meniscus model to be analyzed employs axisymmetric meniscal geometry. The results from this model can then be used for direct comparison to the non-axisymmetric model. If the two-dimensional mesh results were used for direct comparison, it would be impossible to isolate differences in results due to discretization from actual differences in meniscal load bearing. This issue arises from the fact that the three-dimensional mesh must be somewhat coarser than the two-dimensional axisymmetric model in order for the solution to be computationally realizable. The three-dimensional axisymmetric mesh uses the same geometry and material properties as Brown's model, and virtually eliminates discretization effects from the comparison between axisymmetric and non-axisymmetric models.

The axisymmetric meniscus is a wedge-shaped toroid, with inner and outer radii of 6 *mm* and 18 *mm* respectively. The width of the meniscus is therefore 12 *mm*. Noble (1977[48]) reported the average width of the medial meniscus to be 13 *mm*. The outer proximal surface of the meniscus has a radius of curvature of 30 *mm*, chosen to provide congruence between the outer half of the meniscus and the femoral condyle. The inner proximal surface tapers to a thin edge. The distal surface of the meniscus is flat and fully conforming with the tibial plateau.

5.4.3 Material Properties

The range of reported values for the subchondral bone of the distal femur and proximal tibia is extremely broad. Brown [12] modeled the bone of the distal femur as an isotropic, elastic material with a Young's modulus of 1000 *MPa* and a Poisson's ratio of 0.3. Ducheyne *et al.* (1977[19]) reported a range of 60 *MPA* to 3000 *MPa* for the elastic modulus of the femur. The tibial subchondral bone was assumed to be isotropic as well, with an elastic modulus of 500 *MPa* and a Poisson's ratio of 0.3. These are the values used for the three-dimensional meniscus model.

The meniscus is modeled as a transversely isotropic material, and thus requires five independent parameters to completely define the stiffness tensor. Brown (1990[12]) modeled the meniscus as transversely isotropic in the plane orthogonal to the circumferential direction, with a compressive modulus of 15 *MPa*, which was measured in unconfined compression tests. The circumferential elastic modulus is taken to be 120 *MPa*. This value was obtained by averaging values presented by Fithian (1989[23]) for different regions of the medial meniscus. The shear moduli are all equal to 0.2 *MPa*; these values are taken from Anderson (1990[3]). Little experimental data is available for Poisson's ratios; Brown [12] defined the values as $\nu_{rz} = 0.5$ and $\nu_{r\theta} = \nu_{z\theta} = 1$ to satisfy the thermodynamic requirements for a transversely isotropic material. The reader is referred to Brown [12] for a complete discussion of the thermodynamic requirements.

The layers of articular cartilage on the femur and tibia are assumed to be isotropic and elastic, with Young's modulus 12 *MPa* and Poisson's ratio 0.45. These values are taken from Askew and Mow (1978[7]) and Galbraith and Bryant (1989[25]). At high loading rates, articular cartilage is nearly incompressible (Brown, 1990[12]).

5.4.4 Applied Loading

Brown (1990[12]) chose to model the entire knee (femur, tibia, and meniscus) and apply force loading conditions, in lieu of modeling simply the tibia and meniscus and using experimentally determined contact pressures to define the meniscal loading. There are several potential errors present in the experimental determination of femoral contact pressures; modeling of the femur itself results in a more 'natural' distribution of contact pressures on the meniscus. A resultant load of 700 *N* (approximately one times body weight) is placed on the femur. Investigators report values from 3.0 to 4.5 *BW* for the maximum joint contact force which occurs during walking (Morrison, 1968[45]; Harrington, 1976[27]; Fijan, 1990[22]). Since the finite element model is unicondylar, a load of approximately 1 *BW* is reasonable with regard to experimental observations and keeping the number of load steps and therefore the computational cost to a minimum.

5.5 3D Axisymmetric Meniscus Model

The finite element mesh for the 3D axisymmetric meniscus model is shown in Figure 5-3. Figure 5-4 shows a cross-sectional view of the meniscus alone. The elements which comprise the meniscal mesh employ linear interpolation functions on horizontal surfaces, and parabolic interpolation functions on vertical surfaces. This type of element was chosen because the finite element code used requires linear interpolation functions on all contact surfaces. All nodes on the distal surface of the tibia are constrained in the vertical direction, but are free to expand radially. The loading is applied to the center node on the proximal surface of the femur, and all other nodes on this surface are constrained to have the same vertical displacement as the loaded node. This effectively distributes the applied load across the top surface. Soft trusses fix the femur and meniscus to ground in order to prevent the possibility of rigid body motion. (The finite element solution requires that the model contain no rigid body modes, and does not include contact conditions as constraints.) The trusses are highly compliant and thus carry a negligible portion of the load. The axisymmetric meniscus is not constrained on the tibial plateau in any way. There is a truss placed between the subchondral bone of the femur and tibia at the point of initial contact; without this truss, there is a gross amount of overlap in the relatively soft articular cartilage during the first load step and the solution aborts. The truss provides additional stiffness until a sufficient number of contact elements are engaged; it is then removed at an intermediate load step and does not affect the final results.

5.6 Results of the 3D Axisymmetric Model

It is important at this point to address the issue of discretization differences between 2D and 3D axisymmetric models. As stated previously, the 3D model is necessarily less refined than the 2D model for reasons relating to computational cost. The 2D and 3D axisymmetric results are compared here in order to show the effect of this discretization difference. These comparisons will help to establish what differences

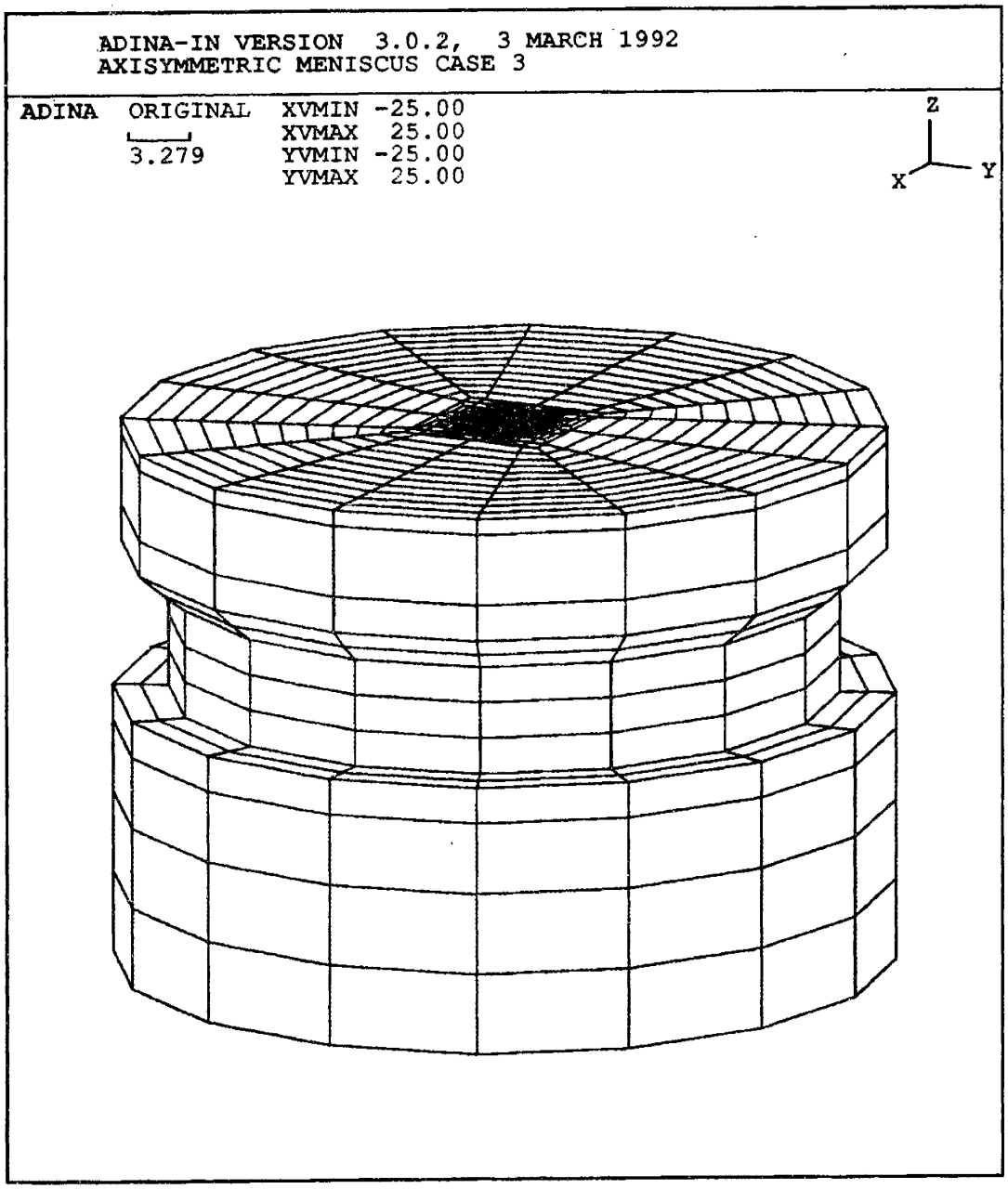

Figure 5-3: 3D axisymmetric meniscus model.

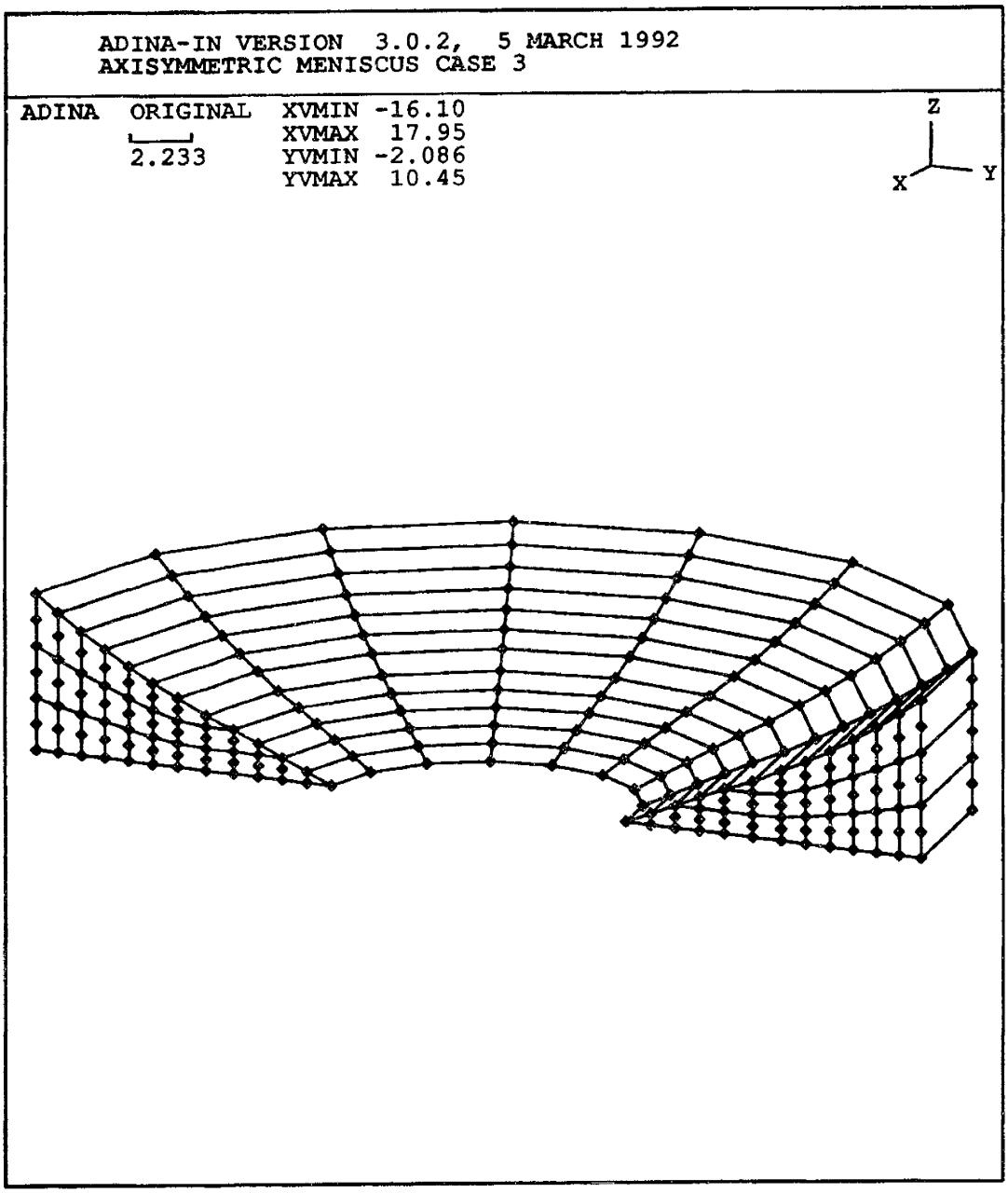

Figure 5-4: Cross sectional view of axisymmetric meniscal mesh

are significant when the axisymmetric and non-axisymmetric models are compared. The parameters used for the comparison are contact pressure, tibial subchondral bone stresses along radial and axial lines, vertical displacement of the top femoral surface as a function of applied load, and radial displacement of the meniscus as a function of applied load. Plots of these parameters are shown in Figures 5-5 through 5-9. In addition, stress band plots of the meniscus and articular cartilage are presented in order to quantify the discretization error present in these areas.

The 2D and 3D axisymmetric models demonstrate considerable agreement. The peak contact pressures predicted by the 2D and 3D models agree to within approximately 10%, and the distributions are very similar in the tibiofemoral and meniscotibial contact regions (see Figure 5-5). The peak subchondral bone stresses predicted by the two models agree to within approximately 5% (see Figures 5-6, 5-7). As shown in Figure 5-8, the total joint stiffnesses also show similar predictions. For a given displacement, the difference in load is less than 13%. The same is true for the radial meniscal displacement comparison at loading levels of interest (Figure 5-9.

Figure 5-10 shows an effective stress plot of a cross-section of the axisymmetric meniscus. The bandwidth of the plot is approximately 7%. The bands are distinguishable throughout most of the elements. Some discontinuities are evident in the triangular elements near the tapered edge; this is not surprising since these elements are degenerate. (The use of degenerate triangular elements is necessary in order to obtain the desired meniscal geometry.) Experience with two-dimensional axisymmetric meniscus models shows that further refinement of the meniscal mesh yields only small improvements in stress band continuity. The level of refinement shown here was therefore deemed acceptable based on both desired accuracy and computational cost considerations.

Figure 5-11 shows an effective stress plot of the tibial articular cartilage in the peak stress region. The bandwidth of this plot is approximately 5%. The bands are very distinguishable, giving confidence to the stress results predicted by the model in this critical region.

Figure 5-12 shows a comparison between contact pressures in the tibial articular

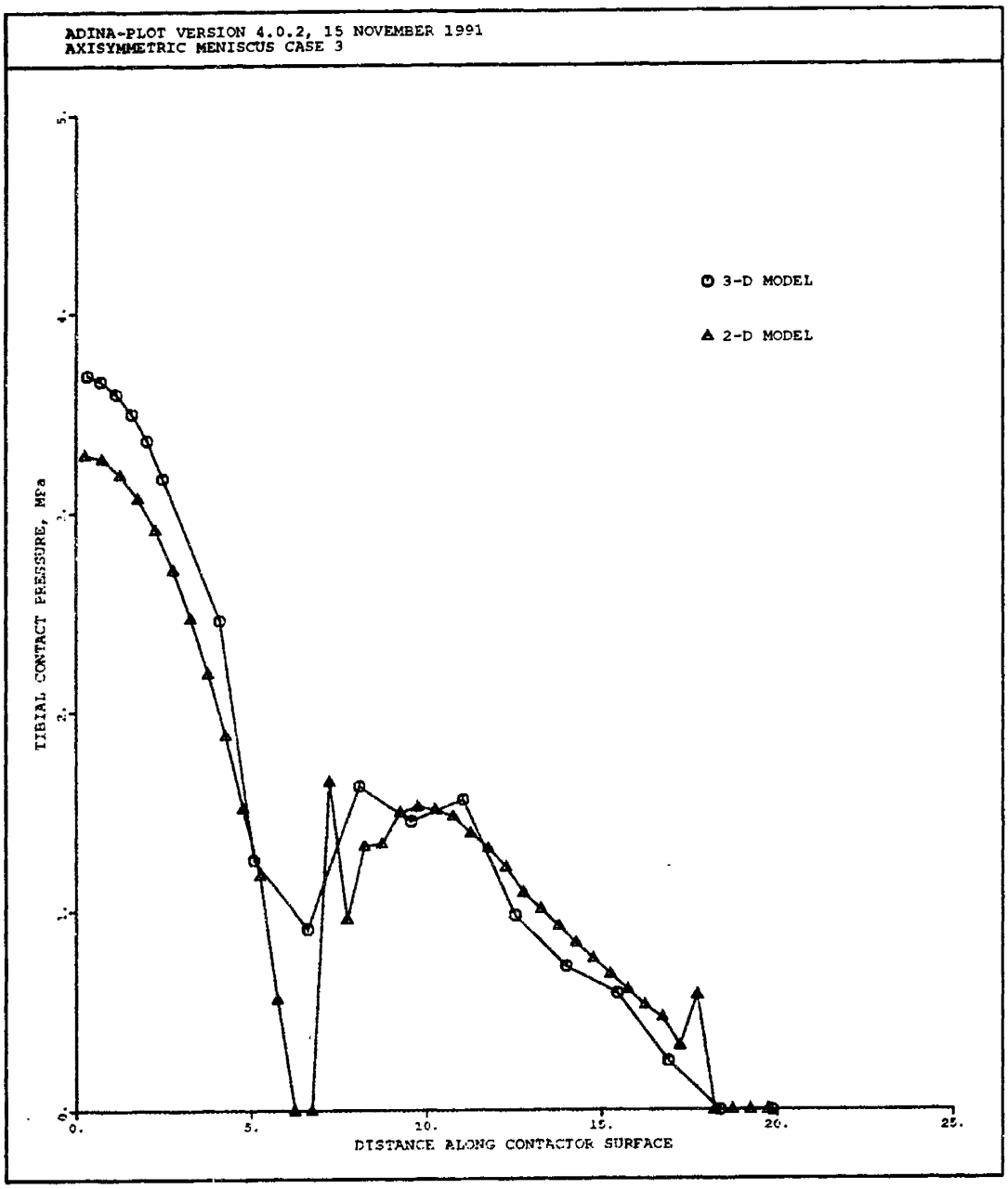

Figure 5-5: Contact pressure distributions in tibial articular cartilage at 1.5 *BW*. Comparison between 2D and 3D axisymmetric models.

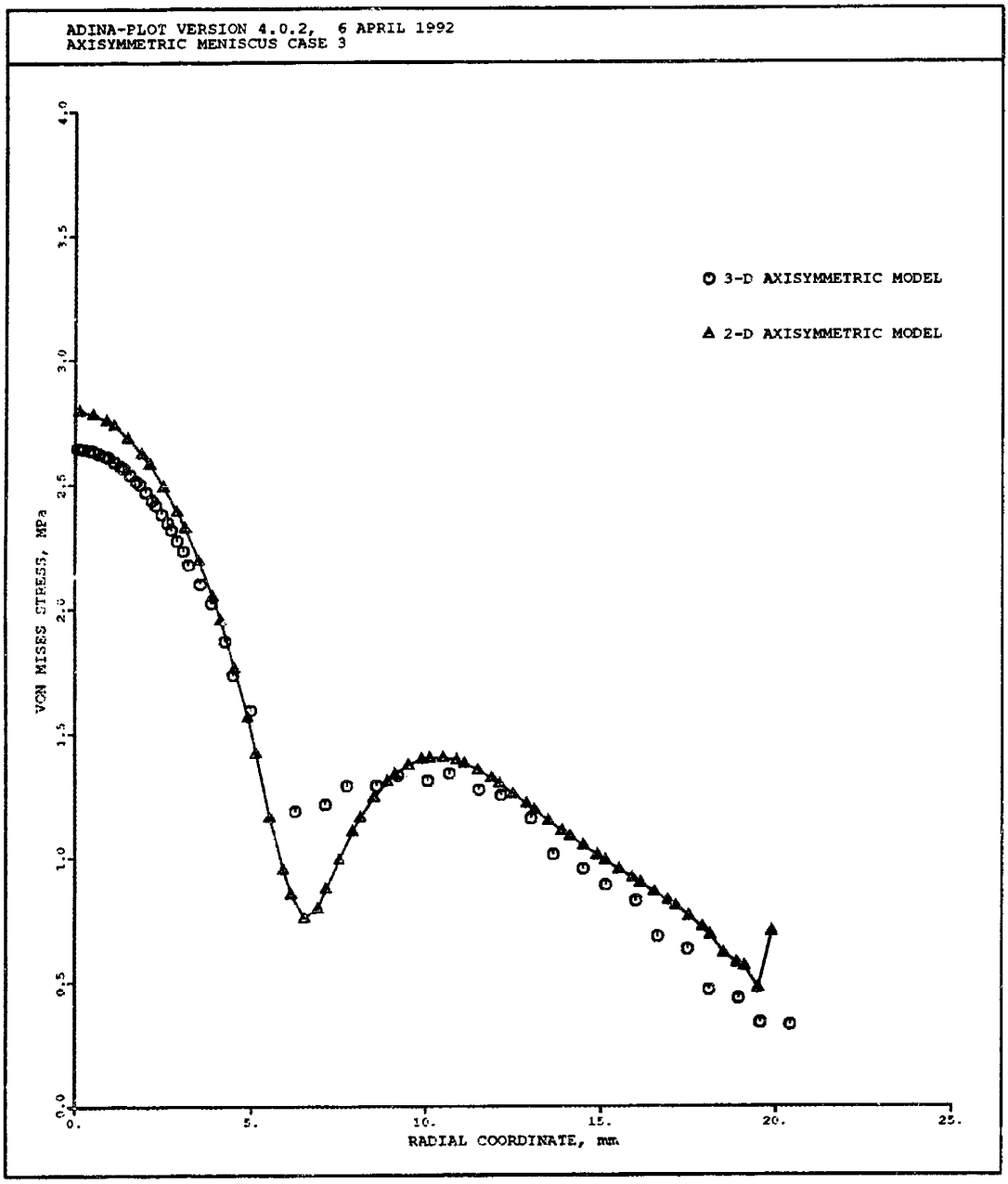

Figure 5-6: Tibial subchondral bone stress along radial line at 1.5 *BW*. Comparison of 2D and 3D axisymmetric models

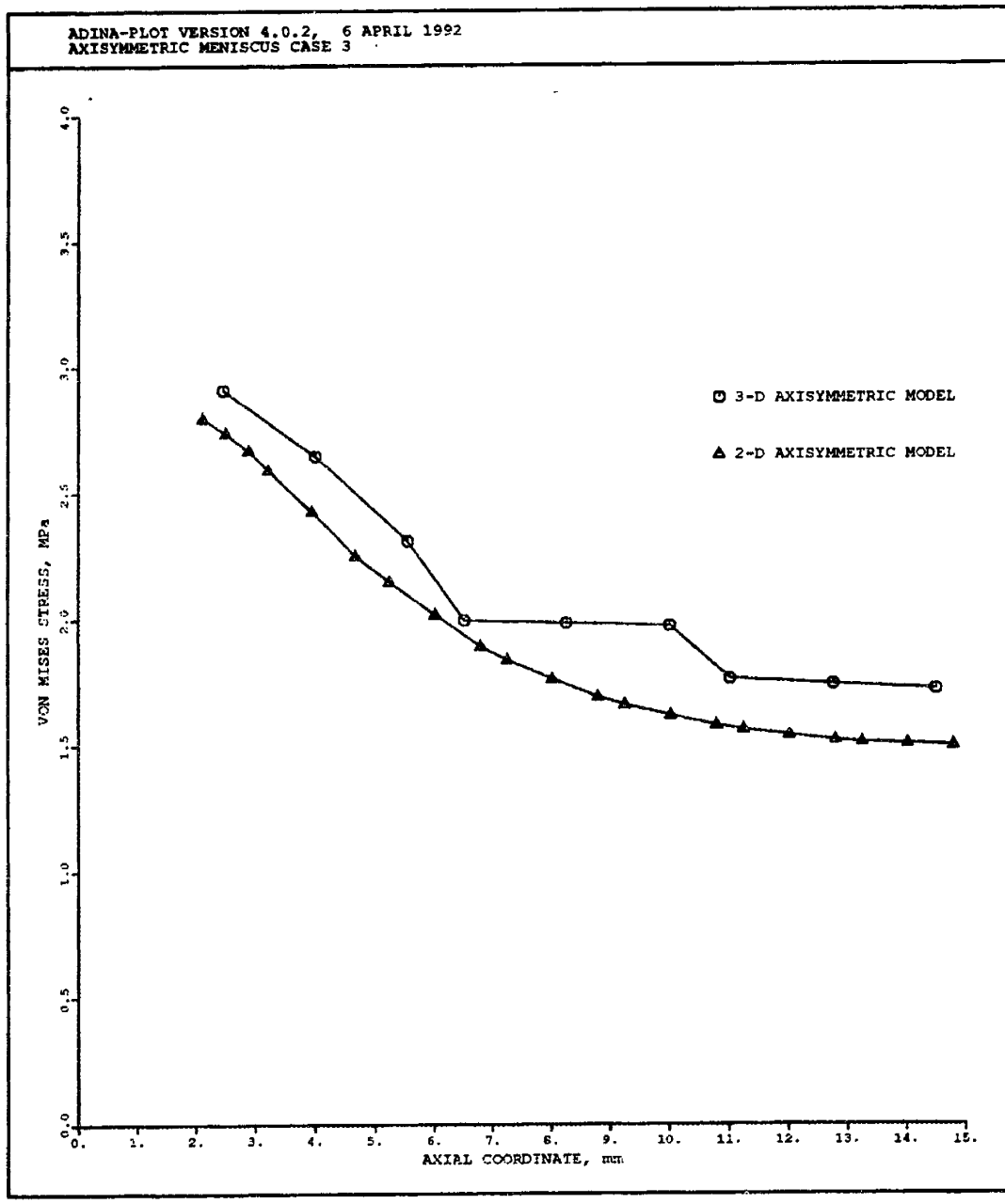

Figure 5-7: Tibial subchondral bone stress along axis of symmetry at 1.5 *BW*. Comparison of 2D and 3D axisymmetric models.

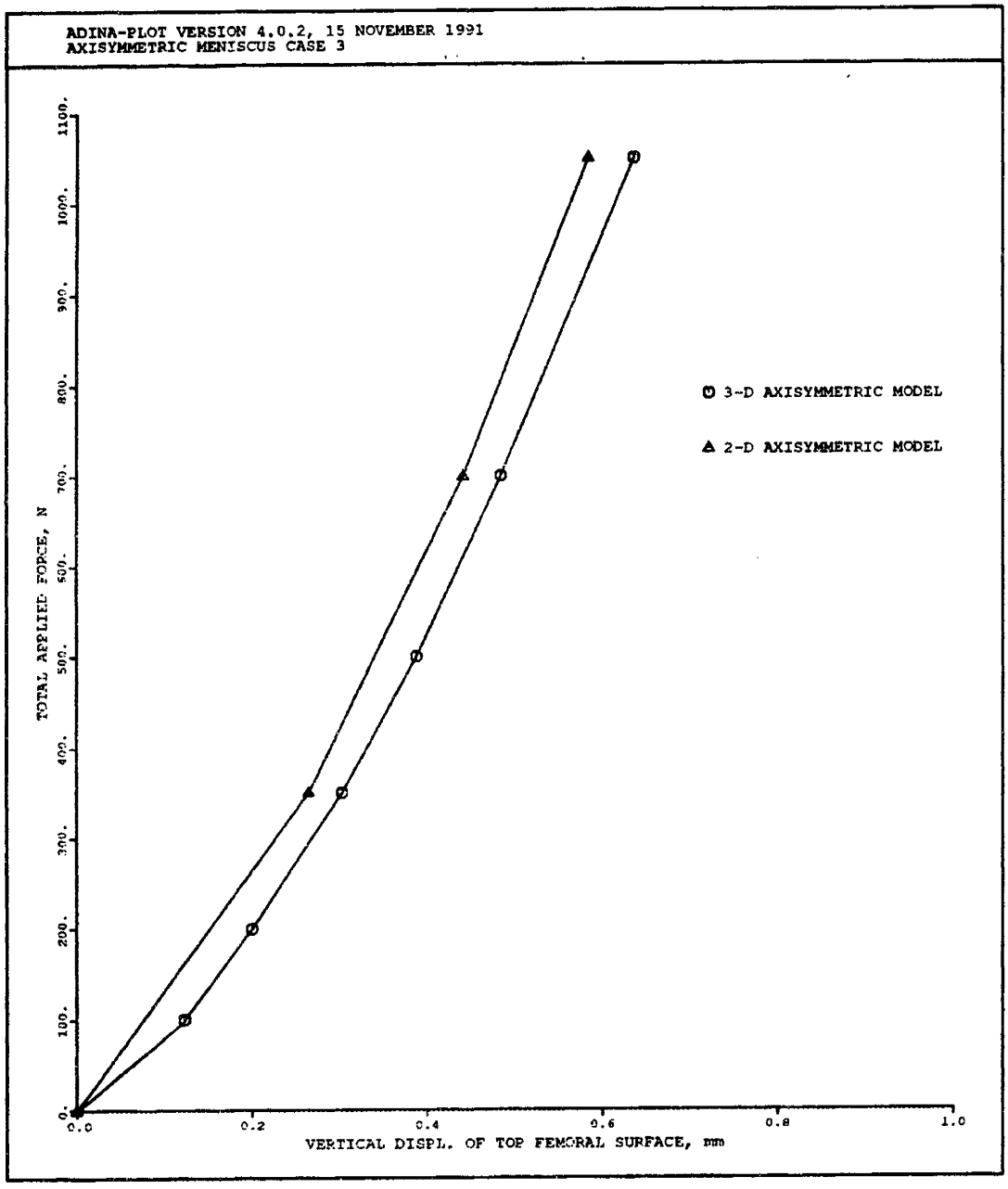

Figure 5-8: Vertical displacement of top femoral surface as a function of applied load, up to 1.5 *BW*. Comparison of 2D and 3D axisymmetric models.

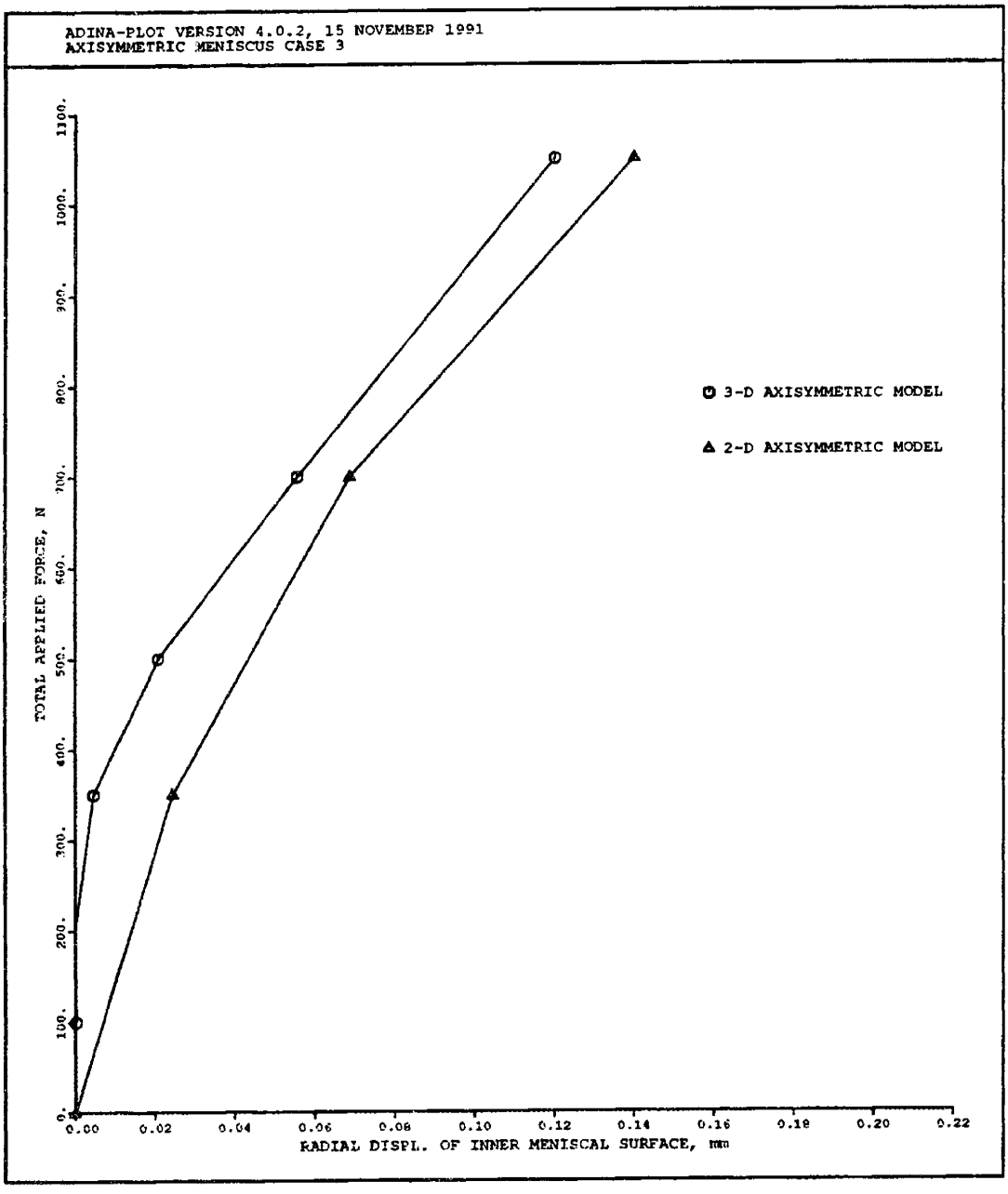

Figure 5-9: Radial displacement of inner meniscal surface as a function of applied load, up to 1.5 *BW*. Comparison of 2D and 3D axisymmetric models.

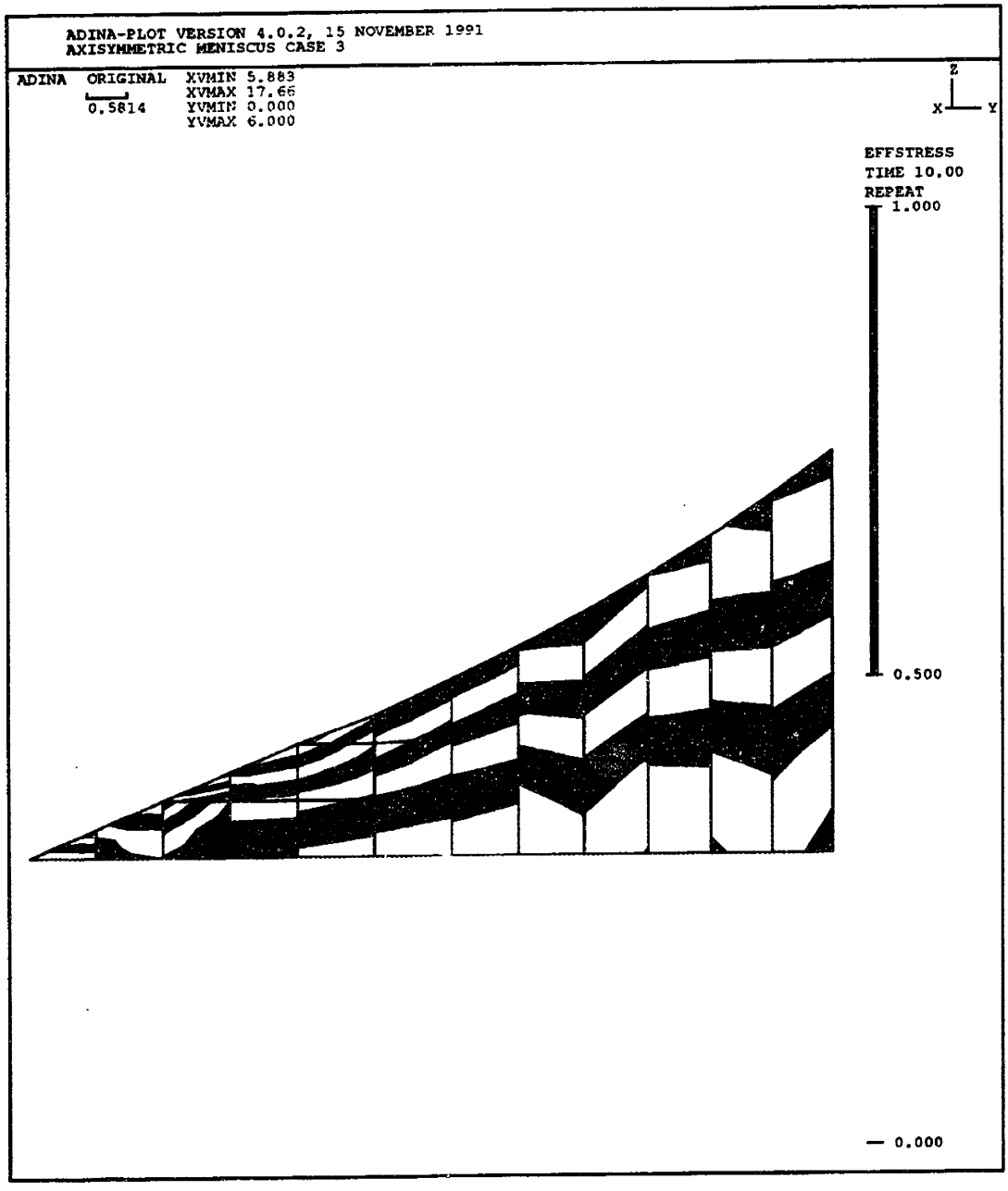

Figure 5-10: Effective stress band plot of axisymmetric meniscus cross section at load of 1.5 *BW*.

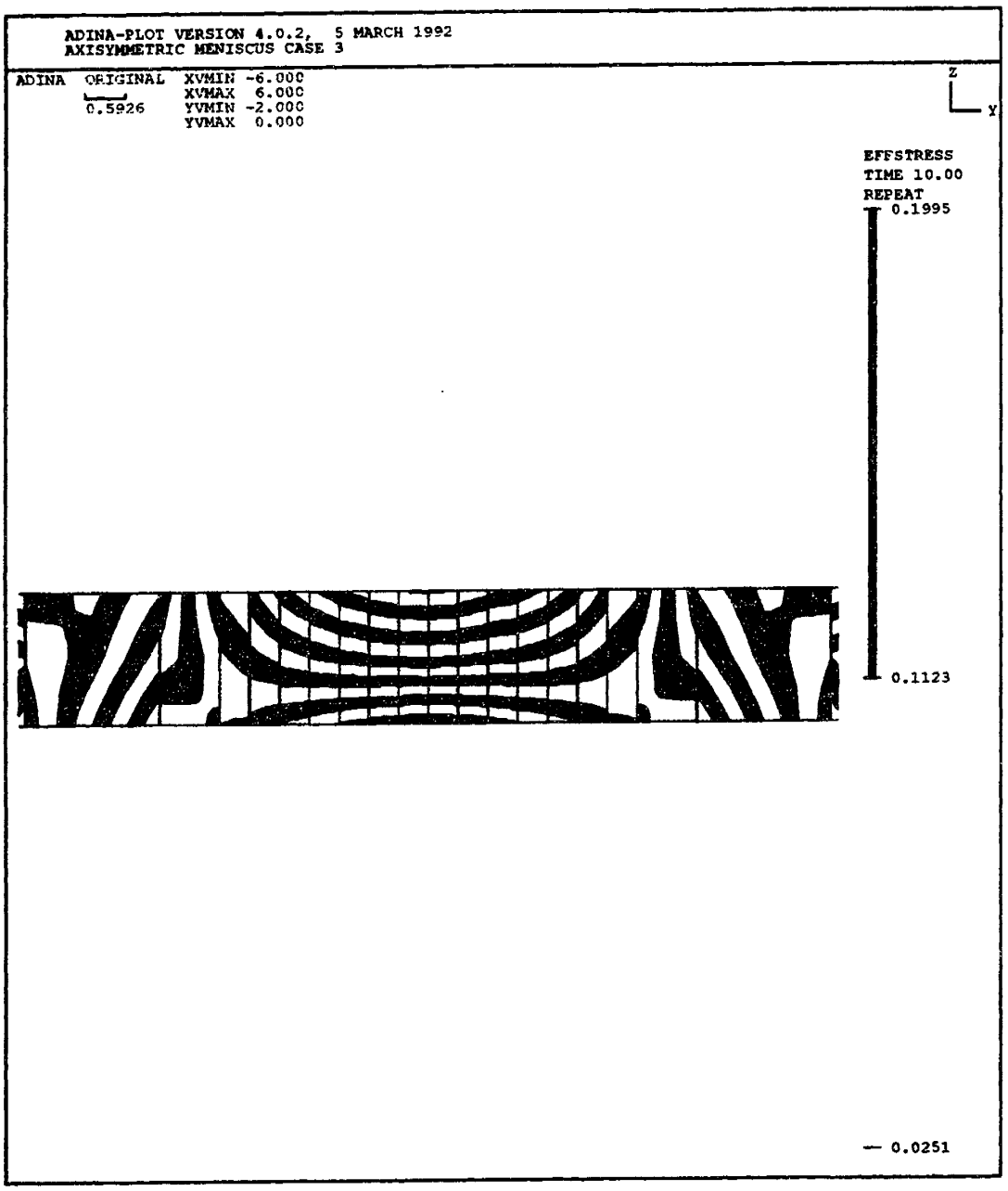

Figure 5-11: Effective stress band plot of articular cartilage in tibiofemoral contact region at load of 1.5 BW.

cartilage along radial lines 45 degrees apart. The results are highly correlated in the important tibiofemoral and meniscotibial contact regions. This result indicates that discretization artifacts have little effect on the 3D contact pressure predictions in the critical regions.

5.7 Non-Axisymmetric Meniscus Model

The mesh design for the femoral and tibial components of the non-axisymmetric meniscus model is identical to that for the axisymmetric model just described. To create the non-axisymmetric meniscal geometry, one quarter of the circumference of the axisymmetric meniscal mesh was removed, and each node in the two exposed cross sections was attached to the tibial plateau via a truss element. Figure 5-13 shows a proximal view of the meniscal mesh. The attachment node on the tibial plateau has all of its translational degrees of freedom deleted. This geometry was chosen to represent an 'average' meniscal shape. The width of the meniscus remains 12 *mm* throughout. The thickness is greatest at the point furthest from the attachment. The outer meniscus conforms with the femur through part of the circumference, and tapers in thickness near the attachment point. Figure 5-14 contains a side view of the meniscus, showing the tapered thickness. This tapering represents an appropriate geometry, since an abrupt cutoff of the meniscus without tapering the thickness would cause non-physiological stress concentrations in the cutoff region.

The stiffness of the attachment elements was chosen to provide physiological continuity between the body of the meniscus and the attachments. In a truly physiological situation, there is no distinct cutoff between 'meniscus' and 'attachments'. Rather, there is a smooth, gradual transition from meniscus into the bone of the tibial plateau. In order to best model this smooth transition, the circumferential stiffness of the axisymmetric meniscus model was calculated and used as a guide in determining the resultant stiffness of the attachments in the non-axisymmetric model.

For an axial load of 1050 *N*, the average circumference of the axisymmetric meniscus increased by approximately 2 *mm*. This gives a circumferential stiffness of 525

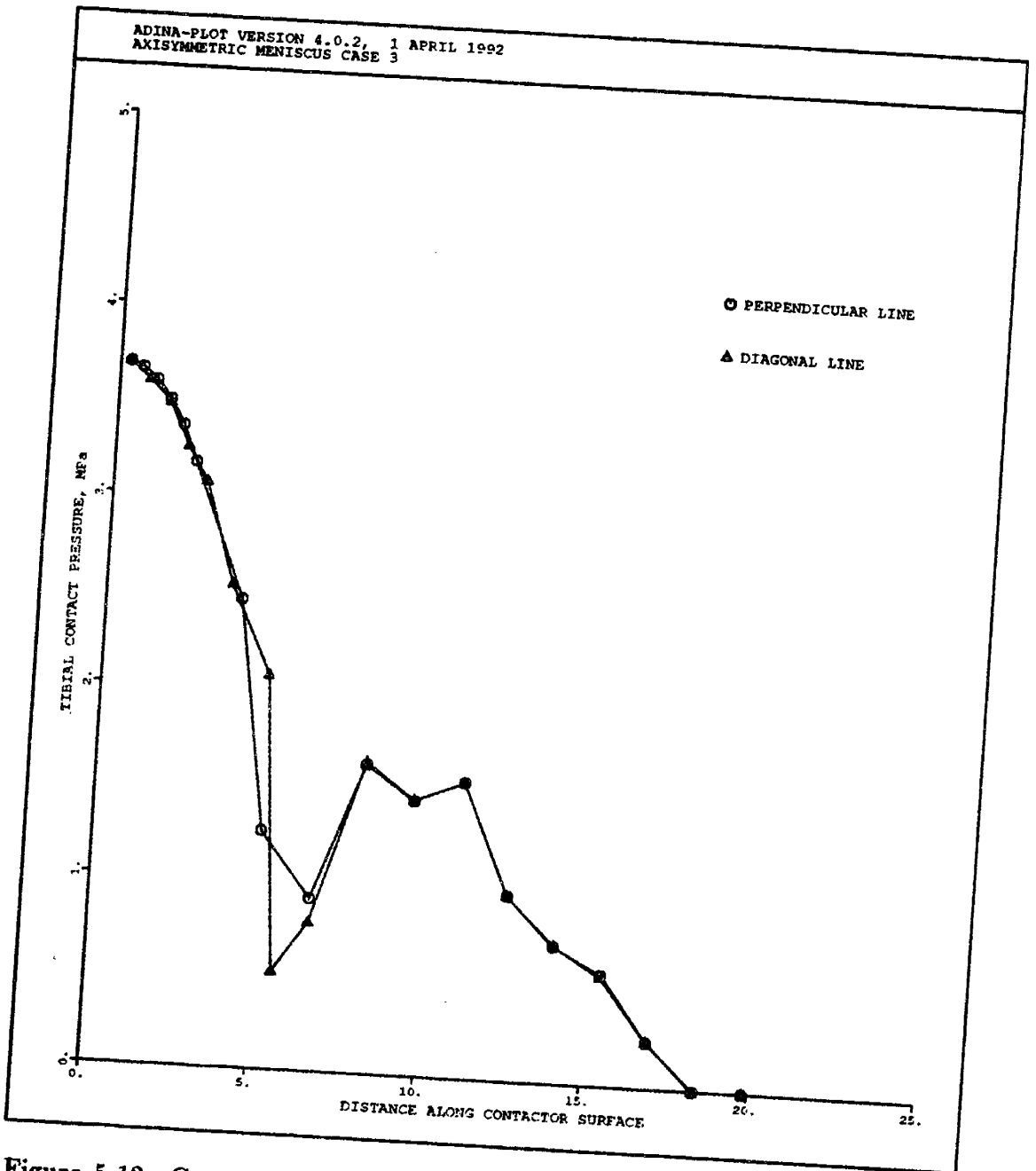

Figure 5-12: Comparison of tibial articular cartilage contact pressure distributions along radial lines 45 degrees apart at 1.5 BW.

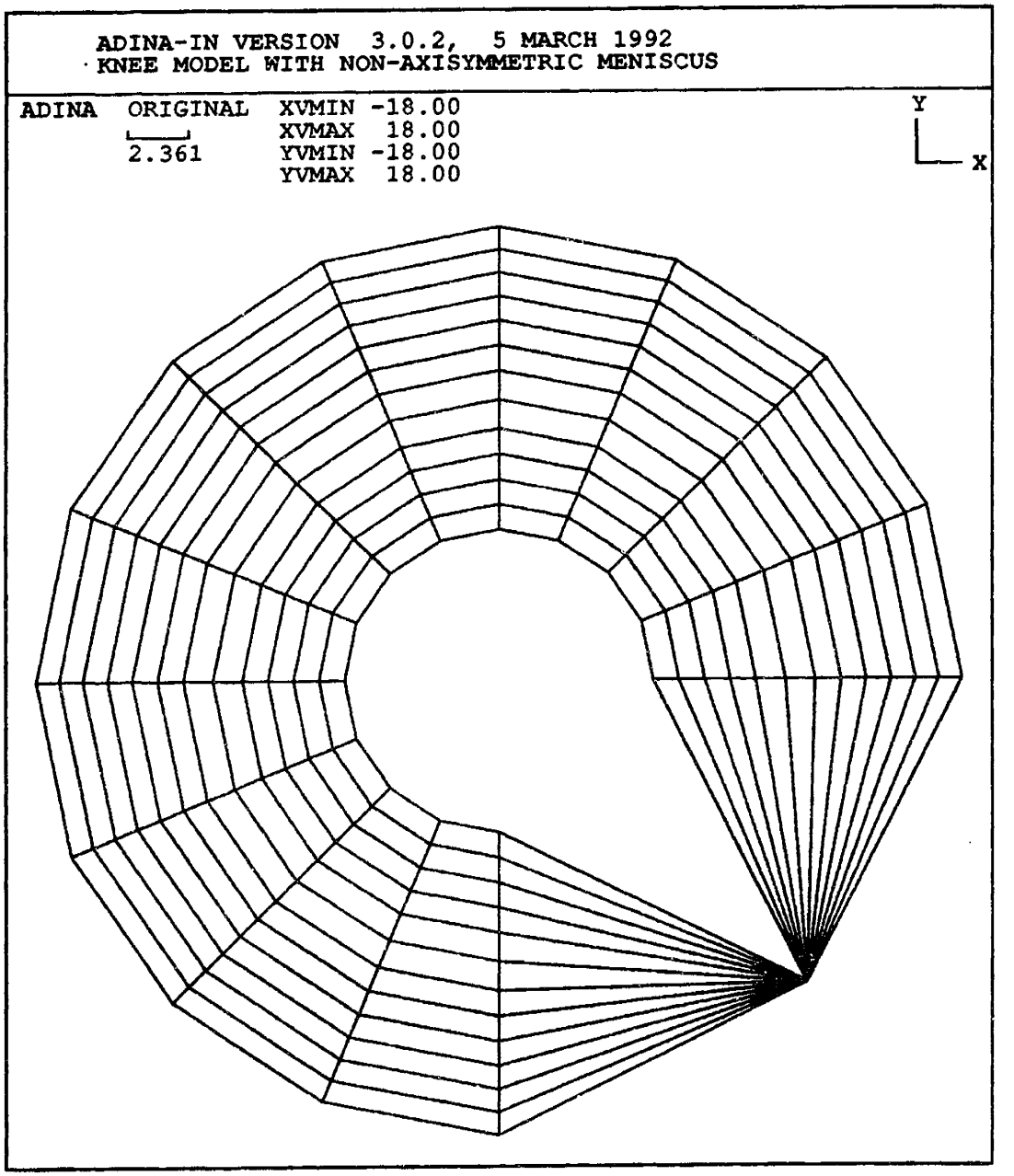

Figure 5-13: Proximal view of non-axisymmetric meniscal mesh.

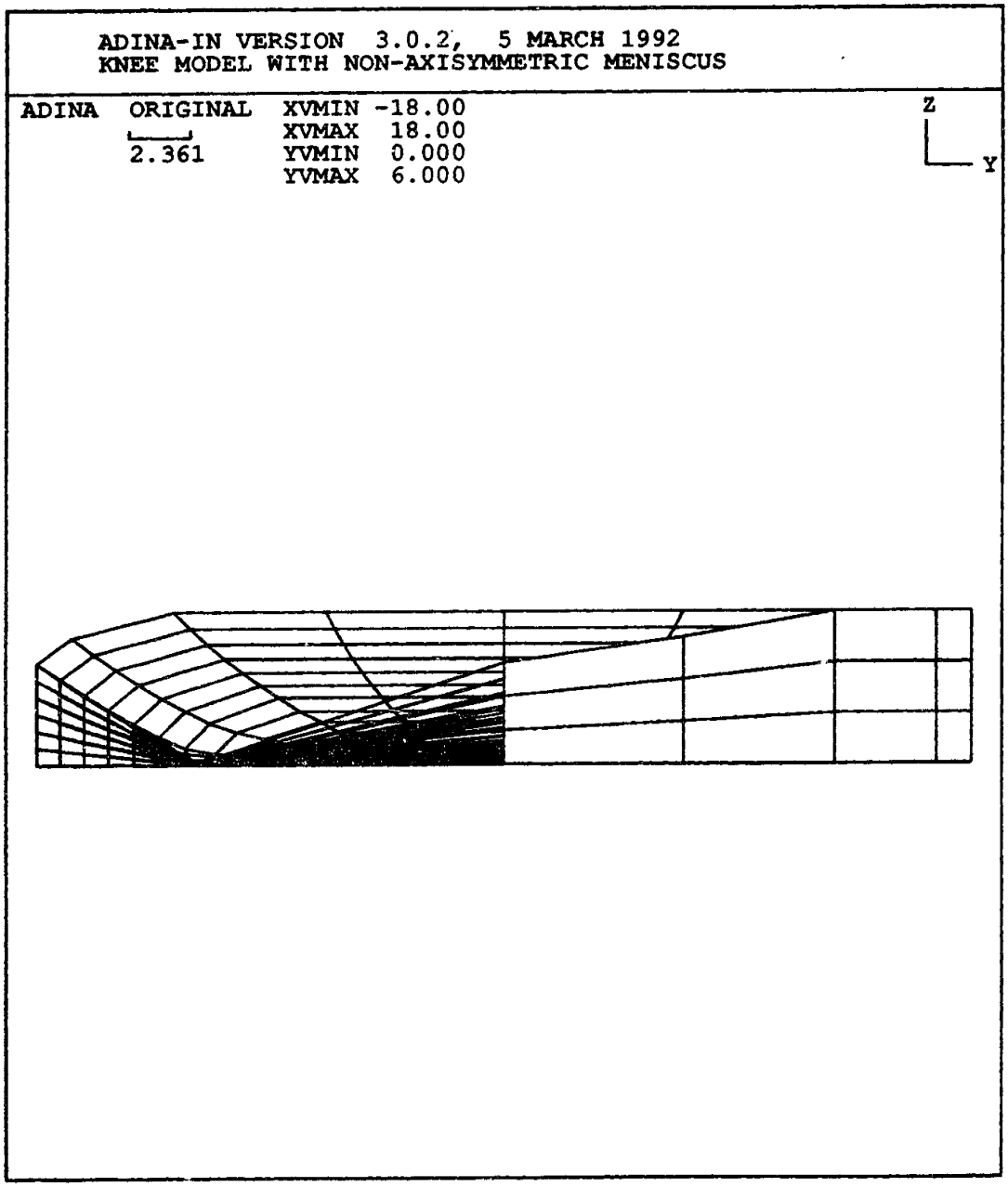

Figure 5-14: Non-axisymmetric meniscal mesh, showing thickness tapering.

N/mm. The total stiffness of each attachment is approximately

$$k = \frac{EA}{L}$$

where E is the elastic modulus, A is the total cross-sectional area of the attachment (sum of the areas of the truss elements), and L is the average truss length. The values of E and A were chosen so that the stiffness of each attachment was approximately equal to 525 *N/mm.*

Chapter 6

Results of the 3D Meniscus Model

There is a tremendous amount of information which can be extracted from a finite element model, particularly one with the level of complexity found in the three-dimensional meniscus model. The results presented here are parameters which are indicators of the role the meniscus plays in load-bearing in the knee joint. These parameters are:

1. Contact pressures on the tibial articular cartilage,
2. Vertical displacement of the top femoral surface as a function of the applied load (total joint stiffness),
3. Radial displacement of the meniscus as a function of applied load,
4. Stresses in the tibial subchondral bone,
5. Average circumferential strain in the meniscus, and
6. The percentage of load transmitted by the meniscus.

Results for the axisymmetric and non-axisymmetric meniscus models are presented simultaneously for comparison purposes. Views of the deformed meshes are presented as well. Quantitative results are presented here; a more in-depth discussion appears in the next chapter.

6.1 Contact Pressures

Figure 6-1 is a plot of contact pressures in the tibial articular cartilage along a radial lines beginning from the point of original tibiofemoral contact. The non-axisymmetric results are shown along three radial lines. One line is through the center of the meniscus, far from the attachment point. The second line passes midway between the center and the edge of the meniscus, and the third passes through the edge of the meniscus. The three non-axisymmetric lines show very similar results in the peak contact pressure region. The meniscotibial contact regions along the three lines from the non-axisymmetric model also show similar trends in contact pressure distribution. The non-axisymmetric model shows significantly higher contact pressures in the tibiofemoral contact region than the axisymmetric model. The peak stress predicted by the axisymmetric model is 2.7 *MPa*, and the prediction of the non-axisymmetric model is 4.7 *MPa*. The non-axisymmetric model also predicts somewhat lower contact pressures in the outer meniscotibial contact region.

6.2 Total Joint Stiffness

Plots of vertical displacement of the top femoral surface as a function of applied joint load are shown in Figure 6-2. These plots provide a measure of the total joint stiffness in the two models. The axisymmetric model predicts less vertical displacement for a given loading level (that is, a stiffer joint). This result has direct bearing on the calculation of the percentage of load transmitted by the meniscus, which will be discussed in more detail below.

6.3 Radial Meniscal Displacement

The radial displacement of the inner and outer edges of the meniscus as a function of applied load are shown in Figures 6-3 and 6-4. The displacements are shown for the nonaxisymmetric model at two points on the meniscus, located at the center of the meniscus, and between the center of the meniscus and the attachments. The graph

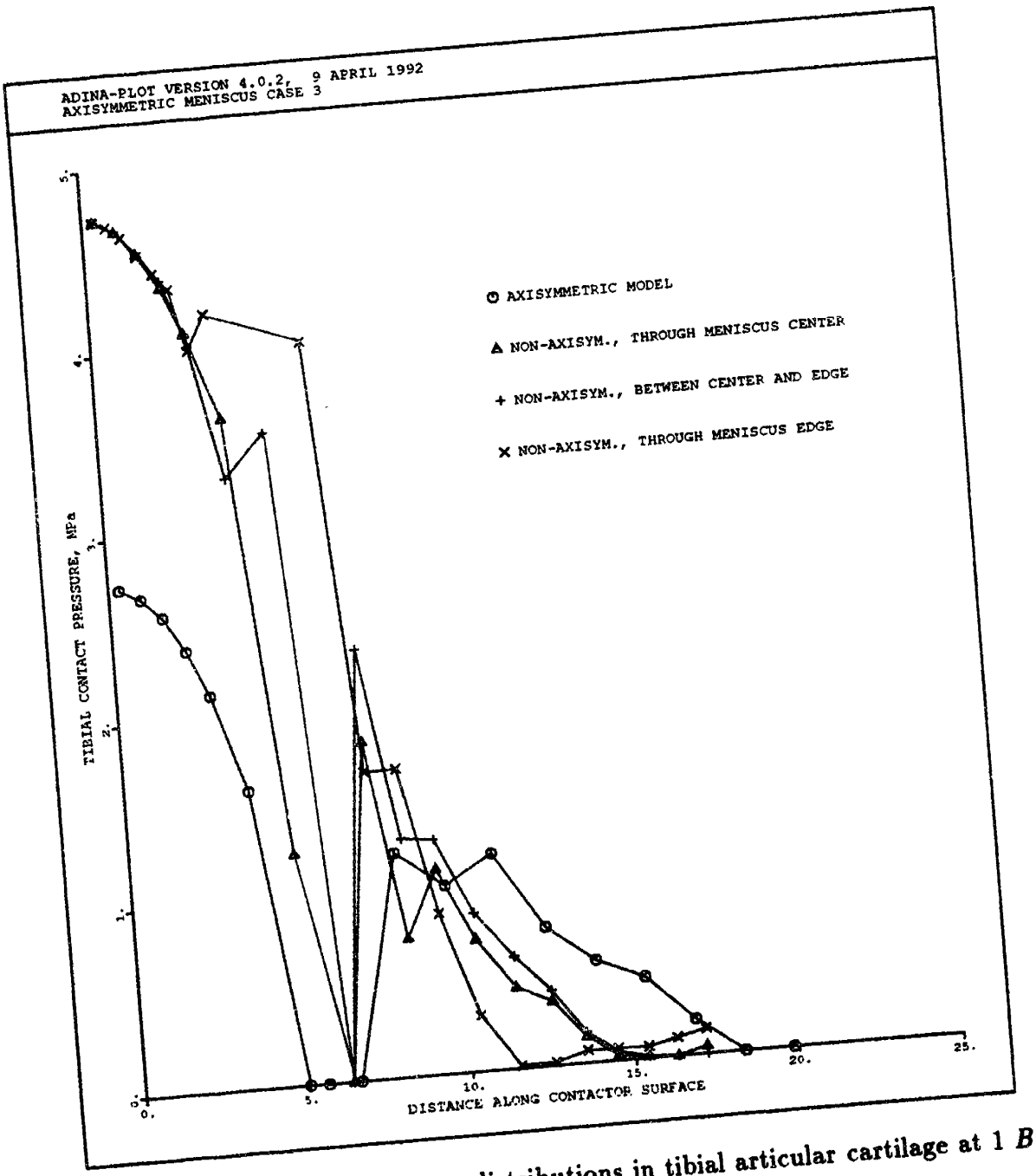

Figure 6-1: Contact pressure distributions in tibial articular cartilage at 1 *BW*.

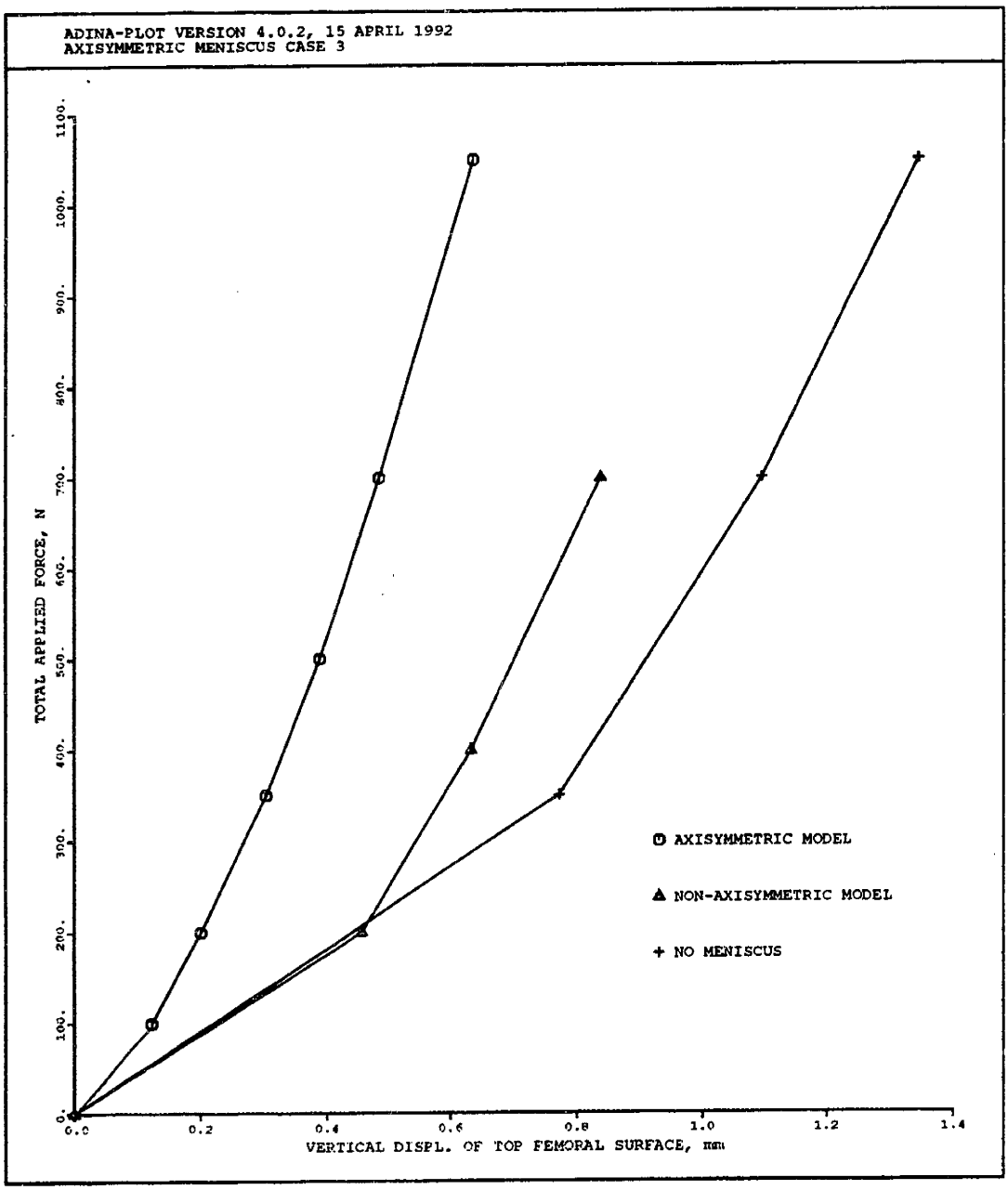

Figure 6-2: Vertical displacement of top femoral surface as a function of applied load.

clearly indicates a substantial difference in the movement of the meniscus on the tibial plateau in the two cases. The non-axisymmetric meniscus experiences significantly more radial displacement under axial loading. Figure 6-5 shows a proximal view of the original and deformed meniscus in the non-axisymmetric model.

6.4 Subchondral Bone Stresses

Figure 6-6 shows the von Mises effective stress in the tibial subchondral bone along a radial line from the point of initial tibiofemoral contact. The non-axisymmetric results are shown along three radial lines, which run parallel to those used to report the tibial contact pressures. The three non-axisymmetric radial lines show consistent subchondral bone stresses, particularly in the peak stress region. The non-axisymmetric model predicts significantly higher subchondral bone stresses than the axisymmetric model in the tibiofemoral and inner meniscotibial contact regions. Figure 6-7 shows the subchondral bone stress along a vertical line just below the point of initial contact. The non-axisymmetric model predicts significantly higher stresses along this line as well.

6.5 Meniscal Circumferential Strains

The average circumferential strain in the meniscus is an effective indicator of the load-bearing role of the meniscus. The average circumferential strain on the outer edge of the meniscus predicted by the axisymmetric model is 2.0% strain. The non-axisymmetric model predicts a value of 2.6% strain. Figure 6-8 shows the general trend of circumferential strains through the thickness of the meniscus. The two models both predict lower strain on the outer edge of the meniscus.

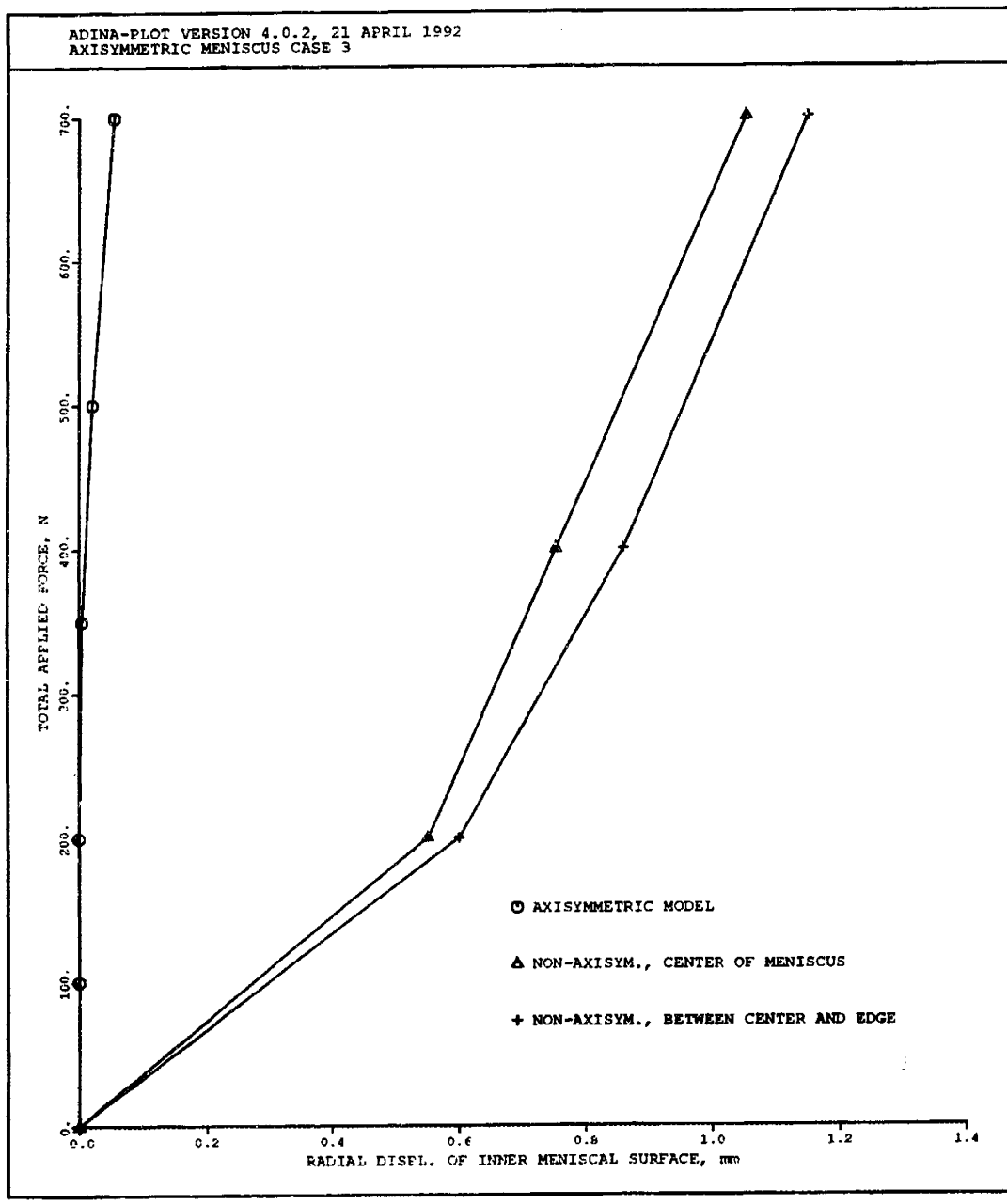

Figure 6-3: Radial displacement of the inner edge of the meniscus as a function of applied load.

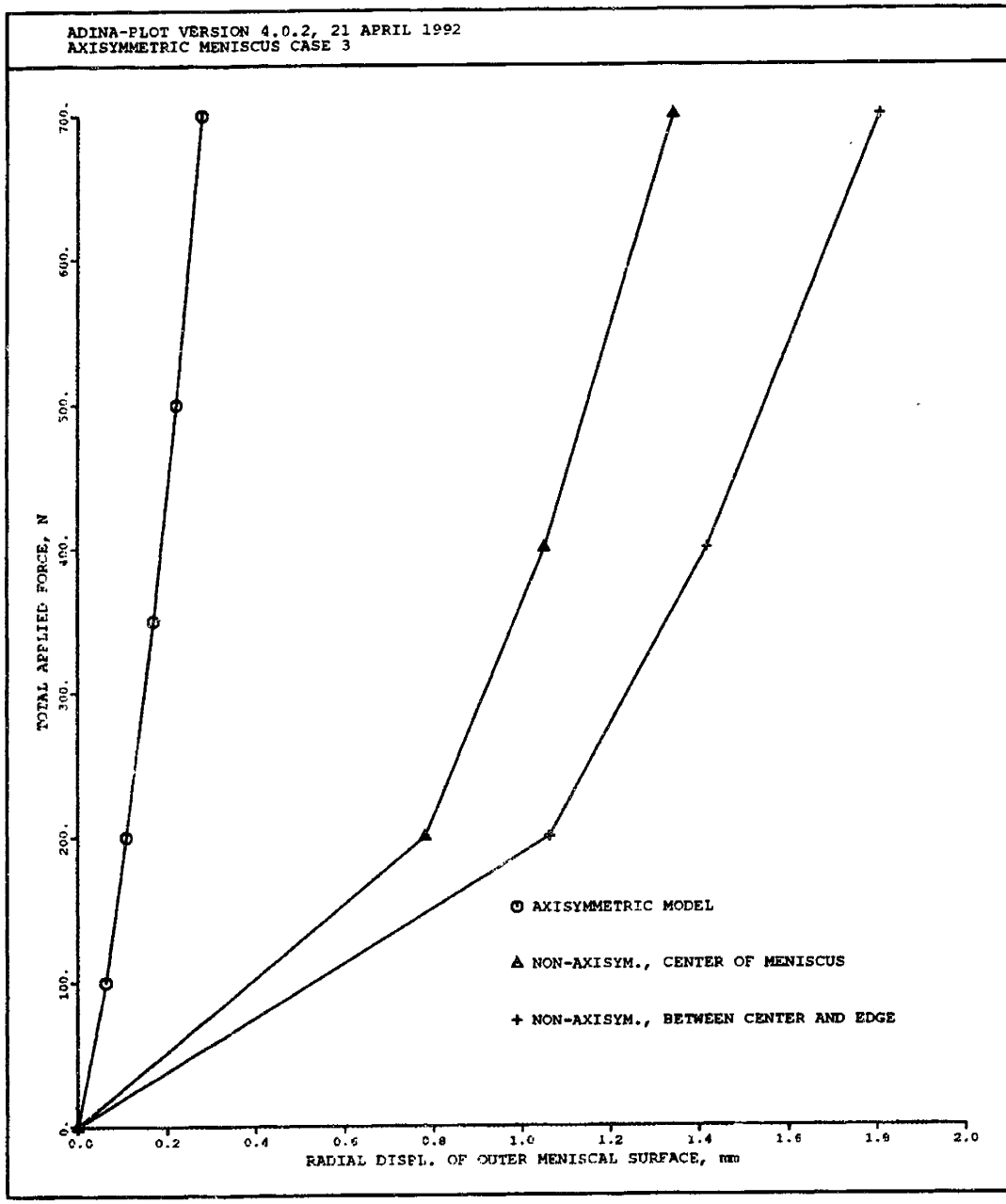

Figure 6-4: Radial displacement of the outer edge of the meniscus as a function of applied load.

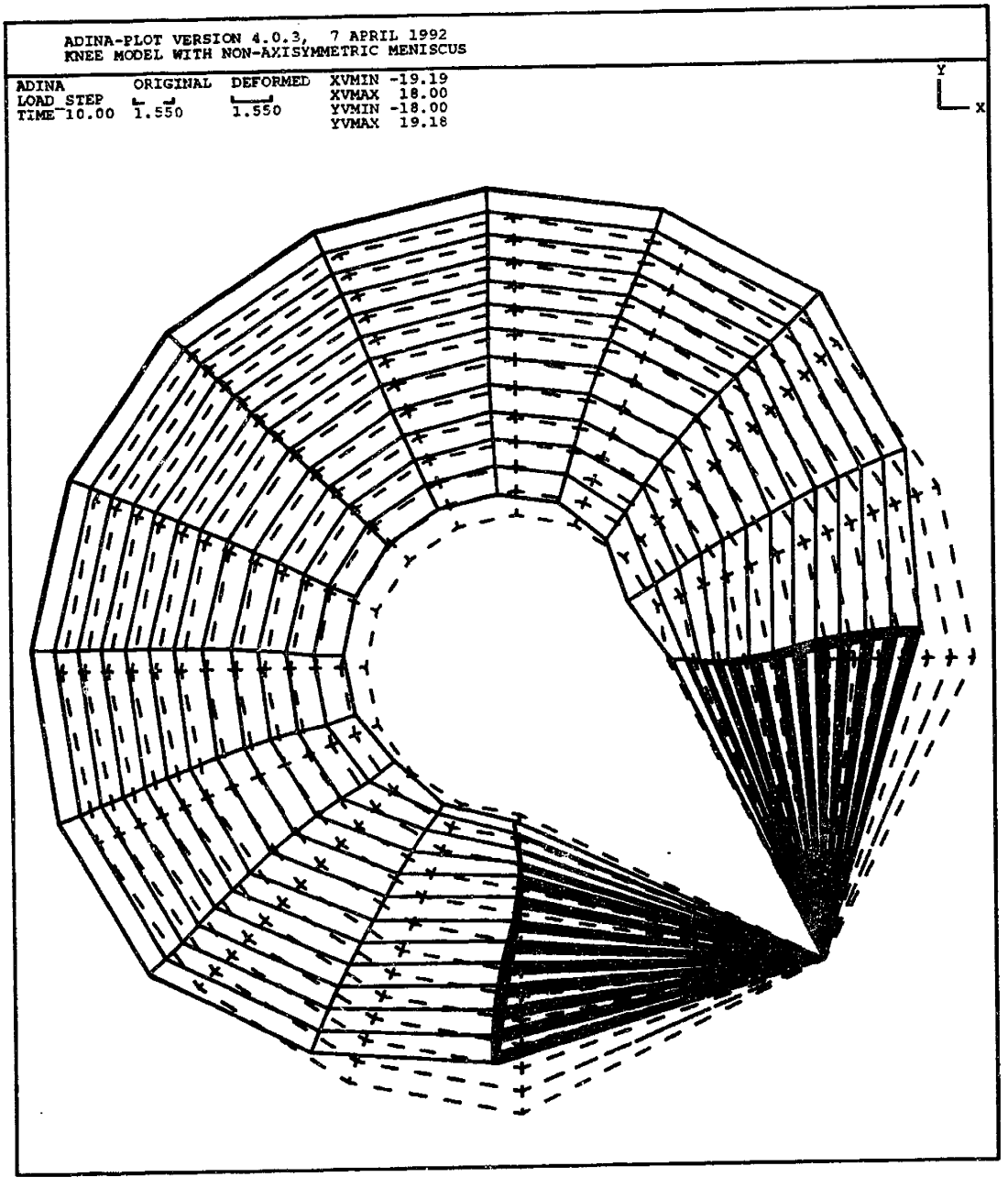

Figure 6-5: Proximal view of deformed meniscus, non-axisymmetric model. Dotted lines indicate the undeformed mesh.

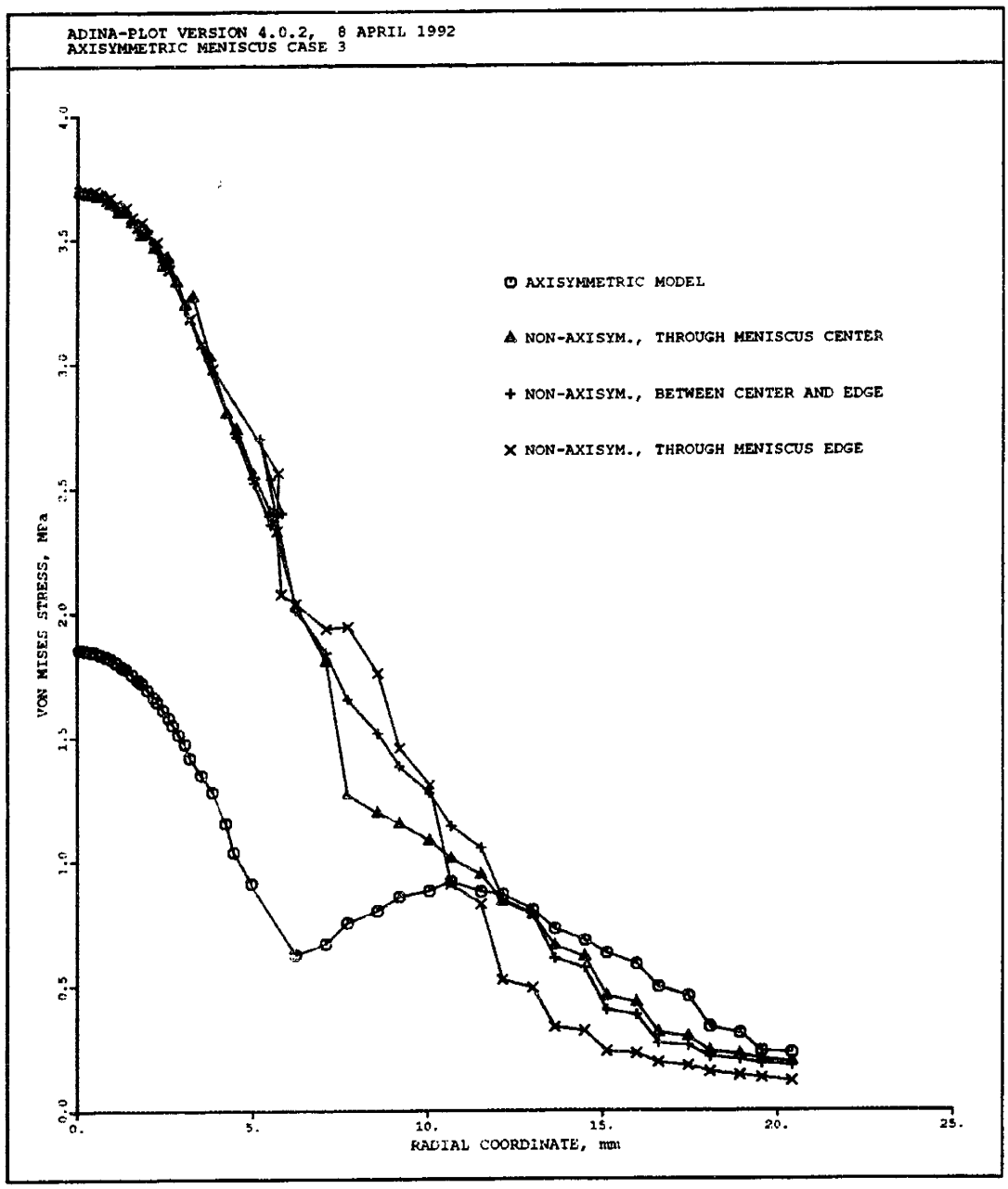

Figure 6-6: Tibial subchondral bone von Mises stress along radial lines at 1 *BW*.

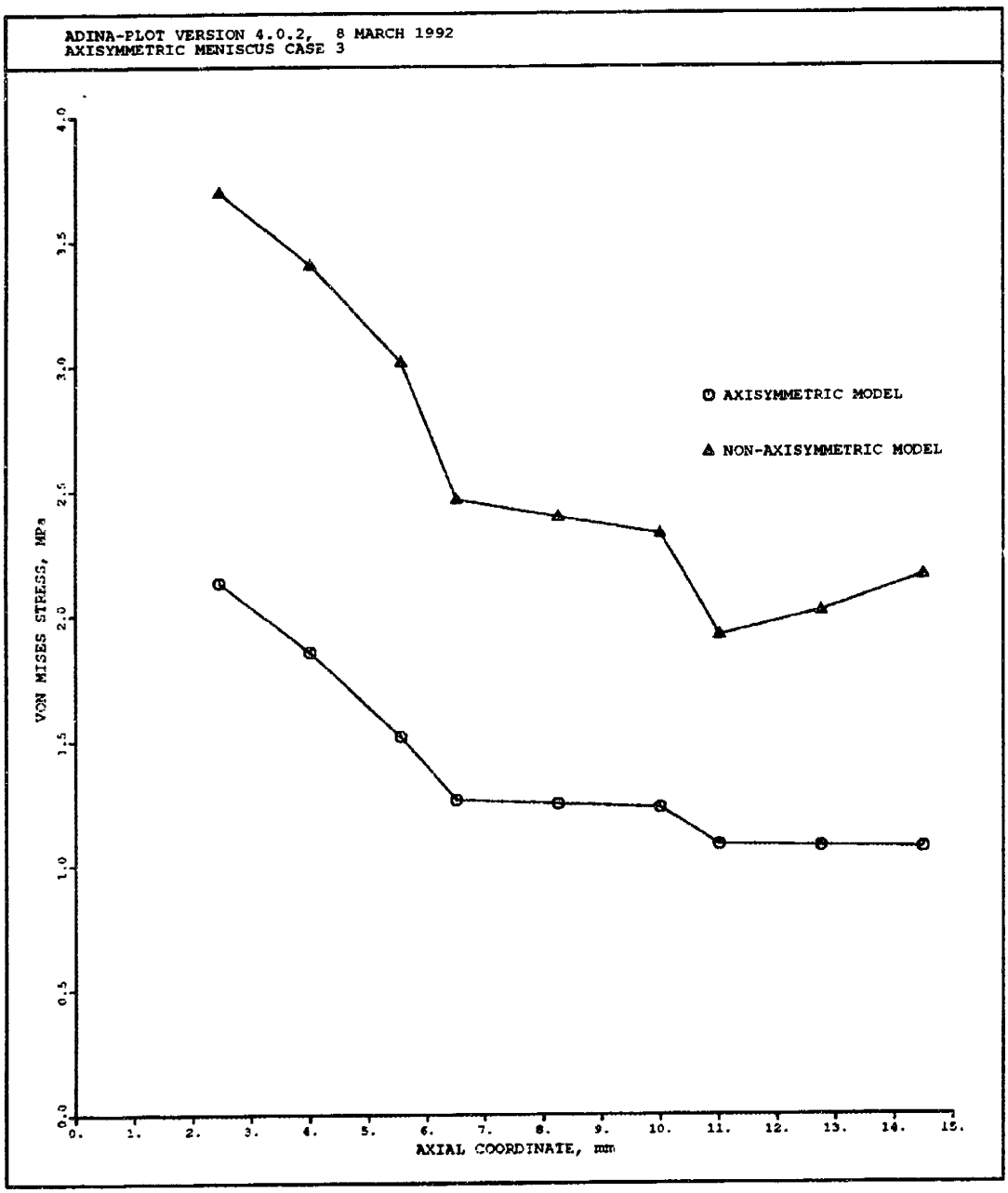

Figure 6-7: Tibial subchondral bone von Mises stress along vertical line below initial tibiofemoral contact point at 1 *BW*.

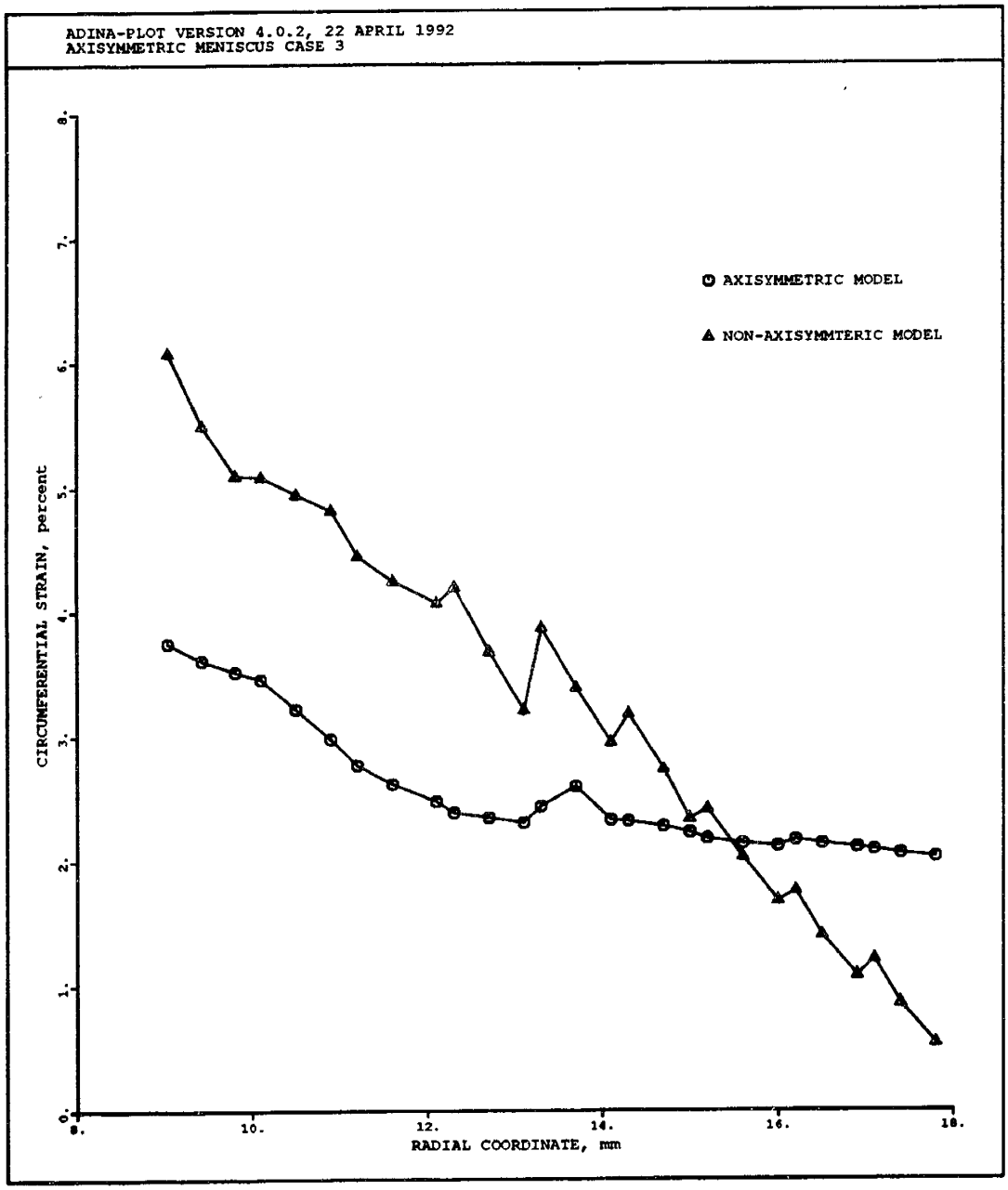

Figure 6-8: Circumferential strain distributions through meniscal cross section at 1 *BW*.

6.6 Percentage of Meniscal Load Transmission

Calculation of the percentage of load transmitted by the meniscus was accomplished using the plot of displacement of the top femoral surface as a function of applied load (see Figure 6-2). For a given displacement, the difference between the amount of load carried by the full meniscus model and a model without the meniscus is the amount of load carried by the meniscus. The values for the case without the meniscus were obtained from the 2D axisymmetric model of the knee used by Brown (1990[12]). Each curve was fit to a quadratic equation for purposes of this calculation. The fitted curves are shown in Figure 6-9, along with the original data points. Figure 6-10 shows the percentage of load transmitted by the meniscus as a function of load for both axisymmetric and non-axisymmetric models. The percentage of load predicted by the axisymmetric model is approximately 74%, while the non-axisymmetric model transmits approximately 40% of the total joint load at loading levels which the knee experiences during normal activities.

Figures 6-11 and 6-12 show deformed cross-sections of the axisymmetric and non-axisymmetric models, respectively. In both cases, it is evident that the all contact surfaces become fully conforming under sufficient loading. Neither the axisymmetric nor the non-axisymmetric meniscus is extruded from the joint space, and therefore both carry load.

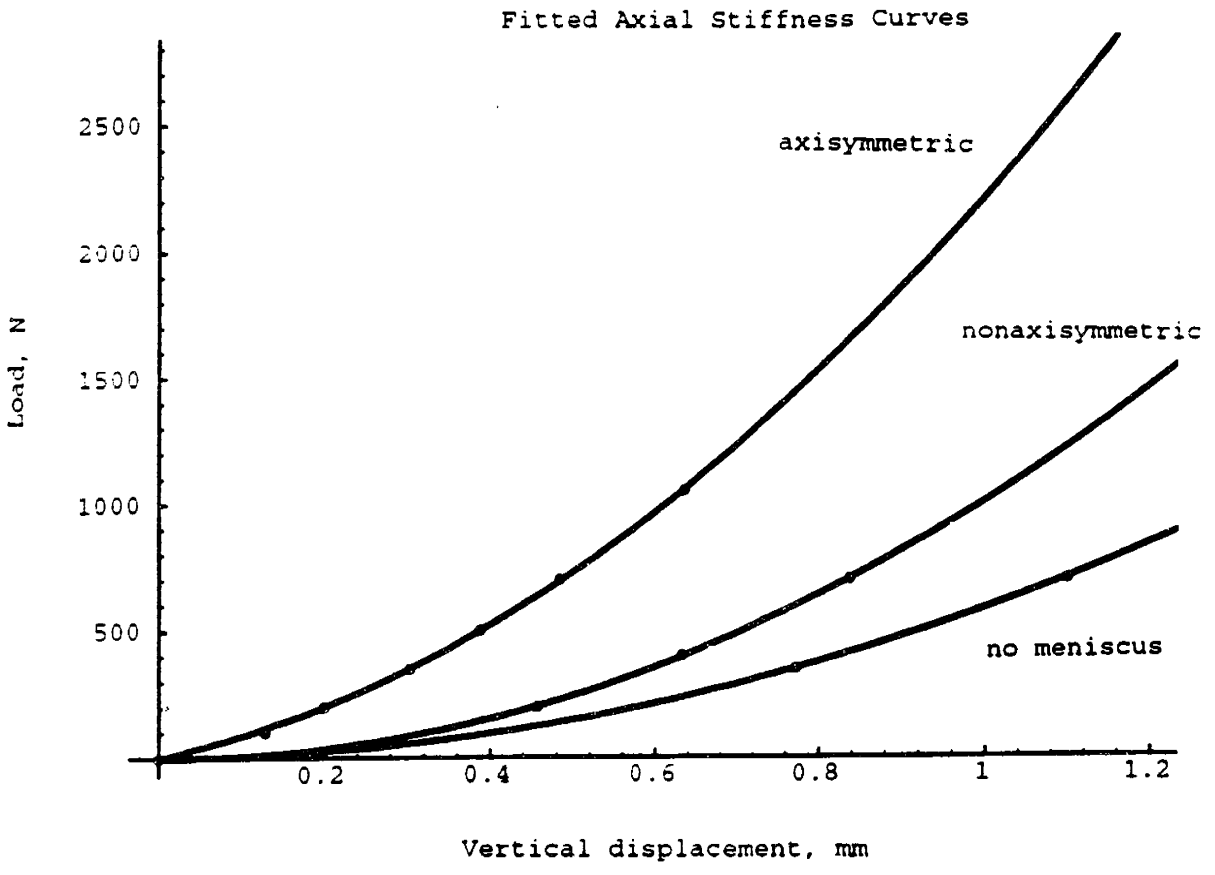

Figure 6-9: Fitted axial stiffness curves for axisymmetric, nonaxisymmetric, and no meniscus models.

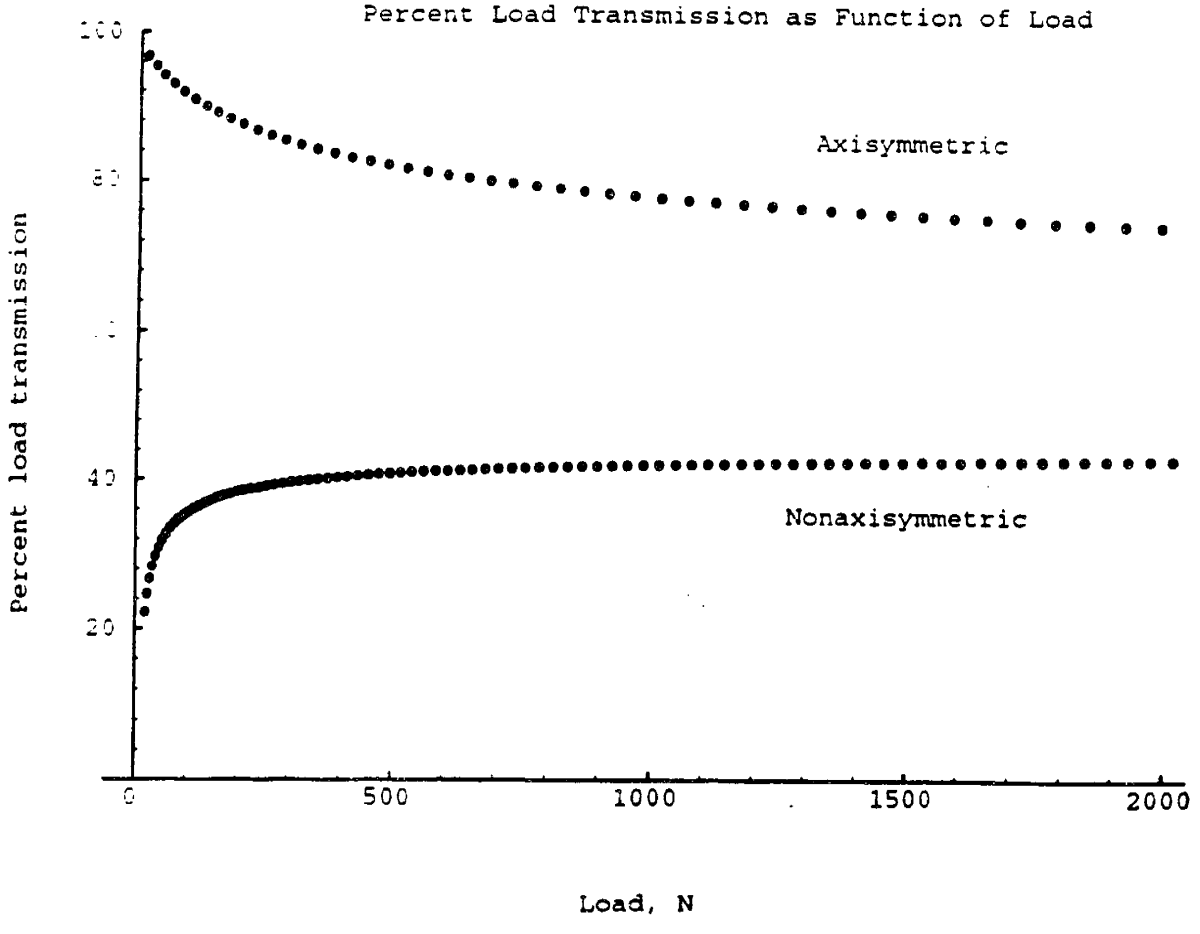

Figure 6-10: Percentage of load transmitted by axisymmetric and nonaxisymmetric menisci as a function of load.

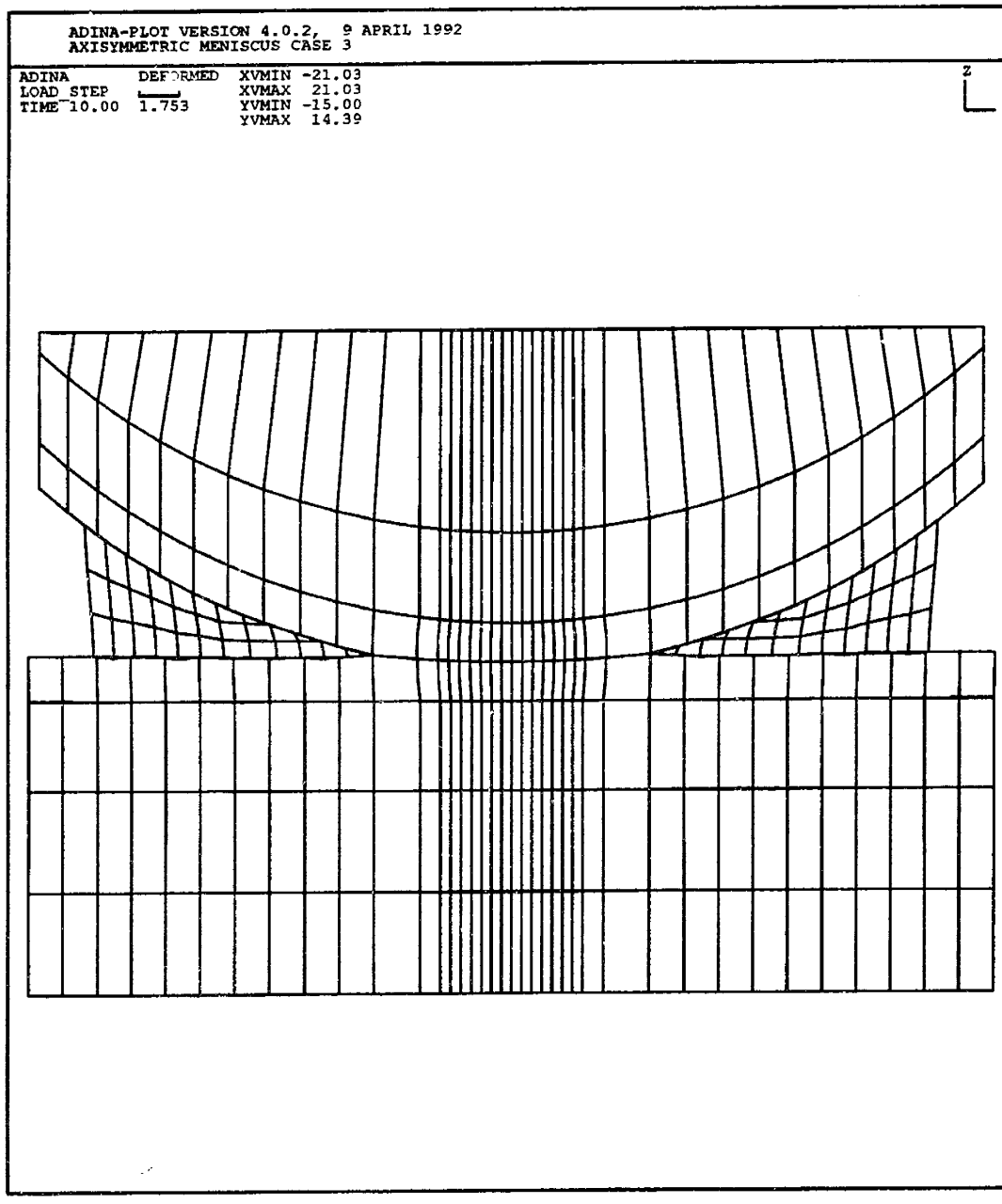

Figure 6-11: Cross-sectional view of deformed axisymmetric model.

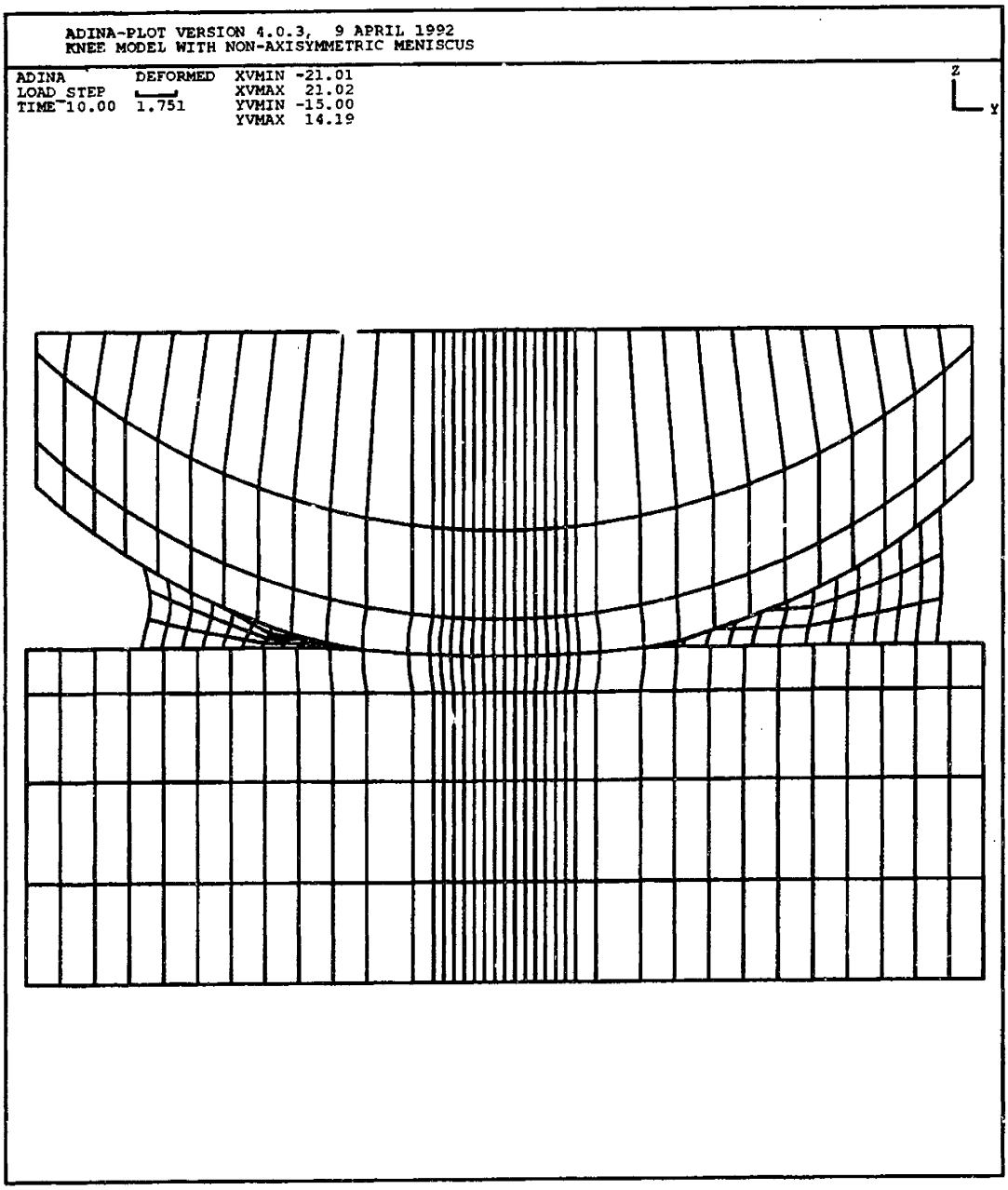

Figure 6-12: Cross-sectional view of deformed non-axisymmetric model.

Chapter 7

Verification and Conclusions

7.1 Model Verification

The modeling process is not complete without verification of the results obtained. In the case of the finite element meniscus model, verification occurs in two parts. The first form of verification involves establishing quantitatively the amount of numerical error present as a result of the discretization process. The finite element method will always yield a solution, and that solution always contains some amount of numerical error. A thorough analysis must include an error estimate for the results to have meaning. The quantification of discretization error in the meniscus model has been accomplished through the use of Hertzian contact and stress band analysis already discussed.

Aside from finite element discretization errors, a more fundamental question arises: How effective is the model in describing the load bearing role of the meniscus *in vivo*? Failure to address this question precludes closure of the modeling process and renders the model results uninterpretable. Unfortunately, *in vivo* data relating to the load-bearing role of the meniscus in humans is not available. However, there is a significant amount of *in vitro* experimental data which can be used to validate the finite element meniscus model. Parameters measured experimentally to determine the role of the meniscus in load bearing include articular cartilage contact pressures, the percentage of load transmitted by the meniscus, meniscal displacements and circumferential

strains.

7.1.1 Contact Pressures

The range of experimentally determined values for peak contact pressures in tibial articular cartilage is extremely broad. One reason for the wide range is variation in experimental technique. The different measurement techniques that have been used include pressure sensitive film (Fukubayashi & Kurosawa, 1980[24]; Baratz *et al.*, 1986[9]; Riegger *et al.*, 1987[52]), a micro-indentation transducer (Ahmed & Burke, 1983[1]), and miniaturized pressure transducers (Walker & Erkman, 1975[69]; Brown & Shaw, 1984[13]). Differences in reported experimental values arise from differences in the level of loading and loading rate, as well as from variation in measurement techniques.

Figure 7-1 shows the results of the 2D and 3D meniscus models with the results from Brown and Shaw's contact pressure study (1984[13]). The load values for the finite element models have been doubled to account for the fact that the models are unicondylar. This assumes that in a bicondylar knee model, the load would be distributed evenly over both condyles. This is a reasonable extrapolation of the finite element results. It is clear from Figure 7-1 that the non-axisymmetric meniscus model predicts peak contact pressures which are more consistent with Brown and Shaw's results.

7.1.2 Percentage Meniscal Load Transmission

The range of reported values for the percentage of meniscal load transmission is extremely broad as well. Seedhom and Hargreaves (1979[58]) reported that the lateral meniscus transmits approximately 50% of the lateral compartmental load at a level of roughly one times body weight. The same study showed that the medial meniscus transmits approximately 80% of the medial compartmental load at the same loading level. Shrive *et al* (1974[60]) reported that the menisci carried less than 60% of the total joint load. In a 1976 study, Seedhom [55] reported that the medial meniscus

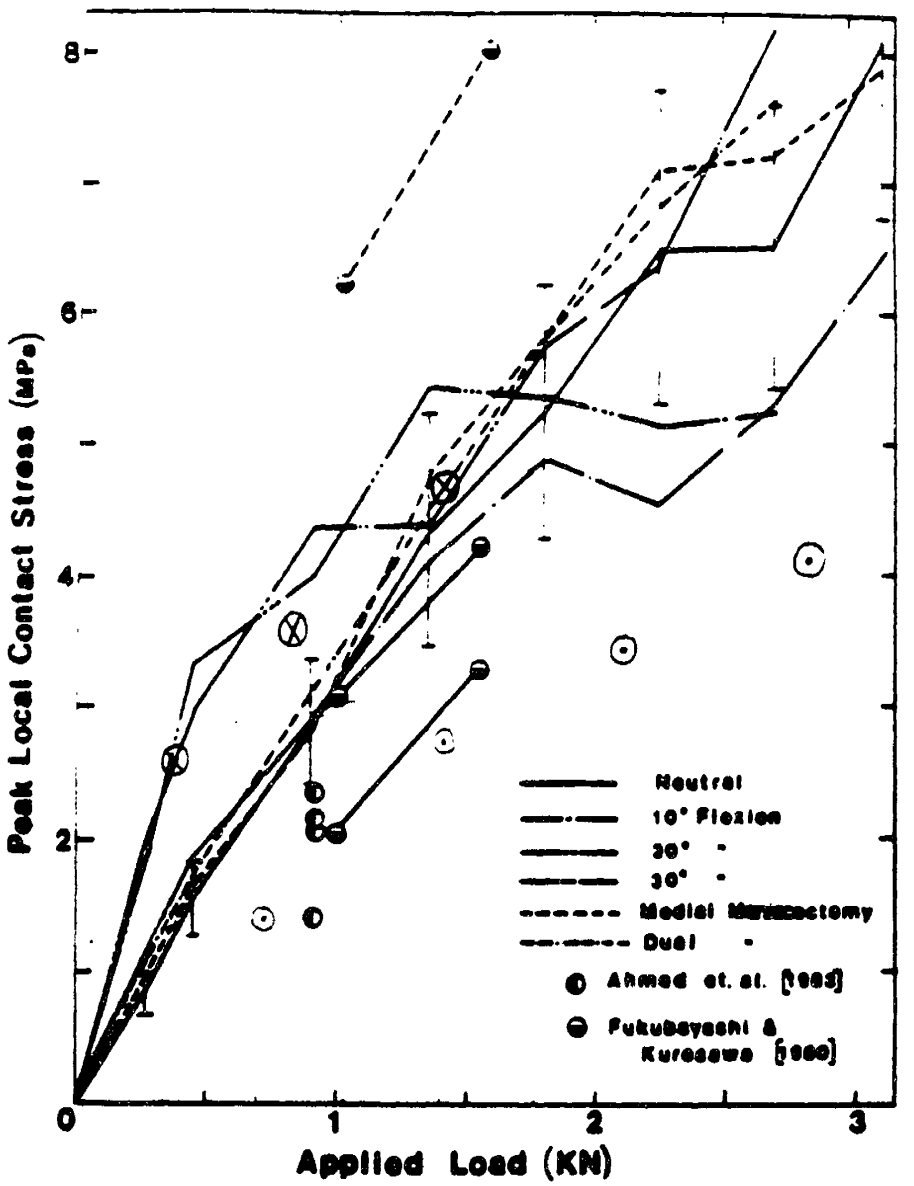

Figure 7-1: Peak contact pressures reported by Brown and Shaw [13]. 2D and 3D model predictions are superimposed (2D predictions ⊙, 3D predictions ⊗).

carries 40-50% of the medial compartmental load, while the lateral meniscus transmits 65-70% of its compartmental load. As with peak contact pressures, it is difficult to draw conclusions concerning model effectiveness given such a wide range of experimental results. The conclusion that can be drawn is that both the axisymmetric and non-axisymmetric models predict meniscal load transmission percentages within the range of reported values.

7.1.3 Meniscal Displacements and Strains

Brown (1990[12]) performed measurements of meniscal radial displacements using stereophotogrammetry for comparison to a two-dimensional finite element model of the meniscus. Brown also calculated the average circumferential strains in the meniscus. For a load of 2 BW, the calculated average circumferential strain of the medial meniscus was $2.1 \pm 0.5\%$ strain. This level of strain is in good agreement with both the axisymmetric and non-axisymmetric model predictions.

The axisymmetric and non-axisymmetric meniscus models predict similar values for average circumferential strains, but markedly different values for radial meniscal displacements. Brown (1990[12]) measured displacements of the meniscus relative to the tibia up to nearly 1 mm under a load of 2 BW. This is inconsistent with the axisymmetric model, which predicts displacements of order 0.1 mm under similar loading conditions. The non-axisymmetric model, however, predicts meniscal displacements which are consistent with the experimental findings.

7.2 Conclusions

The goal of this project was to develop a three-dimensional finite element model of the human knee meniscus for the purpose of quantitatively studying the role of the meniscus in knee joint load transmission. The primary application of the model was the evaluation of axisymmetric meniscal modeling as a means of quantifying meniscal mechanics.

As discussed above, the three-dimensional meniscus model exhibits strong corre-

lation with experimental data. It is evident from the comparison between axisymmetric and non-axisymmetric models that the 3D model is more effective than the axisymmetric model in predicting the meniscal load-bearing parameters. In particular, the 3D model predicts *both* meniscal displacements *and* circumferential strains which are consistent with experimental data; the axisymmetric model predicts reasonable strains, but not displacements. This is due to the increased mobility of the the non-axisymmetric meniscus on the tibial plateau, which more closely resembles the true physiological situation. The comparisons with experiment give a higher degree of confidence to the results of the 3D meniscus model.

Even though it is highly mobile, the non-axisymmetric meniscus is nevertheless capable of transmitting a significant portion of the joint load (40%). This value for percentage of load transmitted by the meniscus is significantly lower, however, than that predicted by the axisymmetric model. A large disparity between axisymmetric and non-axisymmetric models also occurs in the prediction of subchondral bone stresses. The level of subchondral bone stress can be an important factor in the development of osteoarthritis following meniscectomy, according to Radin (1972[50]; 1986[51]). An important factor in Radin's hypothesis is that meniscectomy increases subchondral bone stress, leading to microfractures. According to Wolff's law, the subchondral bone stiffens as a result of the increased stress. The stiffer subchondral bone causes a subsequent increase in articular cartilage stresses, which is followed by degeneration of the cartilage. Brown (1990[12]) predicted a peak subchondral bone stress following meniscectomy of approximately 7 *MPa* for a load of 1 *BW*. The axisymmetric meniscus model predicts a peak subchondral bone stress of approximately 2.1 *MPa*, while the 3D model predicts approximately 3.7 *MPa*. Both models predict an increase in subchondral bone stress following meniscectomy; the predicted amount of increase, however, is markedly different. This difference would be an extremely important factor in any attempt to quantify Radin's hypothesis with a meniscus model.

Given the higher degree of confidence that can be placed in the 3D meniscus model based on experimental comparisons, attempts to *quantify* the mechanical function of the meniscus should be based on models of the meniscus which include non-

axisymmetric geometry. Prior to this study, it was not clear how significant removing the simplifying assumption of axisymmetric geometry would be. The results of the 3D finite element study demonstrate that elimination of the axisymmetric assumption causes an improvement in model predictions. Although effective in providing a first-order description of meniscal mechanics, axisymmetric modeling of the meniscus is not sufficient for specific, quantitative description of the role of the meniscus in knee joint load transmission.

7.3 Future Work

Modeling of the meniscus as an axisymmetric structure has provided significant qualitative insight into the mechanisms of meniscal load bearing, and has provided a basis for more sophisticated models. The step from an axisymmetric to a non-axisymmetric meniscal geometry has added a level of accuracy as well as complexity to the model. The modeling process, however, is not nearly complete. Although the 3D meniscus model is a significant step toward full understanding of meniscal mechanics, it is still a rather simplified model. Development of mesh generation techniques from real anatomic data would significantly increase the accuracy of the model predictions. Further examination of the material properties of bone, cartilage and meniscus would improve the model as well.

The expansion of the meniscus model in to three dimensions makes possible the study of numerous aspects of meniscal mechanics which are not feasible with an axisymmetric model. The development of a bicondylar knee model would allow studies of the effect of torsional loading and could provide insight into the proposed mechanisms of meniscal tears, as well as the importance of meniscal attachments such as that of the medial meniscus to the medial collateral ligament. The role of the meniscus in joint stability could also be examined. In short, there are numerous aspects of knee joint mechanics which remain to be examined with a three-dimensional model of the knee which includes the menisci.

Bibliography

[1] A. M. Ahmed and D. L. Burke. In-vitro measurement of static pressure distribution in synovial joints–part i: Tibial surface of the knee. *Transactions of the ASME*, 105:216–225, 1983.

[2] P. R. Allen, R. A. Denham, and A. V. Swan. Late degenerative changes after meniscectomy. *Journal of Bone and Joint Surgery*, 66-B:666–671, 1984.

[3] D. R. Anderson, M. K. Kwan, S. L.-Y. Woo, W. H. Akeson, L. A. Danzig, and D. H. Gershuni. Viscoelastic shear properties of equine meniscal cartilage. In *Transactions of the 36th Annual Meeting of the Orthopaedic Research Society*, volume 15, page 247. Orthopaedic Research Society, February 1990. New Orleans, LA.

[4] Helge Appel. Late results after meniscectomy in the knee joint. *Acta Orthopedica Scandinavica*, Supplementum No. 133, 1970.

[5] Steven Arnoczky, Mark Adams, Kenneth DeHaven, David Eyre, and Van Mow. Meniscus. In Savio L. Y. Woo and Joseph A. Buckwalter, editors, *Injury and Repair of the Musculoskeletal Soft Tissues*, chapter 12, pages 487–537. American Academy of Orthopaedic Surgeons, Park Lake, Illinois, 1988. Workshop supported by the American Academy of Orthopaedic Surgeons and the National Institute of Arthritis and Musculoskeletal and Skin Diseases held in Savannah, Georgia in June 1987.

[6] M. Askew, A. Melby, L. Good, F. Baniewicz, F. Hurst, and A. Boom. In-vitro kinematic studies of normal, acl deficient, and meniscectomized knees. *Trans-*

actions of the 33rd Annual Meeting of the Orthopedic Research Society, 12:271, 1987.

[7] M. J. Askew and V. C. Mow. The biomechanical function of the collagen fibril ultrastructure of articular cartilage. *J. Biomech. Engng.*, 100:105–115, 1978.

[8] R. M. Aspden. A model for the function and failure of the meniscus. *Engineering in Medicine*, 14:119–122, 1985.

[9] Mark E. Baratz, Freddie H. Fu, and Richard Mengato. Meniscal tears: The effect of meniscectomy and of repair on intraarticular contact areas and stress in the human knee. *The American Journal of Sports Medicine*, 14:270–275, 1986.

[10] Klaus-Jürgen Bathe. *Finite Element Procedures in Engineering Analysis.* Prentice-Hall, Inc., Englewood Cliffs, New Jersey, 1982.

[11] Otto C. Brantigan and Allen F. Voshell. The mechanics of the ligaments and menisci of the knee joint. *Journal of Bone and Joint Surgery*, 23:44–66, 1941.

[12] Gregory A. Brown. *Load-Bearing Role of the Human Knee Meniscus.* PhD thesis, Harvard-MIT Division of Health Sciences and Technology, 1990.

[13] Thomas D. Brown and Daniel T. Shaw. *In vitro* contact stress distribution on the femoral condyles. *J. Orthopaedic Research*, 2(2):190–199, 1984.

[14] Peter G. Bullough, Luis Munuera, Joseph Murphy, and Allan M. Weinstein. The strength of the menisci as it relates to their fine structure. *Journal of Bone and Joint Surgery*, 52–B:564–570, 1970.

[15] David S. Burnett. *Finite Element Analysis.* Addison-Wesley Publishing Company, 1987.

[16] D. I. Bylski, S. A. Goldstein, T. Mcou, D. Moore, S. Reed, and Larry S. Matthews. Experimental determination of meniscal mechanics in intact knee joints. In *Transactions of the 32nd Annual Meeting of the Orthopaedic Research*

Society, volume 11, page 409. Orthopaedic Research Society, February 1986. New Orleans, LA.

[17] S. Ward Casscells. The torn or degenerated meniscus and its relationship to degeneration of the weight-bearing areas of the femur and tibia. *Clinical Orthopedics and Related Research*, 132:196–200, 1978.

[18] R. Chand, E. Haug, and K. Rim. Stresses in the human knee joint. *Journal of Biomechanics*, 9:417–422, 1976.

[19] Paul Ducheyne, Luc Heymans, Marc Martens, Etienne Aernoudt, Paul de Meester, and Jozef Mulier. The mechanical behavior of intracondylar cancellous bone of the femur at different loading rates. *J. Biomechanics*, 10:747–762, 1977.

[20] A. W. Eberhardt, L. M. Keer, J. L. Lewis, and V. Vithoontien. An analytical model of joint contact. *Journal of Biomechanical Engineering*, 112:407–413, 1990.

[21] T. J. Fairbank. Knee joint changes after meniscectomy. *Journal of Bone and Joint Surgery*, 30-B:664–670, 1948.

[22] Robert Scott Fijan. *A Three-Dimensional Mathematical Model of the Human Knee Joint.* PhD thesis, Massachusetts Institute of Technology, Cambridge, MA, April 1990.

[23] D. C. Fithian, M. B. Schmidt, A. Ratcliffe, and V. C. Mow. Human meniscus tensile properties. In *Transactions of the 35th Annual Meeting of the Orthopaedic Research Society*, volume 14, page 205. Orthopaedic Research Society, February 1989. Las Vegas, NV.

[24] Toru Fukubayashi and Hishashi Kurosawa. The contact area and pressure distribution pattern of the knee. *Acta Orthopedica Scandinavica*, 51:871–879, 1980.

[25] P. C. Galbraith and J. T. Bryant. Effects of grid dimensions on finite element models of an articular surface. *J. Biomechanics*, 22:385–393, 1989.

[26] Henry Gray. *Anatomy of the Human Body.* Lea and Febiger, Philadelphia, 1973.

[27] I. J. Harrington. A bioengineering analysis of force actions at the knee in normal and pathological gait. *Biomedical Engineering*, pages 167–172, May 1976.

[28] Mohamed S. Hefzy, Edward S. Grood, and M. Zoghi. An axisymmetric finite element model of the menisci. *Advances in Bioengineering*, pages 51–52, 1987.

[29] Arthur J. Helfet. Mechanism of derangements of the medial semilunar cartilage and their management. *Journal of Bone and Joint Surgery*, 41-B:319–336, 1959.

[30] J. P. Jackson. Degenerative changes in the knee after meniscectomy. *British Medical Journal*, 2:525–527, 1968.

[31] K. L. Johnson. *Contact Mechanics.* Cambridge University Press, 1985.

[32] Robert J. Johnson, Donald B. Kettelkamp, William Clark, and Paul Leaverton. Factors affecting late results after meniscectomy. *Journal of Bone and Joint Surgery*, 56-A:719–729, 1974.

[33] Robert J. Johnson and Malcolm H. Pope. Functional anatomy of the meniscus. In *AAOS Symposium on Reconstructive Surgery of the Knee*, pages 3–13. CV Mosby, 1978.

[34] Uffe Jorgensen, Stig Sonne-Holm, Flemming Lauridsen, and Arne Rosenklint. Long-term follow-up of meniscectomy in athletes. *Journal of Bone and Joint Surgery*, 69-B:80–83, 1987.

[35] Donald B. Kettelkamp and Allen W. Jacobs. Tibiofemoral contact area–determination and implications. *Journal of Bone and Joint Surgery*, 54-A:349–356, 1972.

[36] William R. Krause, Malcolm H. Pope, Robert J. Johnson, and David G. Wilder. Mechanical changes in the knee after meniscectomy. *Journal of Bone and Joint Surgery*, 58-A:599–604, 1976.

[37] H. Kurosawa, P. S. Walker, S. Abe, A. Garg, and T. Hunter. Geometry and motion of the knee for implant and orthotic design. *J. Biomechanics*, 18(7):487–499, 1985.

[38] Hishashi Kurosawa, Toru Fukubayashi, and Hiroyuki Nakajima. Load-bearing mode of the knee joint. *Clinical Orthopedics and Related Research*, 149:283–290, 1980.

[39] I. Martin Levy, Peter A. Torzilli, Jeffrey D. Gould, and Russell F. Warren. The effect of lateral meniscectomy on motion of the knee. *Journal of Bone and Joint Surgery*, 71-A:401–406, 1989.

[40] I. Martin Levy, Peter A. Torzilli, and Russell F. Warren. The effect of medial meniscectomy on anterior–posterior motion in the knee. *Journal of Bone and Joint Surgery*, 64-A:883–888, 1982.

[41] M. A. MacConaill. The function of the intra-articular fibrocartilages with special reference to the knee and inferior radio-ulnar joints. *Journal of Anatomy*, 66:210–227, 1932.

[42] Paul G. J. Maquet. *Biomechanics of the Knee.* Springer-Verlag, 1976.

[43] Keith L. Markolf, William L. Bargar, Stephen C. Shoemaker, and Harlan C. Amstutz. The role of joint load in knee stability. *Journal of Bone and Joint Surgery*, 63-A:570–585, 1981.

[44] Joseph S. Mensch and Harlan C. Amstutz. Knee morphology as a guide to knee replacement. *Clin. Orthop.*, 112:231–241, October 1975.

[45] James B. Morrison. Bioengineering analysis of force actions transmitted by the knee joint. *Biomedical Engineering*, pages 164–170, April 1968.

[46] Alan P. Newman, D. Ron Anderson, A. U. Daniels, and Ken W. Jee. The effect of medial meniscectomy and coronal plane angulation on in vitro load transmission in the canine stifle joint. *Journal of Orthopaedic Research*, 7:281–289, 1989.

[47] H. Nishizaki, N. Ohtsuki, T. Murakami, H. Chikama, T. Toyonaga, and A. Nishio. Photoelastic study of models simulating human knee joint. *Proceedings of the XIIIth International Congress of Biomechanics*, July 1981.

[48] Jonathan Noble. Lesions of the menisci. *Journal of Bone and Joint Surgery*, 59-A:480–483, 1977.

[49] Eric L. Radin, Francois de Lamotte, and Paul Maquet. Role of the menisci in the distribution of stress in the knee. *Clinical Orthopedics and Related Research*, 135:290–294, 1984.

[50] Eric L. Radin, I. L. Paul, and E. M. Rose. Role of mechanical factors in pathogenesis of primary osteoarthritis. *The Lancet*, 1:519–522, 1972.

[51] Eric L. Radin and R. M. Rose. Role of subchondral bone in the initiation and progression of cartilage damage. *Clin. Orthop.*, 213:34–40, 1986.

[52] C. L. Riegger, W. C. Hayes, and T. N. Gerhart. Tibiofemoral contact pressure and area in neutral, varus, valgus, and post-osteotomy conditions. In *Transactions of the 33rd Annual Meeting of the Orthopaedic Research Society*, volume 12, page 223. Orthopaedic Research Society, January 1987. San Francisco, CA.

[53] A. A. H. J. Sauren, A. Huson, and R. Y. Schouten. An axisymmetric finite element analysis of the mechanical function of the meniscus. *Int. J. Sports Med.*, 5(Supplement):93–95, 1984.

[54] K. S. Seale, D. W. Haynes, C. L. Nelson, P. C. McLeod, and M. H. Gerdes. The effect of meniscectomy on knee stability. *Transactions of the 27th Annual Meeting of the Orthopaedic Research Society*, 6:236, 1981.

[55] B. B. Seedhom. Loadbearing function of the menisci. *Physiotherapy*, 62(7):223–226, June 1976.

[56] B. B. Seedhom. Transmission of the load in the knee joint with special reference to the role of the menisci. Part I: Anatomy, analysis and apparatus. *Engineering in Medicine*, 8(4):207–219, October 1979.

[57] B. B. Seedhom, D. Dowson, and V. Wright. The load-bearing function of the menisci: A preliminary study. In O. S. Ingwersen, B. van Linge, T. J. G. van Rens, G. E. Rosingh, B. E. E. M. J. Veraart, and D. LeVau, editors, *The Knee Joint: Recent Advances in Basic Research and Clinical Aspects*, pages 37–42. American Elsevier, New York, 1974.

[58] B. B. Seedhom and D. J. Hargreaves. Transmission of the load in the knee joint with special reference to the role of the menisci. Part II: Experimental results, discussion and conclusions. *Engineering in Medicine*, 8(4):220–228, October 1979.

[59] Stephen C. Shoemaker and Keith L. Markolf. The role of the meniscus in the anterior-posterior stability of the loaded anterior cruciate-deficient knee. *Journal of Bone and Joint Surgery*, 68-A:71–79, 1986.

[60] N. Shrive. The weight–bearing role of the menisci of the knee. *J. Bone Joint Surg.*, 56B(2):381, May 1974. In Proceedings of the British Orthopaedic Research Society.

[61] R. L. Spilker, T. A. Maxian, and V. C. Mow. A fibrous biphasic anisotropic finite element model of the meniscus. In *Transactions of the 36th Annual Meeting of the Orthopaedic Research Society*, volume 15, page 244. Orthopaedic Research Society, February 1990. New Orleans, LA.

[62] Theodore Sussman and Klaus-Jürgen Bathe. Studies of finite element procedures–stress band plots and the evaluation of finite element meshes. *Engineering Computation*, 3:178–191, 1986.

[63] Edward M. Tapper and Norman W. Hoover. Late results after meniscectomy. *Journal of Bone and Joint Surgery*, 51–A:517–526, 1969.

[64] W. O. Thompson, F. H. Fu, F. L. Thaete, and S. F. Dye. Assessment of tibial meniscal kinematics by 3D magnetic resonance imaging. In *Transactions of the 36th Annual Meeting of the Orthopaedic Research Society*, volume 15, page 245. Orthopaedic Research Society, February 1990. New Orleans, LA.

[65] S. P. Timoshenko and J. N. Goodier. *Theory of Elasticity.* McGraw-Hill Book Company, 1970.

[66] M. Tissakht and A. M. Ahmed. Effect of tibial axial rotation on knee meniscal stress: a finite element study. In *Transactions of the 36th Annual Meeting of the Orthopaedic Research Society*, volume 15, page 243. Orthopaedic Research Society, February 1990. New Orleans, LA.

[67] M. Tissakht, R. Farinaccio, and A. M. Ahmed. Effect of ligament attachments on the response of the knee menisci in compression and torsion: a finite-element study. In *Transactions of the 35th Annual Meeting of the Orthopaedic Research Society*, volume 14, page 203. Orthopaedic Research Society, February 1989. Las Vegas, NV.

[68] P. S. Walker and J. V. Hajek. The load-bearing area in the knee joint. *Journal of Biomechanics*, 5:581–589, 1972.

[69] Peter S. Walker and Margaret J. Erkman. The role of the menisci in force transmission across the knee. *Clinical Orthopedics and Related Research*, 109:184–192, 1975.

[70] Ching-Jen Wang and Peter S. Walker. Rotatory laxity of the human knee joint. *Journal of Bone and Joint Surgery*, 56–A:161–170, 1974.